Artif Intell Rev (2019) 52:2319–2380
https://doi.org/10.1007/s10462-018-9616-4

A comprehensive investigation into the performance, robustness, scalability and convergence of chaos-enhanced evolutionary algorithms with boundary constraints

Ahmad Mozaffari[1] · **Mahdi Emami**[2] · **Alireza Fathi**[2]

Published online: 1 February 2018

Abstract The purpose of this research is to investigate the effects of different chaotic maps on the exploration/exploitation capabilities of evolutionary algorithms (EAs). To do so, some well-known chaotic maps are embedded into a self-organizing version of EAs. This combination is implemented through using chaotic sequences instead of random parameters of optimization algorithm. However, using a chaos system may result in exceeding of the optimization variables beyond their practical boundaries. In order to cope with such a deficiency, the evolutionary method is equipped with a recent spotlighted technique, known as the boundary constraint handling method, which controls the movements of chromosomes within the feasible solution domain. Such a technique aids the heuristic agents towards the feasible solutions, and thus, abates the undesired effects of the chaotic diversification. In this study, 9 different variants of chaotic maps are considered to precisely investigate different aspects of coupling the chaos phenomenon with the baseline EA, i.e. the convergence, scalability, robustness, performance and complexity. The simulation results reveal that some of the maps (chaotic number generators) are more successful than the others, and thus, can be used to enhance the performance of the standard EA.

Keywords Evolutionary algorithms · Chaotic maps · Numerical optimization · Power systems

1 Introduction

So far, extensive studies have been carried out to embed the concept of chaos into the structure of metaheuristic optimization algorithms. Intensification (exploitation capability) and diver-

Electronic supplementary material The online version of this article (https://doi.org/10.1007/s10462-018-9616-4) contains supplementary material, which is available to authorized users.

✉ Ahmad Mozaffari
amozaffa@uwaterloo.ca

1 University of Waterloo, Waterloo, ON, Canada

2 Babol University of Technology, Babol, Mazandaran, Iran

sification (exploration capability) are the main properties of such algorithms. Intensification incurs more effective search around local minima, and diversification leads to more covering of the search space which in turn reduces the probability of trapping into local minima and missing the most qualified solutions. Generally, the development of metaheuristic optimization algorithms is performed within two main frames, i.e. introducing novel algorithms and improvement of the existing methods (Goldberg 1989; Yang 2008). Although proposing novel metaheuristics is still welcome according to *no free lunch theorem* (Wolpert and Macready 1997; Karaboga and Basturk 2007; Mozaffari et al. 2012c; Abdechiri et al. 2013), the second field of investigation, i.e. improving intensification/diversification capabilities of the well-established metaheuristics, such as evolutionary algorithms (EAs) and swarm based methods, is of higher importance. The urge for improving the exploration/exploitation capabilities of well-established metaheuristics has come to the mind of many researchers of the both basic and practical science societies, and thus numerous related research papers can be found in literature [see for example Mozaffari et al. (2012a, 2013a), Karaboga and Akay (2009), Civicioglu and Besdok (2013) and references therein].

In the recent years, researchers have been looking for some techniques to replace the stochastic nature of the randomization with a purposeful process (Caponetto et al. 2003; Mozaffari et al. 2015). This is done through embedding orderliness into the stochastic operators (responsible for exploration of metaheuristics) while retaining their unpredictability characteristic.

Fascinating trait of nonlinear dynamical systems (Huaguang and Yongbing 2001), in particular chaotic dynamics, has drawn an increasing attention of researchers. Chaos is mathematically defined as a deterministic nonlinear system which produces randomness (Alatas and Akin 2009; Emami et al. 2016). Some main properties of chaos dynamic systems include ergodicity, semi-stochastic nature and dependence on the initial conditions (Schuster 1988). Promising reports on the successful applications of chaotic systems to a wide spectrum of scientific fields such as mathematics, physics, biology, chemistry and economics have provoked researchers of the engineering community to find out whether it can be of use for other practical tasks. For this purpose, researchers have tried to substitute deterministic chaos-based signals with stochastic ones. The mentioned strategy has been employed in various practical domains such as telecommunication and secure transmissions (Wong et al. 2005), signal, image and video processing (Gao et al. 2006; Abdechiri et al. 2017a, b, c), nonlinear circuits (Arena et al. 2000), DNA computing (Manganaro and Pine dade Gyvez 1997), control (Ott et al. 1990; Kapitniak 1995; Zhang et al. 2014), information decryption (Zelinka and Jasek 2010) and synchronization (Pecora and Carroll 1990; Zhang et al. 2010).

Along with the above-mentioned applications, the concept of substituting chaos sequences with stochastic signals has been used by researchers of the metaheuristic community to improve the randomness of metaheuristic algorithms (Zelinka et al. 2010). As mentioned, chaotic maps improve the exploration/exploitation capabilities of metaheuristics by replacing their stochastic randomness with a deterministic disordered repetitive pattern (Gao et al. 2010). Actually, most of the exerted simulations indicate an obvious enhancement in the accuracy of metaheuristics when they use bounded chaotic based explorative operators instead of pure stochastic processes (Zelinka et al. 2010).

In this work, the impact of combining chaotic maps with EAs, as one of the most popular types of swarm and evolutionary optimizers is empirically analyzed. In particular: (1) different chaotic maps are adopted to select the most compatible one for EAs, (2) the performance improvement and time complexity associated with replacing chaotic sequences with conventional stochastic random procedure is rigorously studied, (3) the robustness of

chaos-enhanced methods are evaluated using statistical metrics, and (4) the scalability of the chaotic methods are tested using numerous scalable benchmarks of different properties considering three different dimensions (50D, 100D and 200D). To the authors' best knowledge, this is the first time that a comprehensive numerical study is carried out which simultaneously verifies the impact of different types of chaotic maps on the algorithmic complexity, robustness, convergence behavior, scalability and performance of EAs. Therefore, it is believed that the findings of the current study can be a good guide which provides a vision for the researchers of metaheuristic computing regarding the efficacy of specific types of chaotic maps for real-life optimization tasks.

The rest of the paper is organized as follows. Section 2 presents the literature review of the advances on chaotic evolutionary computing. Section 3 is devoted to the definition and analysis of chaotic evolutionary algorithms. In Sect. 4, the performances of CEAs are investigated experimentally, and the most efficient chaotic maps are presented. Finally, the paper is concluded in Sect. 5.

2 A review of the theoretical advances and applications of chaotic evolutionary computing

So far, the use of chaotic embedded operators has been examined in different evolutionary algorithms for a wide range of real-life and numerical optimization problems. Table 1 lists the important research papers together with their application and findings.

As can be inferred from the given information, chaos-enhanced EAs have successfully been applied to a wide range of applications, and seem to be used even more in near future for handling complicated optimization problems.

3 The proposed chaotic evolutionary algorithms

3.1 A concise review on the background of evolutionary algorithms

By the middle of twentieth century, the promising reports on using nature-inspired methods for handling complicated problems has drawn an increasing attention from computer scientists. In particular, the use of algorithms mimicking the theory of evolution and survival of the fittest has been found to be very effective for solving complex optimization problems. Investigation on the potentials of evolutionary algorithms (EAs) for optimization has been incepted by a number of independent research groups in 1960s. In 1962, the studies of Holland's research group in Ann Arbor (Holland 1975) and Fogel's research group in San Diego (Fogel et al. 1966) led to the proposition of GA and evolutionary programming (EP), respectively. In 1965, Schwefel and Rechenberg's research in Berlin led to the development of evolutionary strategies (ES) (Beyer and Schwefel 2002). Such pioneering investigations have played a key role in the formation of the field today known as evolutionary computation. There exists an extensive literature regarding the variants of EAs, from which genetic programming (GP) (Brameier and Banzhaf 2007) and differential evolution (DE) (Storn and Price 1997) have gained a remarkable reputation. In spite of the structural differences of the abovementioned algorithms, all of them follow the same concepts for solving a problem, namely the laws of natural competition and survival of the fittest. This is done by executing a series of coupled mathematical operators in the form of selection, crossover and mutation on individuals (chromosomes) to balance the exploitation and exploration rate of search.

Table 1 Chronological progress of the conducted researches on chaos-enhanced evolutionary computing

References	Algorithm	Contribution
Chen and Aihara (1995)	Chaotic simulated annealing (CSA)	Using CSA for training neural network model with transient chaos
Yuan et al. (2002)	Hybrid chaotic genetic algorithm (HCGA)	Implementing a variant of hybrid CGA for short-term hydro system scheduling
Yang and Chen (2002)	Chaotic genetic algorithm (CGA)	Proposing CGA with chaotic mutation for function optimization
Mingjun and Huanwen (2004)	Chaotic SA	Replacing the Gaussian distribution with chaotic sequences in SA for numerical optimization
Liu et al. (2005)	Particle swarm optimization with chaos (CPSO)	Proposing CPSO for global numerical optimization
Jiang and Bompard (2005)	Hybrid CPSO with interior search (HCPSO)	Solving reactive power optimization problems using HCPSO
Zuo and Fan (2006)	Chaos enhanced immune algorithm (CIA)	Using CIA for designing neuro-fuzzy controller method
Xiang et al. (2007)	CPSO	Integrating a chaotic map called piecewise linear chaotic map (PWLCM) with the PSO for numerical optimization
Gong and Wang (2009)	Chaotic ant colony optimization (CACO)	Using CACO for robust engineering optimization
Alatas and Akin (2009)	Chaotically encoded PSO algorithm (CENPSO)	Proposing CENPSO for efficient data mining
Alatas et al. (2009)	CPSO1–CPSO12	Proposing twelve variants of CPSO and comparing them for numerical optimization
Alatas (2010a)	Chaotic harmony search (CHS)	Performing theoretical and numerical analysis for proving the computational efficiency of CHS for both numerical and engineering optimization
Alatas (2010b)	Chaotic artificial bee colony (CABC)	Proposing CABC for global optimization
Alatas (2011)	Uniform big-bang–chaotic big-crunch (UBB–CBC)	Proposing UBB–CBC for numerical optimization
Talatahari et al. (2012)	Chaotic imperialist competitive algorithm (CICA)	Combining imperialist competitive algorithm with chaos for global optimization

Table 1 continued

References	Algorithm	Contribution
Gandomi et al. (2013a)	Chaotic firefly algorithm (CFA)	Combining FA with chaotic maps for global function optimization
Gandomi et al. (2013b)	Chaos-enhanced accelerated PSO (CAPSO)	Proposing CAPSO for global function optimization
Gandomi and Yang (2013)	Chaotic bat algorithm (CBA)	Combining BA with chaotic maps for global function optimization
Askarzadeh and Coelho (2014)	Backtracking search algorithm with Burger's chaotic map	Proposing backtracking search algorithm with Burger's chaotic map for parameter estimation of PEMFC electrochemical model
Zhu and Duan (2014)	Chaotic predator–prey biogeography-based optimization (CPPBBO)	Proposing CPPBBO for optimal path planning of Uninhabited Combat Air Vehicle (UCAV)
Chen et al. (2014)	CPSO	Developing CPSO with multi-kernel support vector machine for the multi-fault diagnosis of a roller bearing
Cheng et al. (2014)	Chaotic differential evolutionary algorithm (CDEA)	Proposing fuzzy clustering CDEA for solving a tedious resource-constrained project scheduling problem
Davendra et al. (2014)	Chaotic discrete self-organizing migrating algorithm (CDSOMA)	Proposing CDSOMA for constraint based lot-streaming flowshop scheduling problem
Coelho et al. (2014)	Chaotic evolutionary algorithm (CEA)	Proposing CEA for the multi-objective optimization of a transformer
He et al. (2014)	CDEA	Using CDEA for short-term cascaded hydroelectric system scheduling tasks
Kaveh et al. (2014)	Chaotic swarming of particles (CSP)	Developing a novel algorithm called CSP for size optimization of truss structures
Lu et al. (2014)	Chaotic differential bee colony optimization algorithm (CDBCO)	Proposing CDBCO for dynamic economic dispatch problems with valve-point effects
Senkerik et al. (2014)	CPSO and CDEA	Comparing the performance of CPSO and CDEA for optimal tuning of PID controller
Singh and Srivastava (2014)	CDEA	Proposing a novel CDEA for multiobjective reactive power management

Table 1 continued

References	Algorithm	Contribution
Tian et al. (2014)	Chaotic non-dominated sorting gravitational search algorithm (CNSGSA)	Proposing CNSGSA for multi-objective optimization of short-term hydrothermal scheduling
Kuru et al. (2015)	CPSO	Using CPSO for the determination of voltage stability boundary values in electrical power systems
Chelliah et al. (2014)	Opposition based CDEA (OCDE)	Proposition of OCDE for the coordination of directional overcurrent relays
Wang et al. (2014)	Chaotic krill herd algorithm (CKHA)	Combining KHA with chaos for global function optimization
Yuan et al. (2015)	Mutative-scale pseudo-parallel chaos optimization (MPCOA)	Proposing MPCOA for function optimization and parameter identification problems
Kuang et al. (2015)	Improved chaotic particle swarm optimization (ICPSO)	Proposing a novel support vector machine (SVM) by combining kernel principal component analysis and ICPSO for intrusion detection
Alikhani Koupaei and Hosseini (2015)	Chaotic search and Golden sectioning search (CS&GSS)	Proposing a novel double stage searching mechanism by combining chaotic local search and golden sectioning search for solving systems of nonlinear equations
Alikhani Koupaei et al. (2016)	CS&GSS	Using CS&GSS for solving multimodal optimization problems
El-Shorbagi et al. (2016)	Chaotic genetic algorithm (CGA)	Proposing CGA for solving nonlinear programming problems
Zhang et al. (2016)	CDEA	Proposing a variant of CDEA for flexible job shop scheduling
Bingol and Alatas (2016)	Chaotic league championship algorithms (CLCA)	Proposing CLCA for function optimization
Mirjalili and Gandomi (2017)	Chaotic gravitational search algorithm (CGSA)	Proposing CGSA for function optimization
Heidari et al. (2017)	Chaotic water cycle algorithm (CWCA)	Proposing CWCA for function optimization and neural network training
Li et al. (2017)	Multi-objective chaos cloud PSO (PM&CCPSO)	Proposing PM&CCPSO for berth and quay crane coordinated scheduling problem

In the next sub-section, the authors explain the steps required for implementing the considered EA.

3.2 Implementation of evolutionary algorithm

To conduct the current experiments, the authors went through the literature to extract some powerful operators suited for developing an accurate and robust EA. Over the past decades, numerous investigations have been carried out to develop powerful operators for EAs (Zhou et al. 2011). In general, the efficacy of each EA depends on the optimality/efficiency of its operators, i.e. the selection, crossover and mutation operators. As the aim of the current study is to investigate the effects of chaotic maps on the performance of EAs, it is crucial to select operators which can be easily combined with chaotic maps. On the other hand, to derive firm conclusions regarding the performance of chaotic maps, we have to ensure that the basic operators of the considered EA are quite efficient. Such facts have motivated us to search the existing literature to find acceptable types of selection, crossover and mutation operators. In what follows the section, the authors scrutinize the operators constructing the algorithmic structure of the considered EA.

3.2.1 Tournament selection

Proposed by Goldberg (1989), tournament selection is one of the most well-known and applicable types of selection mechanisms. In this approach, a pre-defined number of chromosomes are selected randomly and participate in a tournament. The winner of the tournament which is an individual with higher fitness value (as compared to the other rival individuals) is selected for the crossover operation. This can be mathematically expressed as below:

$$T\left(X_1,\ldots,X_u,\ldots,X_r\right)=X_u \;\leftrightarrow\; \max\left(fit\left(X_1\right),\ldots,fit\left(X_u\right),\ldots,fit\left(X_r\right)\right)=fit\left(X_u\right) \tag{1}$$

where T is a function indicating the output of the tournament, X represents an individual, r indicates the maximum number of chromosomes participating in the tournament mechanism, and *fit* shows the fitness function of the individuals.

In general, the tournament selection can be enumerated as a flexible technique as the selection rate can be easily tuned by changing the number of individuals participating in the tournament (r). Obviously, the more the number of individuals participating in the tournament, the higher the probability of exploitation. To be more to the point, when the number of participating individuals is large, the weak chromosomes have smaller chance to be selected as the outputs of the tournament. Consequently, the chromosomes selected for the crossover selection have lots of similar characteristics which in turn foster the exploitation (intensification) capability of EAs. The flexibility of tournament selection provides us with an opportunity to easily tune a rational balance between exploration/exploitation capabilities of the considered EA.

3.2.2 Heuristic crossover

Generally, crossover operators can be considered as a mean for increasing the intensification of EAs. In this phase, two or more chromosomes (depends on the type of crossover mechanism) exchange their information through a phenomenon called intersection. The outputs of such a procedure are the chromosomes known as off-springs. Proposed by Wright (1991), heuristic crossovers (HX) can be considered as one of the most applicable types of crossover

operators. Based on empirical experiments, it has been demonstrated that heuristic crossover can be used for solving nonlinear constraint and unconstraint problems (Michalewicz 1995; Thakur 2013). HX uses two parent chromosomes for generating off-springs. Consider that two parent chromosomes X_1 and X_2 are selected for the process. Then, the off-spring produced by HX can be determined as:

$$\xi = X_1 + \alpha\,(X_1 - X_2) \tag{2}$$

Provided that:

$$\textit{fitness}\,(X_1) > \textit{fitness}\,(X_2) \tag{3}$$

where $\xi = \{\varsigma_1, \varsigma_2, \ldots, \varsigma_D\}$ represents the resulted off-spring, $X = \{x_1, x_2, \ldots, x_D\}$ delegates the vector of parent solutions and α is a random number with uniform distribution spanning the unity [0,1].

In spite of the numerical efficacies provided by HX, it has a remarkable deficiency. Indeed, there is a possibility that the produced solution exceeds the feasible ranges of the solution domain (i.e. $\varsigma_i > x_i^U$ or $\varsigma_i < x_i^L$). In such a situation, it is mandatory to devise a technique which can guide the exceeding solutions towards the feasible domain. The salient asset of HX lies in its simplicity. As it can be inferred, the mathematical steps and criteria required for implementing HX are not demanding in comparison with the other types of crossover operators such as Laplace crossover (Deep and Thakur 2007) and simulated binary crossover (Deb and Agrawal 1995).

3.2.3 Arithmetic graphical search mutation

Goldberg's arithmetic graphical search (AGS) mutation is a self-adaptive mutation operator which has found its place in the realm of evolutionary computation (Goldberg 1989). The adaptive instinct of AGS helps EA to dynamically set a proper balance between exploitation/exploration capabilities. In this regard, at the very beginning of the procedure, AGS fosters the diversification capability of EA and gradually abates the probability of mutation (which in turn decreases the diversification rate) to help the optimizer focus on specific regions to find the most optimum solution. In practice, such mutation operators have been proven to be very effective for optimizing multimodal problems (Mozaffari et al. 2012a; Fathi and Mozaffari 2014). The mathematical formulation of AGS is as follows:

$$\xi = \begin{cases} \begin{cases} X + \delta\left(t, \left(X^{ub} - X\right)\right) \\ or \\ X + \delta\left(t, \left(X - X^{lb}\right)\right) \end{cases} & \textit{if } rand < \lambda \\ X & \textit{if } rand \geq \lambda \end{cases} \tag{4}$$

where λ is a pre-defined value which verifies the chance of mutation, t is the current generation number, ξ shows the resulted chromosome (mutant solution), X shows the chromosome selected for mutation, and $\delta(x, y)$ is calculated as:

$$\delta\,(t, y) = y \times \phi \times \left(1 - \frac{t}{T}\right)^b \tag{5}$$

where T is the number of the maximum iteration, b is a random number larger than 1, and ϕ is a random number within the range of [0,1].

As it can be seen, two alternative equations are considered for the mutation operator ($rand < \lambda$). We implement the operator in a fashion that EA can randomly choose one of them for the exploration. Therefore, each time AGS could select the first equation to

conduct the exploration considering the upper bound, or select the second term and explore the solution domain with respect to lower bound values of the optimization variables.

3.2.4 The proposed boundary constraint handling strategy

As it was mentioned, there is a possibility that the solutions produced by HX and AGS operators exceed from the feasible range of the solution domain. In such cases, the optimization algorithms loose the valid trajectory over the procedure. This may result in finding invalid/impractical solutions and incurring miss-judgments. Hence, it is really necessary to devise a technique capable of controlling/correcting the movements of heuristic agents (chromosomes) over the optimization procedure. In general, such techniques are known as boundary constraint handling strategies (BCHSs).

BCHSs control the positions obtained by the produced chromosomes, and correct them when they are exceeding the admissible solution domain. Indeed, when using BCHSs, we are seeking for a controlling formulation which can detect and modify the position of the violated solutions. The modification is done by using a map which transfers the violated solutions within the admissible range of solution domain. This issue has been clearly addressed by many researchers of the swarm and evolutionary computing society, and there exist several types of such maps in the literature (Gandomi and Yang 2012; Mozaffari et al. 2013b). A previous research by the authors' research group revealed that the following formulation can result in a really powerful BCHS (Mozaffari et al. 2012a):

$$X = \begin{cases} 2 \times X^{lb} - X & if\ X < X^{lb} \\ 2 \times X^{ub} - X & if\ X > X^{ub} \\ X & otherwise \end{cases} \tag{6}$$

where X^{lb} and X^{ub} are the lower and upper bound of the solution domain, respectively. As it can be inferred, after updating each position, the validity of new chromosome is checked using the above map and necessary modifications are inflicted on the chromosome, if required. Based on rigor experimental studies, it has been observed that the above map prevents the optimizer from trapping into local optima, and therefore deters premature convergence of EAs (Tessema 2006). The 2D graphical representation of the considered BCHS is shown in Fig. 1. As seen, by using the considered BCHS, the solutions which violate the constraints (red squares) are mapped into the feasible domain (light green region).

3.2.5 Other parameters and steps

To run the EA, some controlling parameters should be taken into account. As an evolutionary based metaheuristic, the performance of the considered EA is controlled by a set of pre-defined elements such as: crossover probability (P_C), mutation probability (P_m), population size (P_S), number of generations (t), number of elite chromosomes (e), number of chromosomes participating in the tournament (r), the diversification factor of AGS mutation operator (b) and etc. To set the values of the mentioned controlling parameters, we have no choice but to conduct an experimental analysis. To encode the considered EA, the procedure given in Algorithm 1 should be fulfilled.

Now, it is important to find the most optimum values of the controlling parameters. To do so, an empirical analysis is taken into account. Table 2 indicates a set of potential values for the controlling parameters. As it can be seen, 16 different sets of the controlling parameters are considered to find out which of them can yield better results.

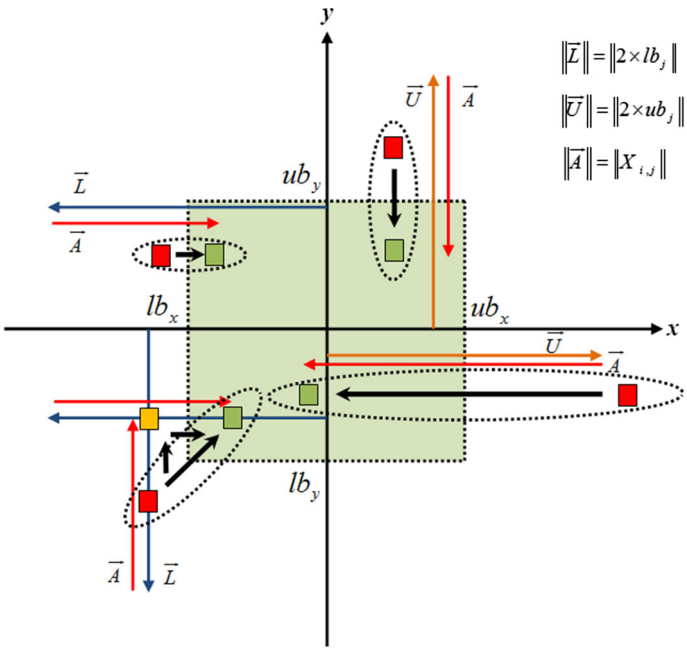

Fig. 1 Performance of the proposed boundary constraint handling technique. (Colour figure online)

Algorithm 1. Pseudo-code of the considered EA

Step 1: Set the controlling parameters, i.e. P_C, P_m, P_S, t, e, t, and b.
Step 2: Initialize the population of chromosomes P_S randomly.
Step 3: Evaluate the fitness of the generated population.
Step 4: Generation Number $= 1$.
Step 5: Perform the tournament selection to select a set of chromosomes for crossover operation.
Step 6: Perform the HX to produce off-springs (ξ) from parent chromosomes X (based on the value of P_C).
Step 7: Archive the elite solution (e) and send the other chromosomes for mutation procedure
Step 8: Apply AGS mutation to produce mutant chromosomes (ξ)
Step 9: Simulate the law of survival of the fittest by sorting the choromosomes and discarding the weak ones from the population (based on their fitness values). Obviously, at this stage, the population is updated.
Step 10: Iteration Number $=$ Iteration Number $+ 1$.
Step 11: If the Iteration Number is equal to Max-Iteration, stop the process, else go to **Step 5**.

These 16 different EAs are used for optimizing 27 different benchmark optimization problems given in "Appendix A". The performance and convergence behavior of the selected cases are considered as the evaluation metrics. The performance metric indicates the capability of the considered EAs in optimizing the benchmark problems (this is done by considering the values of objective value of the chromosomes). The convergence metric indicates the capability of considered EAs in balancing the exploration/exploitation characteristics over the optimization procedure (Mozaffari et al. 2013b). In this research, the numerical analysis is utilized to verify the impact of the considered controlling parameters on the convergence rate of the standard EAs. Obviously, the convergence rate of the chromosomes cannot be evaluated directly by using their fitness functions. Therefore, a proper formulation should

Table 2 Considered sets of the controlling parameters for the standard EA

Sets	P_C	P_m	r	b	Elitism (e)
1.	0.90	0.001	7	1.6	Yes (1)
2.	0.90	0.001	7	2.0	Yes (1)
3.	0.90	0.001	3	1.6	Yes (1)
4.	0.90	0.001	3	2.0	Yes (1)
5.	0.90	0.01	7	1.6	Yes (1)
6.	0.90	0.01	7	2.0	Yes (1)
7.	0.90	0.01	3	1.6	Yes (1)
8.	0.90	0.01	3	2.0	Yes (1)
9.	0.80	0.001	7	1.6	Yes (1)
10.	0.80	0.001	7	2.0	Yes (1)
11.	0.80	0.001	3	1.6	Yes (1)
12.	0.80	0.001	3	2.0	Yes (1)
13.	0.80	0.01	7	1.6	Yes (1)
14.	0.80	0.01	7	2.0	Yes (1)
15.	0.80	0.01	3	1.6	Yes (1)
16.	0.80	0.01	3	2.0	Yes (1)

be taken into account. Based on the results of a recent study by the authors, the following formulation is used to calculate the convergence rate of EA:

$$fitness\ (ObjVal) = \begin{cases} \frac{1}{ObjVal+1} & ObjVal > 0 \\ 1 + |ObjVal| & ObjVal < 0 \end{cases} \tag{7}$$

$$Mean\ fitness = \frac{\sum_{i=1}^{P_S} fitness(ObjVal(X_i))}{P_S} \tag{8}$$

$$Best\ fitness = \max\{fit(ObjVal(X_i))|\ i = 1, \ldots, P_S\} \tag{9}$$

$$Convergence\ rate = \frac{Mean\ fitness}{Best\ fitness} \tag{10}$$

As it can be inferred, the algorithm converges to a specific region when the value of convergence rate (CR) approaches to the proximity of 1. Therefore, the algorithm performs a diverse stochastic search when the value of CR is less than 0.3. It is expected that an efficient EA neatly balances the exploration/exploitation capabilities.

To capture the undesired effects of randomness, all of the experiments are conducted for 30 independent runs with random initial seeds, and the mean values of the considered performance evaluation metrics are reported. Initially, all of the algorithms execute the optimization with $P_S = 40$ (this value has been obtained through a complexity analysis which will be shown later in this section). The generation number (t) is set to be 1000. As the main goal of this experiment is to extract the optimum values of controlling parameters, there is no need for exposing the simple EAs to a scalable optimization framework. Hence, the experiments are conducted by considering the 50D version of the benchmark functions.

Table 3 indicates the mean performances of the standard EAs for the benchmark problems. From the results, it can be realized which sets of the controlling parameters can neatly tune the exploration/exploitation capabilities of EA. The best results are shown in bold. As seen, the best performance belongs to the 6th set of the controlling parameters. In this case, the related

EA outperforms the rival techniques for 10 benchmark functions. Along with the mentioned EA, the 14th set of the controlling parameters show promising results, as it outperforms the rival techniques 8 times.

To ensure the authenticity of the 6th scenario and also avoid any miss-judgment, the second performance evaluation criterion, i.e. convergence analysis, should be taken into account. We claim that the 6th set of the controlling parameters is most optimal if and only if it can show acceptable convergence behavior. To be more to the point, if the exploration/exploitation of chromosomes of the population is deliberate, without any doubt, the 6th scenario yields the most efficient values of the controlling parameters for the EA. Given the mathematical formulations provided, the authors visualize the real-time convergence behavior of the selected EAs in Fig. 2. From the figure, it can be easily inferred that in most of the cases, the selected EA is able to balance its exploration/exploitation capabilities over the optimization procedure. Apparently, at the very beginning of the optimization process, the heuristic agents are diffused over the solution domain and thus, the convergence of EA is really low. However, after a number of iterations, the heuristic agents concentrate on a specific region to exploit for the global optimum solution, and finally the convergence rate approaches the value of 1. This implies that the heuristic agents successfully converge to a unique solution. An interesting observation pertains to the amplitude of the convergence during the process. By checking the benchmark problems, it can be interpreted that when the problem is multimodal, the heuristic agents have an attitude towards exploring a larger domain to avoid trapping into local pitfalls. In the case of uni-modal benchmark problems, a direct ascending behavior can be seen. In such a case, the heuristic agents of EA gradually decrease their distances and converge to a unique solution. As a general remark, it can be expressed that the selected values of the controlling parameters (the 6th set) are not only able to show an acceptable performance, but also can manage the exploration/exploitation capabilities of the chromosomes in order to find the global optimum solutions.

After verifying the optimum values of the controlling parameters, we have to check whether the population size of 40 is the best choice for the experiments. To this aim the both computational complexity and performance should be taken into account. This lets us obtain a logical trade-off between the accuracy and complexity of the EA. In this research, time complexity is used as a mean for evaluating the computational complexity of EAs of different population sizes. The mathematical equations required for implementing the time complexity criterion is given below (Fathi and Mozaffari 2013):

$$Time\_Complexity = \frac{\hat{\tau}_2 - \tau_1}{\tau_0} \tag{11}$$

where τ_0 is the code execution time for 200,000 evaluations of the programming operators, i.e. %, $\times$, +, $-$, $\hat{}$, /, exp, and *ln*, on a simple 2 dimensional vector, τ_1 is the required time for 200,000 function evaluations and $\hat{\tau}_2$ is the mean of 30 execution times.

This time, the experiments are carried out by the population sizes of 20, 40, 60, 80 and 100. Note that for all of the cases, the 6th set of the controlling parameters is used. As in this case, the difference of EAs only refers to the population size, there is no need for a rigor experimental study. For the sake of brevity, the analysis is conducted using f_1, f_6, f_{12}, f_{19} and f_{27} benchmarks. Table 4 lists the obtained results. As it can be seen, for the most of the benchmark problems, the performance of EA with 40 chromosomes is better than the other cases. It seems that the interactions of this amount of heuristic agents through different operators of EA can be really useful for the function optimizations. By taking the results of time complexity into account, one interesting point can be observed. As it can be seen, for most of the cases, the time complexity of EA with a population size of 20 is higher than

Table 3 Mean performances of the standard EAs for benchmark problems

	Set 1	Set 2	Set 3	Set 4	Set 5	Set 6	Set 7	Set 8	Set 9	Set 10	Set 11	Set 12	Set 13	Set 14	Set 15	Set 16
f_1	0.1233	0.2741	0.1389	0.0680	0.0049	0.0025	0.0202	**0.0070**	0.0684	0.0532	0.4579	0.4777	0.0078	0.0039	0.0290	0.0077
f_2	0.0443	0.0083	0.0299	0.0124	0.0009	**0.0006**	0.0016	0.0012	0.0251	0.0866	0.0098	0.0810	0.0036	0.0010	0.0042	0.0032
f_3	−1.259	−1.262	−3.498	−1.262	−3.500	**−3.500**	**−3.500**	**−3.500**	−1.259	**−3.500**	−3.490	−1.259	−1.262	−1.023	**−3.500**	−3.500
f_4	6.56E+4	2.36E+4	1383	573	13.68	4.082	23.8	**2.88**	2610	289.2	498.2	1.12E+5	4.24	3.911	1072	7.538
f_5	−33.64	−31.73	−32.03	−33.28	**−38.89**	−37.98	−38.17	−37.35	−33.68	−31.66	−32.19	−35.09	−38.48	−38.74	−37.58	−36.69
f_6	0.2318	0.4822	0.2049	0.2990	0.0018	**0.0001**	0.0055	0.0024	0.5330	0.1480	0.6205	0.3946	0.0016	0.0003	0.0143	0.0039
f_7	0.2579	0.3473	0.0765	0.1966	0.0124	**0.0123**	0.0420	0.0320	0.0213	0.2987	0.2044	0.1049	0.0247	0.1193	0.1795	0.0322
f_8	5.3E−5	9.9E−6	0.0014	2.3E−5	1.9E−6	**1.8E−7**	2.1E−6	9.7E−7	8.0E−5	5.6E−5	8.6E−5	0.0001	1.1E−6	2.1E−7	5.1E−6	2.1E−6
f_9	−36.56	−39.12	−37.76	−36.79	−38.70	−37.22	−38.83	−41.28	−33.63	−36.82	−37.49	−33.20	−40.28	−38.99	**−41.66**	−35.81
f_{10}	0.0032	0.0008	0.0020	0.0007	3.0E−5	**2.7E−6**	6.9E−5	2.6E−5	0.0106	0.0027	0.0069	0.0025	5.8E−5	1.0E−5	9.1E−5	8.3E−5
f_{11}	0.0008	0.0002	0.0005	0.0004	6.5E−6	2.1E−6	2.6E−5	3.1E−6	0.0004	0.0002	0.0006	6.0E−5	3.8E−6	**1.5E−6**	3.5E−5	9.0E−6
f_{12}	−46.35	−45.41	−45.71	−45.79	−47.80	−47.66	−47.41	−47.45	−45.26	−45.36	−44.35	−46.01	**−48.08**	−47.35	−47.54	−47.23
f_{13}	5.7E+4	2.1E+5	5.1E+4	1.2E+5	4.3E+4	6.8E+4	**2.5E+4**	3.7E+4	2.0E+5	7.9E+4	1.0E+5	1.8E+5	5.6E+4	8.9E+4	4.8E+4	7.9E+4
f_{14}	−9.9E−7	−6.7E−6	−1.2E−5	−6.2E−5	−1.2E−5	−6.2E−5	**−0.0002**	**−0.0002**	−6.6E−6	−1.7E−5	−1.2E−5	−2.3E−5	−1.2E−5	−1.2E−5	−0.0005	−6.2E−5
f_{15}	9.796	8.148	7.835	7.401	8.047	7.544	6.609	6.754	8.427	8.383	8.892	8.328	7.132	7.029	5.770	**5.614**
f_{16}	−9.0E+9	−8.6E+9	−8.0E+9	−7.3E+9	−9.9E+9	**−9.9E+9**	−9.8E+9	−9.7E+9	−8.7E+9	−8.3E+9	−8.1E+9	−7.2E+9	**−9.9E+9**	**−9.9E+9**	−9.8E+9	−9.7E+9

Table 3 continued

	Set 1	Set 2	Set 3	Set 4	Set 5	Set 6	Set 7	Set 8	Set 9	Set 10	Set 11	Set 12	Set 13	Set 14	Set 15	Set 16
f_{17}	1.008	1.001	1.002	**1.000**	**1.000**	**1.000**	**1.000**	**1.000**	1.003	**1.000**	1.003	1.001	**1.000**	**1.000**	**1.000**	**1.000**
f_{18}	4.3E−8	7.9E−10	4.1E−9	1.9E−7	5.6E−13	5.0E−14	2.3E−11	2.2E−12	3.5E−8	2.2E−10	6.2E−8	7.9E−9	1.6E−12	**2.5E−14**	2.8E−11	8.2E−12
f_{19}	7.032	7.059	8.246	15.980	0.001	0.995	0.004	0.001	9.206	11.050	14.140	15.020	0.0016	**0.0006**	0.0047	1.993
f_{20}	865.4	2462	427.6	258.6	36.25	**19.12**	105.6	118.1	146.5	1424	417.7	145.8	140.4	329.4	192.1	136
f_{21}	4.6	4.6	3.3	4.4	1.9	1.2	2.0	2.0	4.0	4.5	3.6	3.8	2.2	1.3	1.7	1.4
f_{22}	−1.7E+4	−1.7E+4	−1.6E+4	−1.7E+4	−1.8E+4	−1.8E+4	−1.8E+4	−1.8E+4	−1.8E+4	−1.7E+4	−1.7E+4	−1.6E+4	−1.8E+4	**−1.9E+4**	−1.8E+4	−1.8E+4
f_{23}	3.2E+4	3.1E+4	8066	1.0E+4	**3675**	4067	4859	4934	2.2E+4	1.9E+4	1.0E+4	1.4E+4	1.1E+4	8427	8393	3783
f_{24}	27.27	25.45	19.2	17.52	0.930	**0.762**	1.175	1.314	22.44	25.99	18.76	21.68	1.192	0.7645	1.448	1.173
f_{25}	0.2674	0.0784	0.1770	0.1535	0.0137	0.0079	0.0295	0.0174	0.1281	0.0860	0.1726	0.2320	0.0109	**0.0074**	0.0275	0.0210
f_{26}	329.9	573.7	289.3	323.8	106.3	293.7	109.0	**97.9**	447.1	474.0	265.8	220.5	103.2	138.7	107.8	126.2
f_{27}	−9E+56	−7E+56	−3E+56	−4E+56	−1E+57	−7E+56	−1E+57	−1E+57	−1E+56	−3E+56	−5E+55	−9E+56	**−2E+57**	**−2E+57**	−1E+57	−4E+56

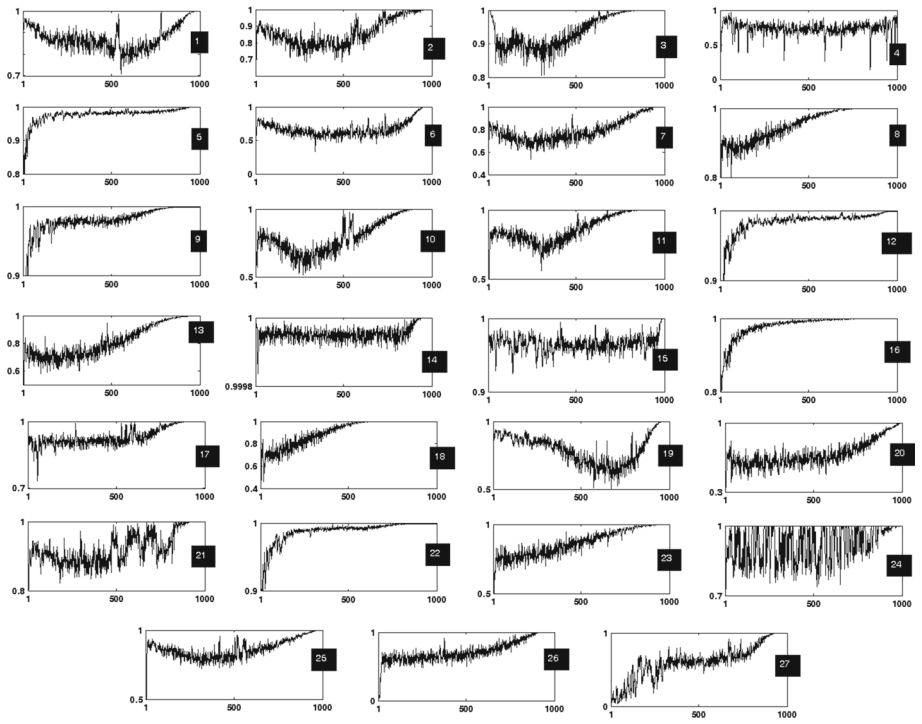

Fig. 2 Convergence behavior of the standard EA with 6th set of controlling parameters for the benchmark problems

the other cases. The reason to this phenomenon should be sought within the algorithmic functioning of EA. Obviously, when the number of chromosomes is low, EA should activate the operators much more than that required for larger number of heuristic agents. To be more to the point, for example, in our case, we have to continue the optimization for 200,000 function evaluations. For a convenient interpretation, let us consider that EA works with HX crossover operator (a pure crossover based metaheuristic). In such a condition, when the number of chromosomes is large (e.g. 100), we can comply with that number of function evaluations by activating the operators for 2000 times. However, for the lower numbers of chromosomes (e.g. 20), the same procedure requires at least 10,000 times of HX activation. Therefore, the computational time of the EA is higher when the number of chromosomes is low. Based on the results obtained, it can be seen that the time complexity of EA with 20 chromosomes is remarkably higher than other scenarios. But, for the other cases, the time complexities are really close. Considering the results of complexity and performance in tandem, it can be seen that the EA with a population size of 40 yields the most promising results (the best performance at the cost of logical computational complexity). Therefore, this number of heuristic agents is considered for the rest of the experiments.

Based on the conducted experiments, the following remarks can be reported regarding the effect of the controlling parameters on the performance of EA:

(1) The results indicated that for the crossover probability of 0.9, the mutation probability of 0.01, and the tournament selection with 7 participants, the EA can show really acceptable results in terms of the both accuracy and convergence behavior. As the number of

Table 4 Performance and complexity of the EAs of different population sizes

P_C	P_m	r	b	Elitism (e)	P_S	Performance	T_0	T_1	T_2	Complexity
f_1										
0.90	0.01	7	2.0	Yes (1)	20	0.0093	0.917616	0.855882	3.017600	2.355798
0.90	0.01	7	2.0	Yes (1)	40	0.0095	0.917616	0.855882	2.646621	1.951512
0.90	0.01	7	2.0	Yes (1)	60	0.0097	0.917616	0.855882	2.713664	2.024575
0.90	0.01	7	2.0	Yes (1)	80	0.0097	0.917616	0.855882	2.870730	2.195742
0.90	0.01	7	2.0	Yes (1)	100	0.0105	0.917616	0.855882	2.905893	2.234062
f_6										
0.90	0.01	7	2.0	Yes (1)	20	0.0033	0.917616	0.573811	2.532927	2.135006
0.90	0.01	7	2.0	Yes (1)	40	0.0036	0.917616	0.573811	2.474313	2.071133
0.90	0.01	7	2.0	Yes (1)	60	0.0039	0.917616	0.573811	2.364886	1.951879
0.90	0.01	7	2.0	Yes (1)	80	0.0038	0.917616	0.573811	2.428294	2.020979
0.90	0.01	7	2.0	Yes (1)	100	0.0038	0.917616	0.573811	2.574341	2.180139
f_{12}										
0.90	0.01	7	2.0	Yes (1)	20	−48.5623	0.917616	1.409868	5.786652	4.769734
0.90	0.01	7	2.0	Yes (1)	40	−47.3126	0.917616	1.409868	4.586607	3.461948
0.90	0.01	7	2.0	Yes (1)	60	−45.8673	0.917616	1.409868	4.349527	3.203583
0.90	0.01	7	2.0	Yes (1)	80	−46.5324	0.917616	1.409868	4.309354	3.159803
0.90	0.01	7	2.0	Yes (1)	100	−45.9231	0.917616	1.409868	3.986649	2.808126
f_{19}										
0.90	0.01	7	2.0	Yes (1)	20	0.2015	0.917616	0.721841	2.891193	2.364117
0.90	0.01	7	2.0	Yes (1)	40	0.2012	0.917616	0.721841	2.746737	2.206692
0.90	0.01	7	2.0	Yes (1)	60	0.2014	0.917616	0.721841	2.642932	2.093567
0.90	0.01	7	2.0	Yes (1)	80	0.2017	0.917616	0.721841	2.823120	2.289933
0.90	0.01	7	2.0	Yes (1)	100	0.2016	0.917616	0.721841	2.882399	2.354534
f_{27}										
0.90	0.01	7	2.0	Yes (1)	20	−1.44E57	0.917616	4.561460	6.878240	2.524782
0.90	0.01	7	2.0	Yes (1)	40	−1.44E57	0.917616	4.561460	6.561023	2.179085
0.90	0.01	7	2.0	Yes (1)	60	−1.43E57	0.917616	4.561460	6.608019	2.235034
0.90	0.01	7	2.0	Yes (1)	80	−1.43E57	0.917616	4.561460	6.777577	2.415081
0.90	0.01	7	2.0	Yes (1)	100	−1.43E57	0.917616	4.561460	6.593092	2.214033

chromosomes participating in the tournament is relatively high, the EA tends to perform exploitive search over the procedure. It is also worth noting that the AGS mutation guarantees the exploration of the EA, as well.

(2) It was observed that the selected set of controlling parameters enables EA to efficiently balance its exploration/exploitation capabilities over the procedure. As it can be seen from Fig. 2, based on the characteristics of the problem, the heuristic agents show explorative behavior to effectively search the solution space, and finally perform an intensive exploitation to find the global optimum solution.

(3) Through conducting a deliberate trade-off among the computational complexity and the computational capability of the EA, the authors have been enabled to find the most optimum number of heuristic agents (chromosomes). The results indicated that by using

the optimum values of the controlling parameters and a relatively low number of chromosomes, we are able to effectively execute the optimization without consuming a remarkable amount of the computational budget.

(4) By finding the most efficient characteristics of the standard EA, we are now able to reliably investigate the effects of chaotic maps, and find out whether they can be useful for improving the exploration/exploitation capabilities of EA.

3.3 Embedding chaos into the structure of EA

In our implementation, the chaotic maps are replaced with a random parameter (α) in the HX crossover and *rand* AGS mutation operators. This allows us evaluate the performances of crossover and mutation operators based on the laws of chaotic sequences, and also, find out whether devising such a policy can improve the searching capabilities of the resulting algorithm. As it was mentioned, the main purpose of using chaotic maps instead of the stochastic random parameter is to find out whether deterministic nonlinear systems capable of producing randomness have positive impacts on the exploration/exploitation capability of EAs. As a dynamic system, the output of chaotic maps (ψ) at generation $t+1$ depends on its value at the current generation t. Let us embed chaos into the structure of HX and AGS operators.

(a) Modified chaotic crossover operator: the mathematical formulation of the modified crossover operator combined with chaotic sequences is given by:

$$\xi = X_1 + \psi(t).(X_1 - X_2) \tag{12}$$

where ψ represents a chaotic sequence, and there is a nonlinear map (Ψ) which produces chaos as:

$$\psi(t+1) = \Psi(\psi(t)) \tag{13}$$

(b) Modified chaotic mutation operator: to modify the mutation operator, the chaotic sequence should be embedded into Eq. (5) to derive the following formulation:

$$\delta(t, y) = y \times \psi(t) \times \left(1 - \frac{t}{T}\right)^b \tag{14}$$

where, the chaotic sequence ψ can be produced based on the formulation given in Eq. (13).

Through the above steps, the chaotic versions of EA can be easily implemented. The exploitation characteristics of the CEA depend on the behavior of the embedded chaos. The mathematical formulation of chaotic maps used in the current study are given in Table 5.

As it can be seen, for each of the above maps, there exists a specific function Ψ which produces chaotic sequences. As an example, for the logistic map, this function can be written as $\Psi(\psi(t)) = \alpha\psi(t)(1-\psi(t))$. In our study, the output of Ψ function is confined within the range of unity. The shape of this iterative function for Chebyshev, logistic, sine and sinusoidal maps are shown in Fig. 3. The salient asset of using the considered maps lies in the bifurcation they are able to produce. In general, the chaotic behavior enables the considered maps to create deterministic randomness suited for evolutionary computation.

Table 5 Mathematical formulation of the considered chaotic maps

Map	Mathematical formulation
(1) Chebyshev map (Huang 2012)	$\psi(t+1) = \cos(t \cos^{-1} \psi(t))$
(2) Circle map (Fourcade and Tramblay 1990)	$\psi(t+1) = \psi(t) + b - (a/2\pi)\sin(2\pi\psi(t)) \bmod (1)$
(3) Gauss/mouse map (Gandomi et al. 2013a)	$\psi(t+1) = \begin{cases} 0 & \psi(t) = 0 \\ 1/\psi(t) \bmod (1) & otherwise \end{cases}$ where $1/\psi(t) \bmod (1) = \frac{1}{\psi(t)} - \left\lfloor \frac{1}{\psi(t)} \right\rfloor$
(4) Liebovitch map (Tavazoei and Haeri 2007)	$\psi(t+1) = \begin{cases} \alpha\psi(t) & 0 < \psi(t) < \nu_1 \\ \frac{\nu_2 - \psi(t)}{\nu_2 - \nu_1} & \nu_1 < \psi(t) < \nu_2 \\ 1 - \beta(1 - \psi(t)) & \nu_2 < \psi(t) < 1 \end{cases}$ where $\alpha = \frac{\nu_2}{\nu_1}(1 - (\nu_2 - \nu_1))$ and $\beta = \frac{1}{\nu_2 - 1}((\nu_2 - 1) - \nu_1(\nu_2 - \nu_1))$
(5) Logistic map (Devaney 1987)	$\psi(t+1) = \alpha\psi(t)(1 - \psi(t))$ where α is equal to 4 and the initial value of the chaotic sequence (ψ_0) can be any value within the range of unity except {0, 0.25, 0.5, 0.75, 1}
(6) Piecewise map (Xiang et al. 2007)	$\psi(t+1) = \begin{cases} \frac{\psi(t)}{\nu} & 0 < \psi(t) < \nu \\ \frac{\psi(t) - \nu}{0.5 - \nu} & \nu < \psi(t) < 0.5 \\ \frac{1 - \nu - \psi(t)}{0.5 - \nu} & 0.5 < \psi(t) < 1 - \nu \\ \frac{1 - \psi(t)}{\nu} & 1 - \nu < \psi(t) < 1 \end{cases}$ where $0 < \nu < 0.5$
(7) Sine map (Devaney 1987)	$\psi(t+1) = \frac{\alpha}{4}\sin(\pi\psi(t))$ where $0 < \alpha \leq 4$
(8) Sinusoidal map (Devaney 1987)	$\psi(t+1) = \alpha\psi(t)^2 \sin(\pi\psi(t))$ where α and ψ_0 are equal to 2.3 and 0.7, respectively
(9) Tent map (Devaney 1987)	$\psi(t+1) = \begin{cases} \frac{\psi(t)}{7} & \psi(t) < 0.7 \\ \frac{10}{3}(1 - \psi(t)) & \psi(t) \geq 0.7 \end{cases}$

4 Results and discussion

4.1 Experimental setup

Before describing the results, some parameters required for experimental procedures should be discussed. For the experiments, the standard EA and 18 chaotic CEAs (9 CEAs with chaotic crossovers and 9 CEAs with chaotic mutations) are taken into account. The selected test bed consists of 27 numerical benchmarks of different landscapes, difficulties and multimodalities. As the characteristics of the selected test bed is really exhaustive, the derived conclusions can be reliably extended for other applications. The selected benchmarks can be found in "Appendix A".

To evaluate the scalability of the considered chaotic maps, three different dimensions, namely 50, 100 and 200, are taken into account. The rival optimization techniques are compared in terms of the performance, robustness, success and complexity. As the algorithmic

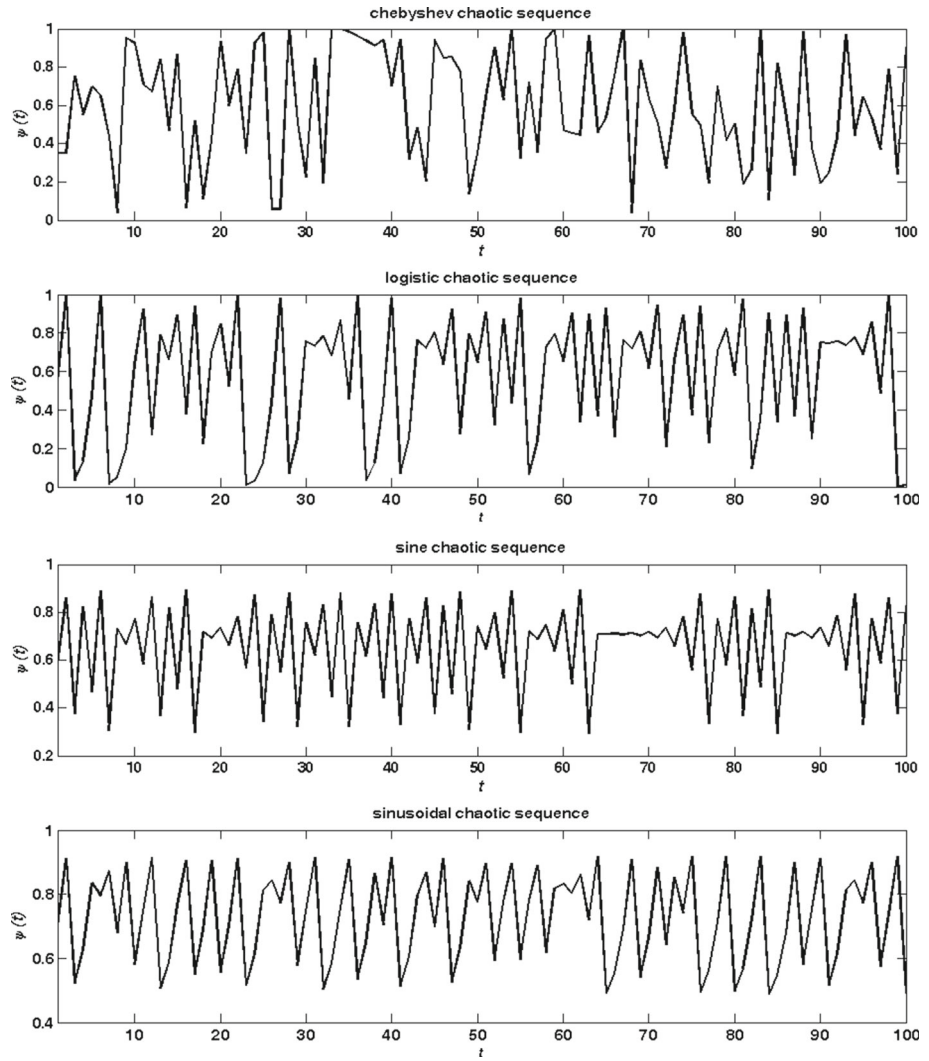

Fig. 3 Iterative chaotic sequences of the Chebyshev, logistic, sine and sinusoidal chaotic maps

functioning of the basic EA is constant, the results of time complexity let us discern the most computationally efficient CEAs. The population size (P_S) of all of the rival algorithms is set to be 40, and the concept of elitism is applied to all of the rival algorithms. The crossover and mutation probabilities are equal to 0.9 and 0.01, respectively. In the tournament selection phase, 7 chromosomes are randomly chosen to participate in the competition, and the diversification factor of AGS mutation (b) is set to be 2.

All of the optimizations are conducted for 1000 iterations. To capture the undesired effects of stochastic optimizations, all of the identification scenarios are conducted for 30 independent runs and the mean, best, worth and standard deviation values are reported. Also, to make sure that the obtained results are unbiased, for each of the optimization scenarios, the starting point (initialization) is taken the same. Thus, all of the algorithms start searching the solution landscape with the same initial condition. All of the algorithms are implemented

in the MATLAB software, and the computational procedures are conducted on a PC with a Pentium IV, Intel Dual core 2.2 GHz and 2 GBs RAM.

4.2 Experimental results

The experimental procedures can be divided into two main parts. Most of the experiments are performed in the first sub-section which is devoted to numerical problems. To attest the authenticity of the obtained results for the real-life problems, a demanding optimization problem, i.e. optimizing the controlling parameters of a power system, is considered which is discussed in the second part of the experiment.

4.2.1 Numerical experiments

In this subsection, the effects of the CEAs with the proposed boundary constraint handling technique are investigated. Through an exhaustive study, the authors will draw some conclusions regarding the impact of the chaotically encoded HX and AGS operators on the performance of the algorithm. The first three stages of the experiment are devoted to the evaluation of the robustness and accuracy of the rival methods for medium scale, semi large-scale, and large-scale benchmark optimization problems. Thus, the results will examine the robustness and accuracy of the algorithms as well as their potentials to be used for the optimization problems of different scales (scalability). Then, based on the results obtained in the previous stags, in the fourth stage of the experiment, the real-time evolution and scalability of the rival methods are tested. The last two stages of the experiment are devoted to analyzing the convergence and time complexity of the rival techniques.

4.2.1.1. Chaotic crossover and mutation: medium scale benchmarks Tables 6 and 7 indicate the statistical results obtained by the rival techniques with chaotically encoded HX operators for the 50D version of the considered benchmark problems. For convenience, in the rest of the section, the best obtained results among the rival algorithms are shown in a bold format. From these two tables, one can easily see that the sinusoidal version of CEA outperforms the other optimizers. Along with the sinusoidal CEA, the logistic and sine versions of CEA show acceptable results too. The success of the other versions of CEAs is not remarkable for the 50D version of the benchmark problems.

Tables 8 and 9 list the statistical results obtained by the rival techniques with chaotically encoded AGS mutation operators for the 50D version of the considered benchmark problems. One of the general observations is that embedding the chaotic maps into the structure of AGS mutation further improves the performance of CEAs as compared to those using the chaotic maps in their HX crossover operator. Indeed, for most of the benchmarks, the obtained mean values are less than those reported in Tables 6 and 7. It can be also observed that for this case, the best performance belongs to the Gauss–Mouse and logistic maps. The piecewise and Liebovitch maps also have acceptable performances as compared to the other maps.

By comparing the results of mutation and crossover experiments, it can be realized that the sinusoidal map which worked well for the crossover operator cannot provide promising results for the mutation operator. This brings us to the conclusion that, at least for the medium scale benchmarks, the logistic map can afford relatively better solutions for the both mutation and crossover experiments. The robustness criterion is the other important element which should be analyzed. Taking the std. values into account, it can be seen that in most of the cases for both mutation and crossover experiments, the robustness of all versions of CEAs is really close. However, it sounds that the circle, Gauss–Mouse and sinusoidal versions of CEAs

Table 6 Statistical results of the optimizations for 50D version of benchmarks ($f_1 - f_{14}$)

Crossover tests	f_1	f_2	f_3	f_4	f_5	f_6	f_7	f_8	f_9	f_{10}	f_{11}	f_{12}	f_{13}	f_{14}
Chebyshev CEA														
Mean	0.0105	0.0016	−3.0524	7.6118	−35.881	0.0067	0.0279	1.26E−6	−38.337	4.80E−5	1.01E−5	−47.263	**31, 235**	−0.0001
Min	0.0089	0.0010	−3.4999	2.3781	−36.278	0.0032	0.0004	8.60E−7	−39.907	3.09E−5	6.43E−6	−47.404	5483	−0.0005
Max	0.0123	0.0027	−1.2624	12.5435	−35.509	0.0112	0.0736	1.78E−6	−36.581	6.90E−5	1.44E−5	−47.159	67,315	−4.88E−6
Std.	0.0015	0.0006	1.00067	4.5216	0.3413	0.0031	0.0299	4.36E−7	1.2838	1.64E−5	2.99E−6	0.1098	22, 397	0.0002
Circle CEA														
Mean	0.0167	0.0023	−3.4999	13.4141	−36.81	0.0105	0.0307	3.15E−6	−39.096	9.84E−5	2.52E−5	−47.092	62,551	−0.0001
Min	0.0147	0.0013	−3.4999	6.6675	−37.856	0.0057	0.0009	1.82E−6	−41.731	6.40E−5	1.34E−5	−47.424	13,126	−0.0004
Max	0.0178	0.0036	−3.4999	17.1461	−35.272	0.0135	0.0720	4.89E−6	−36.111	0.00014	6.00E−5	−46.477	109,501	−6.22E−5
Std.	0.0012	0.0008	4.2E−6	3.9820	0.9948	0.0029	0.0277	1.11E−6	2.0018	3.30E−5	1.96E−5	0.3737	38, 562	0.0001
Gauss–Mouse CEA														
Mean	0.0087	0.0010	−3.4999	5.2657	−36.487	0.0024	0.0198	6.35E−7	−39.526	2.61E−5	9.01E−6	−47.195	47,172	−0.0002
Min	0.0050	0.0007	−3.5000	1.8939	−37.559	0.0011	0.0003	3.72E−7	−41.284	1.87E−5	6.81E−6	−47.519	24,847	−0.0004
Max	0.0116	0.0015	−3.4999	11.525	−35.576	0.0047	0.0491	8.80E−7	−37.414	3.52E−5	1.06E−5	−46.838	94,775	−6.22E−5
Std.	0.0026	0.0003	2.74E−6	3.9602	0.7317	0.0014	0.0185	2.24E−7	1.3997	5.91E−6	1.62E−6	0.2669	29, 896	0.0001
Liebovitch CEA														
Mean	0.0076	0.0014	−3.0500	5.2735	−36.200	0.0013	0.0665	5.01E−7	−38.446	2.18E−5	4.52E−6	−47.105	66,956	−0.0004
Min	0.0054	0.0009	−3.5000	3.8207	−38.200	0.0011	0.0001	3.04E−7	−39.459	1.37E−5	2.36E−6	−47.491	30,355	−0.0020
Max	0.0122	0.0026	−1.2600	7.2231	−34.300	0.0016	0.1511	8.18E−7	−36.800	3.50E−5	7.42E−6	−46.790	103,174	−1.74E−5
Std.	0.0027	0.0006	1.0007	1.7116	1.7900	0.0022	0.0668	2.09E−7	1.2173	7.92E−6	1.96E−6	0.3002	27, 421	0.0009
Logistic CEA														
Mean	0.0059	0.0012	−3.0524	5.0740	−35.784	0.0013	0.0661	2.85E−7	−39.927	1.19E−5	5.49E−6	−47.265	51,613	−0.0001
Min	0.0051	0.0007	−3.5000	1.4251	−36.275	0.0006	0.0099	1.99E−7	−41.586	7.62E−6	1.98E−6	−47.475	25,369	−0.0004
Max	0.0065	0.0024	−1.2624	10.3114	−35.016	0.0021	0.1572	4.14E−7	−39.146	2.38E−5	1.26E−5	−47.054	66,952	−1.27E−5
Std.	0.0005	0.0007	1.0007	3.7623	0.4896	0.0006	0.0648	8.55E−8	1.0261	6.79E−6	4.18E−6	0.1801	16, 982	0.0001

Table 6 continued

Crossover tests	f_1	f_2	f_3	f_4	f_5	f_6	f_7	f_8	f_9	f_{10}	f_{11}	f_{12}	f_{13}	f_{14}
Piecewise CEA														
Mean	0.0106	0.0019	−3.4999	7.7757	−36.908	0.0029	0.0447	9.11E−7	−38.385	3.64E−5	8.13E−6	−47.351	33,610	−5.97E−5
Min	0.0094	0.0009	−3.5000	3.9866	−37.920	0.0010	0.0125	6.61E−7	−39.458	1.66E−5	5.29E−6	−47.561	15,029	−1.18E−4
Max	0.0114	0.0033	−3.4999	12.282	−35.473	0.0058	0.0737	1.56E−6	−36.955	5.25E−5	1.08E−5	−47.136	60,784	−1.27E−5
Std.	0.0008	0.0009	3.13E−6	3.4028	1.2435	0.0018	0.0257	3.67E−7	1.1187	1.38E−5	2.45E−6	0.18171	17, 971	5.35E−5
Sine CEA														
Mean	0.0288	0.0031	−3.4999	62.9057	−35.828	0.0242	**0.0154**	6.36E−6	−38.503	1.95E−4	6.09E−5	−47.235	72,010	−3.17E−4
Min	0.0212	0.0023	−3.4999	20.0719	−36.678	0.0107	0.0019	5.79E−6	−39.617	1.49E−4	4.40E−5	−47.518	53,463	−0.0011
Max	0.0364	0.0037	−3.4999	155.645	−34.310	0.0352	0.0336	8.00E−6	−37.148	2.75E−4	9.95E−5	−46.893	96,766	−9.22E−6
Std.	0.0053	0.0006	2.62E−5	55.9519	0.9532	0.0098	0.0114	9.21E−7	1.0595	5.05E−5	2.34E−5	0.2677	17, 611	4.47E−4
Sinusoidal CEA														
Mean	**0.0049**	0.0013	−2.6049	14.549	**−37.370**	0.0008	0.0470	**2.70E−7**	**−40.040**	**7.14E−6**	**2.78E−6**	**−47.460**	68, 483	−8.78E−6
Min	0.0037	0.0007	−3.5000	1.5536	−38.306	0.0003	0.0125	8.40E−8	−42.943	5.11E−6	1.21E−6	−48.087	1816	−1.74E−5
Max	0.0056	0.0025	−1.2624	49.881	−35.856	0.0013	0.1159	3.78E−7	−37.374	9.49E−6	3.99E−6	−47.052	89,244	−3.55E−6
Std.	0.0007	0.0007	1.2255	20.071	1.0046	0.0004	0.0399	1.12E−7	2.5727	1.88E−6	1.17E−6	0.4221	37, 403	6.10E−6
Tent CEA														
Mean	0.0100	0.0013	**−3.4999**	25.458	−35.526	0.0023	0.0326	7.98E−7	−39.480	3.17E−5	6.30E−6	−47.389	50,232	**−4.90E−4**
Min	0.0084	0.0007	−3.5000	2.5869	−36.192	0.0013	0.0124	5.75E−7	−40.840	2.60E−5	5.00E−6	−47.627	10,135	−0.0015
Max	0.0121	0.0020	−3.4999	74.418	−34.957	0.003	0.0446	1.16E−6	−37.263	4.09E−5	8.52E−6	−47.127	87,979	−3.29E−5
Std.	0.0014	0.0005	1.81E−6	28.320	0.5231	0.0009	0.0126	2.63E−7	1.3795	6.10E−6	1.44E−6	0.1970	27, 836	6.02E−4
Standard EA														
Mean	0.0095	0.0014	−3.4999	**4.8757**	−36.170	0.0036	0.0340	7.64E−7	−37.808	2.37E−5	8.75E−6	−47.312	44, 008	−2.88E−4
Min	0.0069	0.0009	−3.4999	2.9039	−38.366	0.0021	9.2E−5	3.94E−7	−40.084	1.44E−5	6.71E−6	−47.718	21,216	−7.94E−4
Max	0.0124	0.0019	−3.4999	6.4951	−34.846	0.0056	0.1446	1.09E−6	−35.750	3.31E−5	1.30E−5	−47.150	68,161	−2.40E−5
Std.	0.0024	0.0004	5.53E−6	1.5650	1.5105	0.0014	0.0620	2.74E−7	1.8409	7.27E−6	2.45E−6	0.2325	17, 632	3.22E−4

Table 7 Statistical results of the optimizations for 50D version of benchmarks ($f_{15} - f_{27}$)

Crossover tests	f_{15}	f_{16}	f_{17}	f_{18}	f_{19}	f_{20}	f_{21}	f_{22}	f_{23}	f_{24}	f_{25}	f_{26}	f_{27}
Chebyshev CEA													
Mean	7.7551	−9.7E9	1.00002	1.30E−11	0.9975	230.91	1.9598	− 18,197	5640	1.2007	0.0170	129.03	− 1.31E57
Min	6.2692	−9.7E9	1.00007	4.57E−12	0.0021	92.848	1.7998	− 1.91E4	3682	0.8445	0.0106	81.91	− 2.00E57
Max	9.5536	−9.7E9	1.00003	2.57E−11	2.9886	514.32	2.1998	− 17,534	7913	1.4279	0.0255	193.65	− 7.66E56
Std.	1.1954	2.4E7	1.0E−5	8.94E−12	1.2190	168.69	0.1516	5.45E2	1808	0.2538	0.0076	41.460	4.88E56
Circle CEA													
Mean	**6.8092**	−9.5E9	1.00004	6.83E−11	1.0006	380.72	1.7198	− 1.75E4	5349	1.1801	0.0260	107.97	− 1.20E57
Min	5.5491	−9.6E9	1.00001	2.56E−11	0.0038	112.83	1.3998	− 1.82E4	3565	0.8360	0.0222	78.803	− 2.00E57
Max	7.9874	−9.4E9	1.00008	1.32E−10	2.9942	1207.0	2.0998	− 1.69E4	6652	1.6102	0.0287	162.10	− 7.66E56
Std.	0.9972	5.3E7	2.4E−5	4.18E−11	1.2204	463.68	0.2774	6.10E2	1190	0.3021	0.0026	32.782	5.03E56
Gauss–Mouse CEA													
Mean	6.9819	−9.8E9	1.00001	2.34E−12	0.9964	151.14	1.7998	− 1.80E4	4783	0.9552	0.0134	148.21	− 1.67E57
Min	6.3651	−9.8E9	1.00008	3.51E−13	0.0008	140.34	1.5998	− 1.87E4	3805	0.8332	0.0097	64.120	− 2.00E57
Max	7.7413	−9.7E9	1.00001	6.14E−12	1.9915	160.74	2.0998	− 1.73E4	5819	1.2116	0.0175	253.63	− 1.24E57
Std.	0.6611	2.6E7	3.4E−6	2.38E−12	0.9947	7.3560	0.2121	5.43E2	755	0.1473	0.0032	70.672	3.24E56
Liebovitch CEA													
Mean	7.1398	−9.8E9	1.00001	3.13E−12	1.3940	159.06	1.9398	− 1.81E4	5838	0.9584	0.0108	106.54	**− 1.86E57**
Min	6.6346	−9.8E9	1.00000	4.34E−13	0.0008	141.24	1.9010	− 1.92E4	3853	0.7115	0.0065	75.695	− 2.54E57
Max	8.0467	−9.8E9	1.00001	9.52E−12	3.9812	195.37	2.0998	− 1.77E4	8330	1.1716	0.0149	160.07	− 7.66E56
Std.	0.5545	1.3E7	1.8E−6	3.79E−12	1.6650	22.82	0.0894	5.99E2	1635	0.1692	0.0034	33.942	6.54E56
Logistic CEA													
Mean	7.7086	−9.8E9	**1.00000**	5.96E−13	0.1996	149.46	**1.5398**	− 18,509	6939	1.1643	**0.0079**	111.69	− 1.03E57
Min	5.7444	−9.9E9	1.00000	1.81E−13	0.0003	99.80	1.1998	− 18,698	5289	0.8010	0.0056	82.687	− 1.57E57
Max	9.0268	−9.8E9	1.00000	1.22E−12	0.9957	217.92	1.7998	− 18,106	9269	1.4493	0.0137	179.93	− 6.03E56
Std.	1.4162	1.6E7	2.7E−6	4.75E−13	0.4450	42.83	0.2792	245.59	1512	0.2685	0.0033	39.815	3.84E56

Table 7 continued

Crossover tests	f_{15}	f_{16}	f_{17}	f_{18}	f_{19}	f_{20}	f_{21}	f_{22}	f_{23}	f_{24}	f_{25}	f_{26}	f_{27}
Piecewise CEA													
Mean	6.8504	−9.7E9	1.00001	5.18E−12	0.9971	**131.42**	1.7798	−17,925	5362	1.0352	0.0138	129.59	−1.71E57
Min	6.2265	−9.7E9	1.00000	2.40E−12	0.0014	90.09	1.4998	−18,106	3266	0.8557	0.0098	86.418	−3.22E57
Max	7.5357	−9.7E9	1.00002	8.73E−12	1.9928	188.43	1.9998	−17,711	6578	1.2139	0.0213	174.70	−7.66E56
Std.	0.5272	1.0E7	7.2E−6	3.11E−12	0.9952	37.84	0.1788	182.20	1375	0.1532	0.0046	38.539	9.78E56
Sine CEA													
Mean	7.3879	−9.3E9	1.00011	1.84E−10	3.5957	227.76	1.5598	−17,443	**4701**	1.1604	0.0418	**104.26**	−1.10E57
Min	6.4803	−9.3E9	1.00007	6.79E−11	0.0237	109.33	1.2998	−17,948	2874	1.0000	0.0361	81.099	−1.57E57
Max	8.0427	−9.2E9	1.00023	3.28E−10	5.9822	327.59	1.8998	−17,139	6767	1.2697	0.0469	135.89	−7.64E56
Std.	0.6357	3.6E7	6.6E−5	1.00E−10	2.2860	86.31	0.2607	332.27	1811	0.1059	0.0043	20.692	3.09E56
Sinusoidal CEA													
Mean	7.2653	**−9.9E9**	1.00001	**1.54E−13**	**0.0004**	265.84	1.5998	**−18,675**	9523	1.2315	0.0103	170.08	−1.24E57
Min	5.2262	−9.9E9	1.00000	2.87E−14	0.0002	83.81	1.2998	−19,054	6667	0.7848	0.0072	98.184	−2.00E57
Max	9.0085	−9.9E9	1.00001	3.85E−13	0.0006	894.47	1.8998	−18,225	14,556	1.6061	0.0117	222.82	−7.66E56
Std.	1.7826	8.0E6	3.2E−6	1.46E−13	0.0001	352.04	0.2449	387.42	3161	0.3419	0.0017	45.132	4.66E56
Tent CEA													
Mean	7.6771	−9.7E9	1.00001	6.06E−12	0.3999	173.30	1.7198	−17,822	5812	1.1453	0.0125	126.20	−1.03E57
Min	6.6861	−9.7E9	1.00001	1.62E−12	0.0012	139.55	1.2998	−18,106	4972	0.8733	0.0090	85.041	−1.57E57
Max	8.5293	−9.7E9	1.00002	1.81E−11	1.9918	236.53	2.0998	−17,534	7291	1.3462	0.0181	182.67	−6.03E56
Std.	0.7928	2.0E7	5.5E−6	6.77E−12	0.8899	37.08	0.3033	209.18	1028	0.2118	0.0038	35.946	3.84E56
Standard EA													
Mean	6.9642	−9.79	1.00002	4.09E−12	0.2012	164.87	1.5798	−18,217	6117	**0.9544**	0.0117	110.72	−1.44E57
Min	5.3458	−9.7E9	1.00000	1.24E−12	0.0011	139.08	1.2998	−19,054	3611	0.7343	0.0090	53.338	−2.54E57
Max	8.3444	−9.7E9	1.00003	6.62E−12	0.9974	214.70	1.7998	−17,790	9211	1.1645	0.0153	155.51	−9.74E56
Std.	1.0848	1.9E7	1.2E−5	2.26E−12	0.4450	30.25	0.2167	511.06	2417	0.1605	0.0024	43.539	6.22E56

Table 8 Statistical results of the optimizations for 50D version of benchmarks ($f_1 - f_{14}$)

Mutation tests	f_1	f_2	f_3	f_4	f_5	f_6	f_7	f_8	f_9	f_{10}	f_{11}	f_{12}	f_{13}	f_{14}
Chebyshev CEA														
Mean	0.0057	0.0025	−3.0525	7.3466	−37.4206	0.0016	0.0368	3.30E−7	−38.0667	1.37E−5	3.19E−6	**−47.7752**	90, 138	−9.94E−5
Min	0.0052	0.0018	−3.5000	2.5754	−39.0742	0.0011	0.0099	1.64E−7	−40.4648	6.01E−6	2.59E−6	−47.9702	57, 774	−2.22E−4
Max	0.0064	0.0046	−1.2624	10.8715	−36.2031	0.0026	0.0635	5.28E−7	−36.2051	3.27E−5	3.69E−6	−47.4679	114, 530	−9.22E−6
Std.	0.0005	0.0012	1.0007	3.2957	1.4402	0.0006	0.0241	1.60E−7	1.5404	1.11E−5	4.67E−7	0.1861	21, 356	7.93E−5
Circle CEA														
Mean	0.0078	0.0023	−3.5000	9.9960	−36.7703	0.0028	0.0379	6.52E−7	−38.8032	2.32E−5	6.06E−6	−47.5222	59, 617	−1.47E−4
Min	0.0048	0.0009	−3.5000	3.2673	−37.2470	0.0009	0.0001	3.00E−7	−41.5367	1.19E−5	3.13E−6	−47.7432	42, 690	−3.06E−4
Max	0.0103	0.0038	−3.5000	18.8321	−36.1068	0.0057	0.1227	1.42E−6	−36.0132	3.70E−5	9.33E−6	−47.3872	78, 566	−4.53E−5
Std.	0.0020	0.0013	0.0000	7.0949	0.5446	0.0024	0.0490	4.40E−7	2.0507	9.82E−6	2.28E−6	0.1788	15, 377	1.04E−4
Gauss–Mouse CE														
Mean	0.0034	0.0006	−3.5000	**1.8028**	−37.0501	0.0003	0.1198	1.08E−7	**−38.8617**	**2.75E−6**	5.69E−7	−47.4449	63, 443	−7.75E−5
Min	0.0020	0.0003	−3.5000	0.2229	−38.0374	0.0001	0.0708	4.02E−8	−40.7933	2.44E−6	3.37E−7	−47.5887	11, 956	−1.62E−4
Max	0.0046	0.0010	−3.5000	3.2394	−36.0000	0.0005	0.2045	1.46E−7	−37.4482	3.44E−6	9.84E−7	−47.1359	123, 727	−1.27E−5
Std.	0.0012	0.0003	0.0000	1.1629	0.7938	0.0002	0.0606	4.08E−8	1.3079	3.97E−7	2.54E−7	0.1887	40, 742	6.15E−5
Liebovitch CEA														
Mean	0.0036	0.0008	−3.0525	2.2422	−35.5449	0.0004	0.1234	1.59E−7	−38.0730	4.75E−6	1.06E−6	−47.5661	81, 915	−3.72E−5
Min	0.0016	0.0004	−3.5000	0.7755	−37.6826	0.0002	0.0123	6.91E−8	−39.1681	2.37E−6	4.85E−7	−47.8886	60, 812	−8.56E−5
Max	0.0057	0.0015	−1.2624	6.9319	−34.1354	0.0005	0.3135	2.48E−7	−36.9638	7.81E−6	1.42E−6	−47.2278	114, 155	−4.88E−6
Std.	0.0015	0.0004	1.0007	2.6436	1.3441	0.0001	0.1136	7.55E−8	0.9278	2.27E−6	3.99E−7	0.3023	21, 801	3.11E−5
Logistic CEA														
Mean	**0.0016**	**0.0005**	−2.6050	0.6660	**−38.4168**	**0.0002**	0.0944	**4.03E−8**	−37.7903	3.46E−6	**4.58E−7**	−47.5692	71, 846	−2.19E−5
Min	0.0012	0.0002	−3.5000	0.2367	−40.3261	0.0002	0.0000	1.71E−8	−41.8471	8.32E−7	1.98E−7	−47.8306	43, 339	−6.23E−5
Max	0.0025	0.0010	−1.2624	1.4534	−36.9534	0.0003	0.1388	6.24E−8	−36.2811	7.23E−6	6.52E−7	−47.2642	122, 535	−1.37E−6
Std.	0.0005	0.0003	1.2256	0.4785	1.4444	0.0001	0.0566	1.63E−8	2.3041	2.60E−6	1.96E−7	0.2101	33,891	2.40E−5

Table 8 continued

Mutation tests	f_1	f_2	f_3	f_4	f_5	f_6	f_7	f_8	f_9	f_{10}	f_{11}	f_{12}	f_{13}	f_{14}
Piecewise CEA														
Mean	0.0035	0.0009	−3.5000	3.4337	−37.1373	0.0003	**0.0339**	1.47E−7	−38.7029	1.08E−5	2.41E−6	−47.5143	**42, 546**	−4.88E−5
Min	0.0021	0.0005	−3.5000	0.2559	−38.3151	0.0001	0.0000	8.90E−8	−40.3202	3.09E−6	1.11E−6	−47.7208	23,638	−1.62E−4
Max	0.0046	0.0014	−3.5000	6.9649	−35.1513	0.0005	0.0736	2.32E−7	−37.0078	1.82E−5	4.86E−6	−47.1845	52,688	−1.27E−5
Std.	0.0010	0.0004	0.0000	2.6893	1.2781	0.0001	0.0288	5.89E−8	1.3776	6.51E−6	1.44E−6	0.2169	12,892	6.37E−5
Sine CEA														
Mean	0.0146	0.0038	−3.5000	14.5337	−36.9937	0.0034	0.0431	8.66E−7	−38.1403	4.63E−5	1.42E−5	−47.6485	97,364	−2.93E−5
Min	0.0112	0.0022	−3.5000	7.4773	−38.0394	0.0017	0.0102	6.26E−7	−39.3020	3.19E−5	9.14E−6	−47.7732	43,504	−3.29E−5
Max	0.0167	0.0060	−3.5000	21.3641	−35.2532	0.0075	0.1012	1.24E−6	−37.2366	7.78E−5	2.34E−5	−47.4593	186,063	−2.40E−5
Std.	0.0021	0.0014	0.0000	6.1433	1.1913	0.0023	0.0368	2.48E−7	0.8467	1.90E−5	5.85E−6	0.1188	54,671	4.92E−6
Sinusoidal CEA														
Mean	0.0283	0.0081	−2.6049	953.337	−37.3980	0.0519	0.0825	5.59E−6	−37.1803	2.29E−4	8.10E−5	−47.2721	12,5748	−4.94E−6
Min	0.0203	0.0055	−3.5000	23.8999	−39.9539	0.0107	0.0059	2.99E−6	−40.0460	1.33E−4	3.77E−5	−47.7804	62,330	−1.27E−5
Max	0.0467	0.0117	−1.2622	3243.75	−35.5850	0.1534	0.1710	8.70E−6	−35.8617	3.55E−4	1.60E−4	−46.3390	176,976	−1.36E−6
Std.	0.0107	0.0024	1.2256	1353.96	1.8009	0.0585	0.0671	2.09E−6	1.6628	8.90E−5	5.25E−5	0.5516	41,475	4.85E−6
Tent CEA														
Mean	0.0046	0.0007	−3.0525	4.9543	−37.5837	0.0012	0.0192	1.61E−7	−37.9036	8.49E−6	2.59E−6	−47.4812	42,955	−8.41E−5
Min	0.0030	0.0005	−3.5000	0.3769	−39.4523	0.0003	0.0000	6.65E−8	−39.5365	4.75E−6	6.76E−7	−47.6856	14,277	−2.22E−4
Max	0.0054	0.0010	−1.2624	9.4864	−35.6719	0.0034	0.0491	2.66E−7	−36.5043	1.12E−5	7.15E−6	−47.2515	73,266	−4.53E−5
Std.	0.0010	0.0002	1.0007	4.1189	1.3590	0.0013	0.0189	7.23E−8	1.2821	2.64E−6	2.62E−6	0.2013	26,957	7.77E−5
Standard EA														
Mean	0.0095	0.0014	−3.4999	4.8757	−36.17	0.0036	0.034	7.64E−7	−37.808	2.37E−5	8.75E−6	−47.312	44,008	**−2.88E−4**
Min	0.0069	0.0009	−3.4999	2.9039	−38.366	0.0021	9.2E−5	3.94E−7	−40.084	1.44E−5	6.71E−6	−47.718	21,216	−7.94E−4
Max	0.0124	0.0019	−3.4999	6.4951	−34.846	0.0056	0.1446	1.09E−6	−35.75	3.31E−5	1.30E−5	−47.15	68,161	−2.40E−5
Std.	0.0024	0.0004	5.53E−6	1.565	1.5105	0.0014	0.062	2.74E−7	1.8409	7.27E−6	2.45E−6	0.2325	17,632	3.22E−4

Table 9 Statistical results of the optimizations for 50D version of benchmarks ($f_{15} - f_{27}$)

Mutation tests	f_{15}	f_{16}	f_{17}	f_{18}	f_{19}	f_{20}	f_{21}	f_{22}	f_{23}	f_{24}	f_{25}	f_{26}	f_{27}
Chebyshev CEA													
Mean	7.1924	**−9.98E+9**	1.000009	4.36E−13	0.00108	113.1904	1.7999	−19,030.4	8254	1.0269	0.0112	135.5061	−1.36E+57
Min	6.2226	−9.98E+9	1.000004	1.06E−13	0.00048	73.3437	1.4999	−19,527.9	6160	0.7886	0.0082	87.1970	−2.00E+57
Max	8.5357	−9.98E+9	1.000013	8.30E−13	0.00238	143.5666	2.1999	−18,580.4	13, 019	1.3334	0.0150	226.2186	−7.66E+56
Std.	0.9167	2.67E+6	3.44E−06	2.72E−13	0.00077	33.9790	0.2550	413.687	2800	0.2168	0.0029	53.5192	4.56E+56
Circle CEA													
Mean	6.4061	−9.88E+9	1.000028	1.53E−12	0.59801	109.8184	1.7199	−17,609.2	**5045**	0.6148	0.0146	158.1378	−1.51E+57
Min	5.8545	−9.88E+9	1.000009	3.81E−13	0.00087	44.4340	1.4999	−17,909.2	2938	0.4042	0.0108	94.2554	−2.54E+57
Max	6.6767	−9.87E+9	1.000062	3.31E−12	0.99676	180.8260	1.8999	−17,178.8	7128	0.7829	0.0187	285.8465	−9.73E+56
Std.	0.3539	7.76E+6	2.09E−05	1.21E−12	0.54498	49.0432	0.2049	337.140	1652	0.1668	0.0037	76.9778	6.11E+56
Gauss–Mouse CEA													
Mean	6.6943	−9.89E+9	1.000001	2.58E−14	0.19910	**86.9267**	1.5599	−18,098.7	7033	0.8559	0.0041	135.0339	−1.43E+57
Min	4.6650	−9.91E+9	1.000001	8.85E−15	6.71E−05	37.7298	1.3999	−18,225.1	5209	0.7277	0.0029	86.6846	−2.00E+57
Max	7.5315	−9.87E+9	1.000002	5.08E−14	0.99513	118.8322	1.6999	−18,007.9	10, 173	0.9807	0.0055	205.3942	−7.66E+56
Std.	1.1689	1.46E+7	4.79E−07	1.75E−14	0.44500	30.6132	0.1517	92.167	2004	0.0970	0.0010	45.8185	4.58E+56
Liebovitch CEA													
Mean	6.7503	−9.93E+9	1.000002	3.33E−14	**0.00019**	118.9728	1.6599	−18,560.6	6805	0.9125	0.0045	157.7782	**−1.82E+57**
Min	5.2898	−9.94E+9	1.000000	1.27E−14	7.28E−05	66.6051	1.1999	−19,054.1	5180	0.6557	0.0034	108.2130	−2.54E+57
Max	7.5400	−9.92E+9	1.000005	6.31E−14	0.00027	157.5582	1.9999	−18,225.1	8945	1.1117	0.0076	239.4710	−1.24E+57
Std.	0.9205	9.18E+6	1.79E−06	2.55E−14	7.68E−05	34.2611	0.2881	349.789	1643	0.1996	0.0018	50.6505	6.65E+56
Logistic CEA													
Mean	7.1703	−9.98E+9	**1.000001**	**1.40E−14**	0.19909	172.7476	1.7999	**−19,077.8**	8137	1.6057	**0.0030**	163.6597	−1.35E+57
Min	5.6223	−9.98E+9	1.000000	6.24E−15	4.07E−05	146.0444	1.4999	−19,883.2	6455	1.1813	0.0014	117.0558	−2.54E+57
Max	9.5602	−9.97E+9	1.000001	3.05E−14	0.99515	216.8700	1.9999	−18,580.4	9739	2.4282	0.0047	231.7417	−7.66E+56
Std.	1.6120	4.93E+6	3.11E−07	9.87E−15	0.44501	28.2860	0.1871	545.331	1461	0.4958	0.0013	44.1281	6.92E+56

Table 9 continued

Mutation tests	f_{15}	f_{16}	f_{17}	f_{18}	f_{19}	f_{20}	f_{21}	f_{22}	f_{23}	f_{24}	f_{25}	f_{26}	f_{27}
Piecewise CEA													
Mean	7.0860	−9.92E+9	1.000005	6.20E−14	0.19925	151.1716	1.7399	−18,347.4	6525	0.6295	0.0065	145.9120	−1.06E+57
Min	6.2062	−9.93E+9	1.000002	3.25E−14	0.00017	74.9361	1.1999	−18,817.3	3919	0.5765	0.0053	102.9579	−1.24E+57
Max	8.0662	−9.92E+9	1.00001	1.39E−13	0.99533	215.6909	2.0999	−17,178.9	9606	0.6793	0.0079	219.6033	−6.03E+56
Std.	0.6599	6.43E+6	3.46E−06	4.44E−14	0.44502	55.6024	0.4159	661.267	2028	0.0405	0.0011	47.8073	2.79E+56
Sine CEA													
Mean	**6.3741**	−9.89E+9	1.000134	1.79E−12	0.20444	128.9987	**1.4999**	−18,177.7	6998	**0.5753**	0.0181	152.4626	−1.68E+57
Min	5.7268	−9.90E+9	1.000088	4.32E−13	0.00289	71.1067	1.2999	−18,817.3	4594	0.3574	0.0161	101.8143	−3.22E+57
Max	7.1762	−9.87E+9	1.000206	3.04E−12	1.00182	212.5642	1.8999	−17,514.4	9049	0.9034	0.0208	193.7381	−9.72E+56
Std.	0.5590	1.41E+7	4.68E−05	1.07E−12	0.44575	53.0809	0.2828	624.473	1694	0.2088	0.0022	40.2985	9.56E+56
Sinusoidal CEA													
Mean	6.9374	−9.97E+9	1.000216	4.41E−11	0.21382	134.4032	2.6999	−18,730.3	13,997	2.4845	0.0640	310.0365	−1.20E+57
Min	5.4471	−9.99E+9	1.000141	2.02E−11	0.01063	90.3043	2.2999	−19,291	7976	1.4878	0.0464	249.1375	−1.99E+57
Max	7.8660	−9.94E+9	1.000324	8.11E−11	1.00781	261.6071	3.2999	−18,481.6	20,059	3.2834	0.0948	410.6770	−6.00E+56
Std.	1.0868	1.73E+7	7.01E−05	2.98E−11	0.44386	71.7739	0.4062	322.769	4682	0.9124	0.0213	72.9631	5.09E+56
Tent CEA													
Mean	6.9605	−9.91E+9	1.000003	5.63E−14	0.00015	101.1116	1.6599	−18,110.6	7009	0.8049	0.0064	137.3879	−9.19E+56
Min	5.0722	−9.93E+9	1.000001	3.58E−14	7.27E−05	80.4046	1.4999	−18,461.9	5376	0.6764	0.0043	82.9411	−1.57E+57
Max	8.0498	−9.90E+9	1.000005	8.89E−14	0.00023	157.2688	1.8999	−17,415.7	7667	0.9565	0.0077	202.2101	−4.75E+56
Std.	1.2268	9.49E+6	1.63E−06	2.23E−14	5.53E−05	31.9793	0.2191	410.379	992	0.1280	0.0014	47.9889	4.27E+56
Standard EA													
Mean	6.9642	−9.79E+9	1.00002	4.09E−12	0.2012	164.87	1.5798	−18,217	6117	0.9544	0.0117	**110.72**	−1.44E+57
Min	5.3458	−9.70E+9	1	1.24E−12	0.0011	139.08	1.2998	−19,054	3611	0.7343	0.009	53.338	−2.54E+57
Max	8.3444	−9.70E+9	1.00003	6.62E−12	0.9974	214.7	1.7998	−17,790	9211	1.1645	0.0153	155.51	−9.74E+56
Std.	1.0848	1.90E+7	1.20E−5	2.26E−12	0.445	30.25	0.2167	511.06	2417	0.1605	0.0024	43.539	6.22E+56

can afford much more promising outcomes in terms of the robustness metric. By taking the characteristics of the chaotic maps into account, it can be inferred that the logistic, sinusoidal, and Gauss–Mouse chaotic maps are not only able to effectively improve the performance of the standard EA, but also can generate random deterministic chaotic sequences with a low computational budget (as their mathematical formulation is really straight forward).

By comparing the results of CEAs with those obtained by the standard EAs, it can be seen that embedding chaotic sequences into the structure of EA can effectively improve its accuracy and robustness. This fact can be concluded by taking the mean performance into account. As seen, it is just for f_{24} benchmark problem that the EA outperforms its chaotic embedded counterpart. Besides, for the most of the benchmark problems, the robustness of CEAs is really higher than the standard EA. Such observations augur the remarkable improvements afforded by embedding chaos into the structure of the baseline EA, at least for the 50D benchmark problems.

4.2.1.2. Chaotic crossover and mutation: semi large scale benchmarks At the second step of the experiment, the 100D versions of the benchmark problems are considered for evaluating the performance of EAs with chaotic crossover and mutation operators. This allows us realize whether the same observations are valid when the dimensionalities of the landscapes of benchmark functions are increased. To be more to the point, considering a higher dimension of benchmark problems yield some results regarding the scalability of CEAs.

Tables 10 and 11 summarize the statistical results of numerical experiments for the rival techniques with chaotically encoded HX operators. Interestingly, for the 100D problems, the best performance belongs to the sinusoidal version of CEA. It seems that the sinusoidal map can be neatly combined with the EA so that the exploration/exploitation features remain qualified for solving semi large-scale optimization problems.

Tables 12 and 13 list the obtained statistical results for the rival techniques with chaotically encoded AGS operators. Once more, it can be seen that the solutions obtained by the EAs with chaotically encoded AGS operators are more qualified than those of the crossover experiments. This, in turn, endorses the fact that the EAs with chaotic mutation operator can outperform the EAs with chaotically encoded crossovers even when the dimensionality of the benchmarks increases. It is interesting that for most of the cases, the best performance belongs to the mutation operator with Gauss–Mouse chaotic map. It can be also seen that for some of the benchmarks, the Chebyshev, circle and piecewise maps show acceptable performances. Once more, the results indicate that the sinusoidal map is best suited to be combined with the crossover operator and the Gauss–Mouse map is the fittest one for the mutation operator.

As a general remark, it can be inferred that the results of the other CEAs are not as promising as those obtained in the 50D experiments. Apparently, except the sinusoidal and Gauss–Mouse CEAs, the other CEAs can outperform the other optimizers at most for one time. However, the standard EA outperforms its chaotic counterparts for the f_7 and f_{23} benchmark problems for the crossover experiments and the f_{21} benchmark for the mutation experiment. This spontaneously implies that the chaotic maps (except the sinusoidal for crossover and the Gauss–Mouse for mutation) could not retain their acceptable performance when the dimensionality of the benchmarks increases. However, it is worth mentioning that their performance is still fine as compared to the standard EA. By considering the results of the standard deviation, it can be concluded that the robustness of the standard EA, sinusoidal, tent, circle and Leibovitch CEAs is acceptable for this experiment. Once more, it has been observed that the chaotic maps are not only able to improve the accuracy of the standard EA, but also can retain their robustness at a standard level.

Table 10 Statistical results of the optimizations for 100D version of benchmarks ($f_1 - f_{14}$)

Crossover tests	f_1	f_2	f_3	f_4	f_5	f_6	f_7	f_8	f_9	f_{10}	f_{11}	f_{12}	f_{13}	f_{14}
Chebyshev CEA														
Mean	0.0916	0.0540	−3.0510	2791	−67.239	0.4882	0.0475	0.00015	−76.604	0.0043	0.0010	−89.071	2,993,580	−1.04E−6
Min	0.0848	0.0343	−3.4988	1559	−68.086	0.3888	0.0257	0.00012	−81.034	0.0033	0.0008	−90.846	2,000,792	−2.58E−6
Max	0.1031	0.0826	−1.2606	5205	−65.548	0.5720	0.1023	0.00020	−72.800	0.0050	0.0013	−86.719	4,211,530	−8.38E−9
Std.	0.0082	0.0207	1.0008	1407	1.0182	0.0882	0.0329	3.32E−5	3.4363	0.0007	0.0002	1.9465	828,045	1.15E−6
Circle CEA														
Mean	0.1005	0.0639	−3.4985	5889	−65.143	0.5783	0.0697	0.00018	−76.003	0.0051	0.0016	−87.364	2,813,759	**−4.69E−6**
Min	0.0856	0.0364	−3.4987	3469	−67.318	0.4728	0.0271	0.00013	−79.926	0.0044	0.0012	−88.711	2,212,026	−1.26E−5
Max	0.1230	0.0948	−3.4981	7903	−63.057	0.7135	0.1038	0.00024	−71.614	0.0058	0.0020	−85.481	4,227,411	−5.25E−7
Std.	0.0142	0.0237	0.0002	1914	1.8881	0.1034	0.0308	4.35E−5	2.9633	0.0007	0.0003	1.3772	855,060	4.74E−6
Gauss–Mouse CEA														
Mean	0.0625	0.0299	**−3.4993**	1096	−67.894	0.2491	0.0357	6.60E−5	−77.265	0.0026	0.0007	−88.675	2,848,089	−6.12E−7
Min	0.0581	0.0225	−3.4994	815	−70.049	0.1722	0.0093	4.89E−5	−80.822	0.0021	0.0005	−89.779	2,139,544	−1.88E−6
Max	0.0695	0.0344	−3.4991	1370	−66.23	0.3045	0.0591	7.99E−5	−74.838	0.0031	0.0010	−87.138	3,598,150	−7.78E−8
Std.	0.0044	0.0050	0.0001	224	1.6865	0.0673	0.0222	1.31E−5	2.2308	0.0003	0.0002	1.0197	564,097	7.52E−7
Liebovitch CEA														
Mean	0.0678	0.0402	−3.0515	1108	−67.853	0.2441	0.0613	6.84E−5	−77.004	0.0027	0.0007	−89.330	2,786,515	−1.09E−6
Min	0.0643	0.0328	−3.4992	868	−69.436	0.1688	0.0209	5.18E−5	−81.245	0.0014	0.0004	−90.982	1,285,470	−4.87E−6
Max	0.0707	0.0535	−1.2611	1344	−66.862	0.3145	0.1468	9.02E−5	−74.818	0.0034	0.0009	−88.129	4,646,694	−2.99E−8
Std.	0.0024	0.0082	1.0008	174	1.0408	0.0594	0.0534	1.60E−5	2.4848	0.0008	0.0002	1.2056	1,257,318	2.12E−6
Logistic CEA														
Mean	0.0581	0.0349	−3.0519	566	−69.953	0.2224	0.0289	5.78E−5	**−77.544**	0.0021	0.0004	−90.308	2,544,404	−3.02E−7
Min	0.0458	0.0282	−3.4995	369	−71.792	0.1786	0.0073	3.77E−5	−80.081	0.0013	0.0004	−91.811	1,220,316	−5.25E−7
Max	0.0628	0.0420	−1.2617	852	−67.239	0.2474	0.0496	7.01E−5	−76.000	0.0027	0.0006	−88.897	4,187,257	−5.66E−8
Std.	0.0070	0.0059	1.0007	191	1.6951	0.0301	0.0206	1.32E−5	1.87451	0.0005	7.5E−5	1.0578	1,102,704	2.12E−7

Table 10 continued

Crossover tests	f_1	f_2	f_3	f_4	f_5	f_6	f_7	f_8	f_9	f_{10}	f_{11}	f_{12}	f_{13}	f_{14}
Piecewise CEA														
Mean	0.0722	0.0385	−3.4991	1770	−66.105	0.3347	0.0510	0.00010	−76.113	0.0030	0.0010	−88.519	2,195,916	−5.72E−7
Min	0.0638	0.0326	−3.4992	1474	−69.383	0.2707	0.0226	8.28E−5	−81.062	0.0023	0.0007	−91.226	1,038,509	−1.87E−6
Max	0.0795	0.0440	−3.4991	1911	−62.988	0.3972	0.1003	0.00014	−72.861	0.0036	0.0014	−86.331	3,688,088	−5.66E−8
Std.	0.0060	0.0046	5.3E−5	174	3.1362	0.0536	0.0297	2.60E−5	3.0526	0.0004	0.0002	2.1512	985,312	7.48E−7
Sine CEA														
Mean	0.1276	0.0686	−3.4974	12,084	−63.327	0.9421	0.0707	0.00029	−76.285	0.0100	0.0025	−86.566	2,739,396	−2.23E−6
Min	0.1015	0.0561	−3.4980	7914	−65.688	0.8224	0.0383	0.00024	−77.436	0.0076	0.0018	−88.001	1,660,392	−6.69E−6
Max	0.1596	0.0792	−3.4965	20,594	−61.762	1.1702	0.1365	0.00034	−74.494	0.0127	0.0044	−84.366	3,502,884	−5.24E−7
Std.	0.0214	0.0094	0.0005	5186	1.5672	0.1373	0.0386	3.85E−5	1.1268	0.0023	0.0010	1.4363	846,316	2.55E−6
Sinusoidal CEA														
Mean	**0.0395**	**0.0190**	−2.1571	**289**	**−71.747**	**0.1216**	0.0628	**−3.38E−5**	−76.893	**−0.0013**	**−0.0002**	**−94.486**	**−2,053,492**	−6.26E−8
Min	0.0366	0.0152	−3.4997	142	−74.652	0.1110	0.0052	2.73E−5	−78.555	0.0011	0.0002	−95.191	1,585,819	−2.78E−7
Max	0.0434	0.0252	−1.2620	455	−69.408	0.1509	0.2110	4.35E−5	−73.520	0.0016	0.0003	−94.112	2,480,179	−2.5E−10
Std.	0.0024	0.0041	1.2255	111	2.1729	0.0165	0.0861	6.24E−6	1.9984	0.0001	2.3E−5	0.4184	336,043	1.21E−7
Tent CEA														
Mean	0.0779	0.0407	−3.0516	1601	−66.988	0.3418	0.0301	8.65E−5	−75.390	0.0033	0.0007	−87.925	2,263,655	−8.87E−7
Min	0.0727	0.0329	−3.4994	810	−69.094	0.2736	0.0184	5.16E−5	−78.139	0.0023	0.0006	−89.253	1,551,318	−3.54E−6
Max	0.0862	0.0497	−1.2615	2642	−64.612	0.3940	0.0581	0.00011	−73.967	0.0046	0.0008	−86.698	4,485,820	−2.99E−8
Std.	0.0053	0.0062	1.0006	859	1.7479	0.0514	0.0169	2.75E−5	1.7148	0.0009	0.0001	1.1791	1,253,004	1.49E−6
Standard EA														
Mean	0.0833	0.0366	−3.4990	1709	−66.024	0.2880	**0.0295**	8.76E−5	−76.700	0.0028	0.0008	−88.896	3,420,142	−4.56E−7
Min	0.0678	0.0293	−3.4994	1023	−69.399	0.2432	0.0188	7.10E−5	−78.681	0.0023	0.0006	−89.753	1,718,578	−9.92E−7
Max	0.0901	0.0448	−3.4986	2450	−63.855	0.3165	0.0482	0.00010	−72.985	0.0037	0.0009	−87.805	5,990,808	−1.58E−8
Std.	0.0090	0.0060	0.0003	532	2.1282	0.0293	0.0126	1.52E−5	2.2627	0.0005	0.0001	0.8222	1,603,879	4.49E−7

Table 11 Statistical results of the optimizations for 100D version of benchmarks ($f_{15} - f_{27}$)

Crossover tests	f_{15}	f_{16}	f_{17}	f_{18}	f_{19}	f_{20}	f_{21}	f_{22}	f_{23}	f_{24}	f_{25}	f_{26}	f_{27}
Chebyshev CEA													
Mean	18.1	−6.79E19	1.0019	4.13E−8	45.012	526.26	1.8198	−32,453	30,674	3.5148	0.2630	**279.79**	−5.64E+113
Min	16.0	−7.13E19	1.0015	2.33E−8	41.943	395.35	1.5998	−34,987	18,168	2.7037	0.2141	251.99	−1.40E+114
Max	20.5	−6.60E19	1.0023	5.81E−8	49.956	794.07	1.9998	−31,296	42,034	4.9922	0.3268	300.66	−3.44E+112
Std.	1.67	2.01E18	6.9E−4	1.27E−8	3.1511	157.69	0.1643	1468	9269	0.8770	0.0408	19.500	5.92E+113
Circle CEA													
Mean	18.680	−5.81E19	1.0043	8.51E−8	46.144	536.99	1.8798	−31,181	17,726	2.8304	0.2984	410.56	−6.72E+112
Min	14.693	−5.97E19	1.0031	6.09E−8	38.001	377.89	1.6998	−32,322	10,720	2.0008	0.2806	249.26	−1.62E+113
Max	21.242	−5.59E19	1.0056	1.14E−7	50.921	719.84	2.0998	−29,993	27,350	3.4639	0.3137	493.54	−1.89E+110
Std.	2.8101	1.60E18	0.0009	1.99E−8	5.1372	140.75	0.1483	977	6768	0.5903	0.0140	98.136	7.44E+112
Gauss–Mouse CEA													
Mean	18.699	−6.99E19	1.0014	2.83E−8	39.923	588.41	2.0798	−32,750	25,208	2.7710	0.1698	294.45	−6.12E+113
Min	18.193	−7.12E19	1.0011	1.58E−8	33.971	408.90	1.8998	−33,863	22,291	2.4438	0.1507	196.09	−1.20E+114
Max	19.372	−6.77E19	1.0019	4.85E−8	53.883	855.23	2.2998	−31,692	27,016	3.0717	0.1889	376.69	−6.79E+112
Std.	0.4768	1.34E18	0.0003	1.22E−8	8.4276	178.60	0.1483	860	1904	0.2662	0.0167	77.984	4.09E+113
Liebovitch CEA													
Mean	19.273	−7.17E19	1.0017	1.85E−8	39.689	532.63	2.1798	−32,351	24,270	**2.6012**	0.1944	305.57	−8.63E+113
Min	17.428	−7.40E19	1.0013	1.43E−8	32.930	407.99	1.7998	−33,527	17,326	1.7108	0.1679	223.67	−1.38E+114
Max	21.085	−6.85E19	1.0020	2.94E−8	44.846	814.62	2.3998	−30,942	34,104	3.1380	0.2306	368.03	−2.17E+113
Std.	1.6802	2.14E18	0.0002	6.20E−9	4.4084	164.68	0.2387	1002	7029	0.5793	0.0285	63.652	5.35E+113
Logistic CEA													
Mean	18.994	−7.76E19	1.0013	1.70E−8	35.895	783.21	2.3598	−33,030	30,491	3.7509	0.1756	319.02	−2.03E+114
Min	17.037	−7.94E19	1.0008	1.03E−8	27.942	360.91	2.0998	−34,199	24,452	3.2055	0.1466	260.90	−4.41E+114
Max	20.958	−7.63E19	1.0017	3.16E−8	41.867	1957.1	2.4998	−31,929	40,483	4.1097	0.1983	395.45	−5.83E+113
Std.	1.6112	1.16E18	0.0003	8.37E−9	5.1241	667.04	0.1673	946	6441	0.3372	0.0186	49.124	1.62E+114

Table 11 continued

Crossover tests	f_{15}	f_{16}	f_{17}	f_{18}	f_{19}	f_{20}	f_{21}	f_{22}	f_{23}	f_{24}	f_{25}	f_{26}	f_{27}
Piecewise CEA													
Mean	19.870	− 6.87E19	1.0020	3.45E−8	33.962	388.71	1.9998	− 31,936	22,273	3.3338	0.2061	398.74	− 7.10E+113
Min	17.778	− 7.01E19	1.0015	1.81E−8	28.965	310.07	1.8998	− 33,192	19,149	2.7339	0.1712	272.37	− 1.26E+114
Max	21.716	− 6.73E19	1.0025	4.40E−8	35.910	497.66	2.0998	− 31,474	27,206	3.7497	0.2516	548.53	− 3.16E+113
Std.	1.7418	1.34E18	0.0004	1.01E−8	2.8228	72.020	0.1	714	3080	0.3906	0.0304	110.68	3.94E+113
Sine CEA													
Mean	20.739	− 5.33E19	1.0072	1.24E−7	57.295	638.33	**1.6798**	− 30,513	21,867	3.2868	0.4033	418.50	− 5.15E+111
Min	18.852	− 5.50E19	1.0064	7.58E−8	53.035	476.52	1.4998	− 31,848	15,925	2.4740	0.3684	192.84	− 1.86E+112
Max	22.629	− 5.12E19	1.0085	1.91E−7	60.993	1035.7	1.8998	− 29,142	28,343	4.0785	0.4445	635.13	− 3.36E+108
Std.	1.3635	1.41E18	0.0008	4.28E−8	3.3335	227.78	0.1483	1057	4589	0.6593	0.0337	181.94	7.77E+111
Sinusoidal CEA													
Mean	**16.374**	**− 8.61E19**	**1.0006**	**3.68E−9**	**16.165**	**333.36**	2.4798	**− 34,436**	36,112	3.7487	**0.1313**	311.74	**− 2.65E+114**
Min	15.779	− 8.64E19	1.0005	1.92E−9	10.969	293.83	1.9998	− 35,127	24,700	2.7628	0.1194	250.36	− 4.45E+114
Max	17.934	− 8.56E19	1.0006	5.39E−9	20.940	358.25	2.8998	− 33,548	47,939	4.6129	0.1547	387.98	− 1.71E+114
Std.	0.8878	2.92E17	6.6E−5	1.35E−9	4.8479	28.474	0.3492	599	10,633	0.7165	0.0138	56.788	1.07E+114
Tent CEA													
Mean	19.056	− 6.75E19	1.0023	2.94E−8	39.942	423.74	2.0598	− 31,991	23,190	2.9907	0.2044	347.41	− 3.06E+113
Min	17.129	− 6.94E19	1.0018	2.32E−8	29.974	333.16	1.9998	− 33,744	17,740	2.6412	0.1740	239.27	− 7.25E+113
Max	20.822	− 6.48E19	1.0030	3.76E−8	43.946	582.15	2.1998	− 30,270	25,427	3.4766	0.2467	440.48	− 1.03E+113
Std.	1.3410	1.83E18	0.0004	6.04E−9	5.7658	98.599	0.0894	1431	3110	0.3130	0.0269	76.931	2.57E+113
Standard EA													
Mean	18.039	− 6.73E19	1.0020	2.22E−8	47.295	430.85	2.0798	− 32,497	**17,433**	3.0025	0.2260	334.26	− 8.67E+113
Min	16.476	− 6.98E19	1.0016	1.42E−8	33.943	360.20	1.8998	− 33,251	14,236	2.4451	0.1837	215.57	− 3.36E+114
Max	20.081	− 6.56E19	1.0023	2.89E−8	57.872	470.22	2.1998	− 31,514	20,415	3.3962	0.2496	446.70	− 4.74E+112
Std.	1.3578	1.68E18	0.0002	5.57E−9	9.3973	43.270	0.1303	733	2785	0.3535	0.0263	87.590	1.42E+114

Table 12 Statistical results of the optimizations for 100D version of benchmarks ($f_1 - f_{14}$)

Mutation tests	f_1	f_2	f_3	f_4	f_5	f_6	f_7	f_8	f_9	f_{10}	f_{11}	f_{12}	f_{13}	f_{14}
Chebyshev CEA														
Mean	0.0521	0.0224	−2.6044	331.196	**−73.4914**	0.1361	0.0576	4.44E−5	**−76.9485**	0.0018	0.0004	−93.8136	3.52E+6	−1.62E−7
Min	0.0388	0.0172	−3.4996	254.211	−77.2957	0.1230	0.0190	2.93E−5	−79.4602	0.0012	0.0003	−95.0138	2.13E+6	−7.22E−7
Max	0.0581	0.0282	−1.2616	462.781	−70.4712	0.1576	0.1141	6.54E−5	−75.3121	0.0026	0.0005	−92.5433	4.67E+6	−3.23E−9
Std.	0.0077	0.0049	1.2257	94.6112	2.7969	0.0137	0.0396	1.33E−5	1.8699	0.0006	0.0001	1.1404	1.14E+6	3.14E−7
Circle CEA														
Mean	0.0622	0.0318	−3.0519	478.458	−72.1366	0.2101	0.0432	5.90E−5	−75.5151	0.0020	0.0004	−93.8324	3.37E+6	**−7.91E−7**
Min	0.0557	0.0183	−3.4996	322.596	−75.8407	0.1482	0.0107	5.01E−5	−78.3316	0.0018	0.0002	−94.8728	2.45E+6	−1.88E−6
Max	0.0709	0.0385	−1.2616	720.736	−67.9723	0.3114	0.1276	7.00E−5	−73.3790	0.0025	0.0006	−93.1677	4.03E+6	−4.11E−8
Std.	0.0058	0.0080	1.0008	146.5201	2.8015	0.0700	0.0483	8.84E−6	2.0414	0.0003	0.0002	0.6456	6.25E+5	7.99E−7
Gauss–Mouse CEA														
Mean	**0.0238**	**0.0131**	−2.1573	**72.402**	−70.4095	**0.0357**	0.0554	**9.32E−6**	−76.6947	**0.0004**	**0.0001**	−93.7094	**3.23E+6**	−2.08E−7
Min	0.0211	0.0094	−3.4999	56.1478	−72.0811	0.0261	0.0134	4.98E−6	−78.0858	0.0002	0.0001	−94.2345	2.14E+6	−7.22E−7
Max	0.0260	0.0184	−1.2623	84.2107	−68.6169	0.0445	0.1284	1.41E−5	−73.9713	0.0005	0.0001	−93.2020	4.30E+6	−4.44E−9
Std.	0.0023	0.0033	1.2256	13.0501	1.5872	0.0072	0.0493	3.70E−6	1.5967	0.0001	0.0000	0.4342	8.94E+5	2.99E−7
Liebovitch CEA														
Mean	0.0266	0.0136	−2.1095	84.6621	−71.0421	0.0382	0.0378	1.09E−5	−76.0041	0.0005	0.00014	−93.6729	3.27E+6	−1.85E−7
Min	0.0225	0.0100	−3.4999	39.1398	−73.3662	0.0295	0.0013	8.85E−6	−78.0067	0.0003	0.0001	−94.6154	2.55E+6	−7.22E−7
Max	0.0325	0.0179	−1.0231	128.924	−68.9232	0.0460	0.1422	1.37E−5	−74.0125	0.0005	0.0002	−92.7453	3.63E+6	−4.77E−10
Std.	0.0038	0.0037	1.2730	42.2422	1.7267	0.0073	0.0610	2.12E−6	1.5329	7.65E−5	0.0000	0.7298	4.35E+5	3.04E−7
Logistic CEA														
Mean	0.0290	0.0184	−2.5569	88.2940	−72.8346	0.0584	0.0335	1.37E−5	−76.0142	0.0007	0.0002	**−94.2213**	3.39E+6	−3.93E−8
Min	0.0220	0.0062	−3.4999	49.1906	−75.0572	0.0224	0.0019	7.79E−6	−78.5957	0.0005	0.0001	−94.7354	1.60E+6	−1.07E−7
Max	0.0405	0.0361	−1.0228	136.257	−70.8901	0.0837	0.0746	2.06E−5	−71.6916	0.0009	0.0002	−93.5304	5.62E+6	−9.03E−10
Std.	0.0072	0.0109	1.2939	43.3034	1.8908	0.0263	0.0281	5.46E−6	2.7580	0.0001	0.0000	0.5147	1.56E+6	4.42E−8

Table 12 continued

Mutation tests	f_1	f_2	f_3	f_4	f_5	f_6	f_7	f_8	f_9	f_{10}	f_{11}	f_{12}	f_{13}	f_{14}
Piecewise CEA														
Mean	0.0314	0.0142	**−3.4998**	169.337	−71.2336	0.0594	**0.0179**	1.86E−5	−75.9188	0.0007	0.0002	−93.8632	3.66E+6	−1.25E−7
Min	0.0233	0.0122	−3.4999	114.464	−73.6719	0.0490	0.0016	1.49E−5	−77.4255	0.0005	0.0001	−94.5553	2.25E+6	−2.78E−7
Max	0.0385	0.0149	−3.4997	220.027	−68.5108	0.0729	0.0342	2.20E−5	−73.9100	0.0010	0.0002	−93.1159	4.54E+6	−1.58E−8
Std.	0.0069	0.0011	7.02E−05	48.7996	2.2260	0.0104	0.0127	3.54E−6	1.4973	0.0002	0.0000	0.6911	1.10E+6	1.14E−7
Sine CEA														
Mean	0.0843	0.0459	−2.6035	886.847	−73.2134	0.4226	0.0473	1.16E−4	−73.2601	0.0037	0.0009	−93.9718	4.81E+6	−3.49E−7
Min	0.0750	0.0300	−3.4986	647.7319	−74.7214	0.3205	0.0081	8.91E−5	−75.8271	0.0030	0.0006	−94.3801	3.19E+6	−1.36E−6
Max	0.0949	0.0565	−1.2609	1351.742	−70.0994	0.5582	0.1437	1.45E−4	−70.1635	0.0048	0.0011	−93.2302	6.30E+6	−4.43E−9
Std.	0.0072	0.0104	1.2255	275.282	1.8915	0.1056	0.0555	2.63E−5	2.1637	0.0007	0.0002	0.4695	1.25E+6	5.78E−7
Sinusoidal CEA														
Mean	0.0818	0.0545	−2.5563	2024.90	−74.0650	0.3009	0.0630	7.44E−5	−76.0031	0.0039	0.0007	−94.7757	8.62E+6	−1.61E−8
Min	0.0598	0.0444	−3.4993	1120.39	−75.1889	0.2441	0.0216	5.39E−5	−76.9996	0.0033	0.0006	−95.2216	3.16E+6	−5.66E−8
Max	0.0974	0.0708	−1.0225	2778.31	−73.1994	0.3938	0.1201	1.10E−4	−74.5860	0.0047	0.0009	−94.4104	1.23E+7	−3.47E−10
Std.	0.0138	0.0103	1.2938	616.136	0.7539	0.0628	0.0375	2.14E−5	0.9990	0.0006	0.0001	0.3066	3.77E+6	2.33E−8
Tent CEA														
Mean	0.0329	0.0143	−3.4996	151.156	−72.1358	0.0808	0.0466	2.04E−5	−76.2494	0.0008	0.00013	−94.4081	3.04E+6	−2.71E−8
Min	0.0276	0.0123	−3.4999	102.080	−76.3241	0.0550	0.0034	1.46E−5	−77.9539	0.0005	0.0001	−95.4640	2.28E+6	−7.78E−8
Max	0.0402	0.0190	−3.4997	241.891	−67.7025	0.0932	0.0917	2.78E−5	−74.0053	0.0012	0.0002	−93.2511	3.87E+6	−8.38E−9
Std.	0.0054	0.0028	6.34E−05	53.8504	3.2147	0.0152	0.0395	5.87E−6	1.6609	0.0003	0.0001	1.0824	7.25E+5	2.88E−8
Standard EA														
Mean	0.0833	0.0366	−3.4990	1709	−66.024	0.288	0.0295	8.76E−5	−76.7	0.0028	0.0008	−88.896	3.42E+6	−4.56E−7
Min	0.0678	0.0293	−3.4994	1023	−69.399	0.2432	0.0188	7.10E−5	−78.681	0.0023	0.0006	−89.753	1.72E+6	−9.92E−7
Max	0.0901	0.0448	−3.4986	2450	−63.855	0.3165	0.0482	0.0001	−72.985	0.0037	0.0009	−87.805	5.99E+6	−1.58E−8
Std.	0.009	0.006	0.0003	532	2.1282	0.0293	0.0126	1.52E−5	2.2627	0.0005	0.0001	0.8222	1.60E+6	4.49E−7

Table 13 Statistical results of the optimizations for 100D version of benchmarks ($f_{15} - f_{27}$)

Mutation tests	f_{15}	f_{16}	f_{17}	f_{18}	f_{19}	f_{20}	f_{21}	f_{22}	f_{23}	f_{24}	f_{25}	f_{26}	f_{27}
Chebyshev CEA													
Mean	**16.3196**	**−9.29E+19**	1.0006	9.45E−9	**15.2004**	489.942	2.9999	−**36,750**	30,336	2.5911	0.1585	377.137	−2.48E+114
Min	15.0513	−9.36E+19	1.0003	3.49E−9	12.0144	333.856	2.6999	−37,575	26,417	2.2043	0.1422	330.540	−4.44E+114
Max	18.0819	−9.23E+19	1.0010	1.41E−8	19.9912	631.134	3.1999	−36,134	38,696	3.2305	0.1816	421.249	−6.53E+113
Std.	1.3147	4.55E+17	0.0003	3.94E−9	3.1086	129.297	0.2345	628	4812	0.4355	0.0144	39.1652	1.61E+114
Circle CEA													
Mean	17.1327	−8.10E+19	1.0012	1.11E−8	20.9678	482.792	2.7199	−32,853	**16,888**	**1.4059**	0.1921	315.994	−1.66E+114
Min	15.6845	−8.18E+19	1.0008	9.24E−9	13.9970	416.825	2.3999	−33,568	14,768	1.2749	0.1825	218.476	−2.14E+114
Max	19.2555	−8.04E+19	1.0017	1.32E−8	26.9557	654.230	3.0999	−31,949	20,785	1.5851	0.2019	473.040	−1.33E+114
Std.	1.5708	5.40E+17	0.0004	1.76E−9	5.2224	97.8637	0.2588	813	2568	0.1261	0.0077	106.785	3.43E+113
Gauss–Mouse CEA													
Mean	17.0496	−8.19E+19	1.0002	**5.56E−10**	19.9196	**323.215**	2.8799	−33,485	33,023	2.7669	**0.0680**	384.648	−2.10E+114
Min	15.3910	−8.33E+19	1.0001	1.81E−10	16.9302	261.742	2.4999	−34,081	27,063	2.2510	0.0538	322.598	−3.53E+114
Max	18.5058	−7.99E+19	1.0002	1.03E−9	22.9080	356.893	3.2999	−32,936	40,254	3.7814	0.0755	536.387	−6.60E+113
Std.	1.4622	1.46E+18	3.81E−5	3.73E−10	2.8149	36.3853	0.3194	522	5006	0.5957	0.0083	86.2398	1.09E+114
Liebovitch CEA													
Mean	16.7598	−8.51E+19	1.0003	7.19E−10	20.5200	364.760	2.9999	−34,851	25,587	3.5651	0.0737	324.920	−1.81E+114
Min	14.9059	−8.59E+19	1.0002	1.80E−10	16.9508	270.038	2.6999	−35,562	18,723	2.9081	0.0622	202.424	−2.77E+114
Max	19.8767	−8.44E+19	1.0004	1.66E−9	23.8928	475.401	3.3999	−34,140	31,151	4.1305	0.0864	378.261	−5.55E+113
Std.	2.0281	5.89E+17	0.0001	5.90E−10	2.8591	74.2747	0.3317	677	5330	0.5084	0.0095	70.5407	8.65E+113
Logistic CEA													
Mean	16.6320	−9.22E+19	**1.0001**	2.26E−9	15.7440	351.417	3.2999	−36,454	38,100	4.9578	0.0703	444.851	−8.82E+113
Min	15.3233	−9.30E+19	1.0001	4.90E−10	11.9615	284.728	2.8999	−37,299	32,577	4.1400	0.0491	316.998	−1.35E+114
Max	18.0783	−9.05E+19	1.0002	6.34E−9	21.9087	460.218	3.9999	−35,700	44,552	5.9333	0.0949	586.315	−4.09E+113
Std.	1.2640	9.91E+17	3.81E−5	2.34E−9	3.6811	69.8570	0.4359	643	5215	0.7183	0.0191	127.660	4.01E+113

Table 13 continued

Mutation tests	f_{15}	f_{16}	f_{17}	f_{18}	f_{19}	f_{20}	f_{21}	f_{22}	f_{23}	f_{24}	f_{25}	f_{26}	f_{27}
Piecewise CEA													
Mean	16.4368	−8.51E+19	1.0003	1.13E−9	16.1568	371.658	2.9999	−33,860	25,571	2.3248	0.0857	**277.133**	−2.43E+114
Min	15.3895	−8.61E+19	1.0002	5.01E−10	11.9693	334.394	2.6999	−34,575	15,915	1.8474	0.0810	230.548	−4.47E+114
Max	17.5770	−8.44E+19	1.0003	1.95E−9	20.9395	448.272	3.2999	−32,542	31,796	2.6476	0.0911	342.531	−6.58E+113
Std.	0.7860	6.37E+17	6.20E−5	5.75E−10	3.4051	48.9370	0.2550	773	5986	0.2968	0.0047	56.1469	1.56E+114
Sine CEA													
Mean	16.5857	−8.38E+19	1.0034	1.70E−8	17.7241	499.841	2.7399	−33,385	24,327	1.4554	0.3058	355.291	**−2.69E+114**
Min	13.3735	−8.46E+19	1.0026	1.14E−8	14.1597	447.135	2.4999	−34,179	18,987	1.2259	0.2523	261.635	−4.33E+114
Max	18.0363	−8.23E+19	1.0047	2.22E−8	21.0229	532.403	2.9999	−31,691	31,892	1.8204	0.3624	458.677	−1.03E+114
Std.	1.8589	1.04E+18	0.0009	4.73E−9	2.6634	33.6128	0.2074	1001	5931	0.2270	0.0447	94.9596	1.24E+114
Sinusoidal CEA													
Mean	14.9922	−9.21E+19	1.0034	1.18E−8	3.9750	424.413	4.1799	−36,268	59,093	10.7916	0.3400	681.839	−1.02E+114
Min	14.2921	−9.46E+19	1.0029	4.51E−9	0.1713	345.878	3.2999	−36,943	49,902	6.8977	0.2796	402.155	−1.68E+114
Max	15.4822	−8.99E+19	1.0041	3.12E−8	6.1726	523.537	4.6999	−35,185	66,474	14.4850	0.4299	882.911	−3.34E+113
Std.	0.5292	1.82E+18	0.0006	1.12E−8	2.4895	73.9393	0.5357	715	8030	2.9714	0.0606	174.627	5.05E+113
Tent CEA													
Mean	16.3109	−8.43E+19	1.0003	1.80E−9	13.7608	389.838	2.8999	−33,829	24,056	2.2802	0.1110	323.661	−2.36E+114
Min	15.0191	−8.53E+19	1.0002	6.85E−10	11.9678	335.788	2.2999	−34,871	17,475	2.0082	0.0935	198.163	−4.47E+114
Max	18.0152	−8.30E+19	1.0003	2.64E−9	14.9672	420.781	3.0999	−32,265	29,227	2.4905	0.1457	400.308	−6.59E+113
Std.	1.1096	1.03E+18	5.87E−5	8.12E−10	1.3030	34.1670	0.3391	964	4886	0.1825	0.0223	75.8744	1.41E+114
Standard EA													
Mean	18.039	−6.73E+19	1.002	2.22E−8	47.295	430.85	**2.0798**	−32,497	17,433	3.0025	0.226	334.26	−8.67E+113
Min	16.476	−6.98E+19	1.0016	1.42E−8	33.943	360.2	1.8998	−33,251	14,236	2.4451	0.1837	215.57	−3.36E+114
Max	20.081	−6.56E+19	1.0023	2.89E−8	57.872	470.22	2.1998	−31,514	20,415	3.3962	0.2496	446.7	−4.74E+112
Std.	1.3578	1.68E+18	0.0002	5.57E−9	9.3973	43.27	0.1303	733	2785	0.3535	0.0263	87.59	1.42E+114

4.2.1.3. Chaotic crossover and mutation: large scale benchmarks As a final experiment, the rival methods are exposed to a very demanding and large-scale version of the considered benchmark problems (200D version). This final numerical test helps us to make some firm decisions regarding the scalability of CEAs as well as their accuracy when facing to large-scale multimodal problems. The results of the experiment for the CEAs with chaotically encoded crossover operators are presented in Tables 14 and 15. Once more, the sinusoidal CEA shows an explicit domination over the other optimizers. Such a fact demonstrates the high potential of the sinusoidal CEA for handling large-scale optimization problems. However, it seems that for some of the problems, other versions of the CEAs, i.e. Leibovitch, and sine CEAs, can yield acceptable results as well. This is while such an observation was not valid for 100D benchmarks. This brings us to the conclusion that the performance of CEA with sinusoidal crossover shows a slight degeneration for the 200D problems.

Tables 16 and 17 list the simulation results for the CEAs with chaotically encoded mutation operators. An interesting observation pertaining to this set of the experiments is that most of the rival techniques could show acceptable results, at least, for one of the benchmark problems. However, the Gauss–Mouse map is still the most dominant chaotic sequence at the heart of mutation operator. For this experiment, the relatively same observation is valid. It can be seen that the standard EA preserves its acceptable performance while the EAs with chaotic mutation could not keep their performance by increasing the dimensionality of benchmark problems. For this set of the experiments, the standard EA retains its quality as it outperforms its chaotic counterparts for two of the benchmark problems. Based on such facts, it can be concluded that embedding the chaotic maps within the algorithmic functioning of EAs makes them very sensible.

Obviously, some types of chaotic maps improve the performance of the standard EA while some other types undermine its performance significantly. Hence, the selection of a suitable chaotic map is really important. The same conclusion is valid in view of the robustness capability of the rival techniques. Among the 27 problems, for both of the experiments, the standard EA shows a very acceptable rate of the robustness for 18 problems. For these cases, only a few types of CEAs can show comparative robustness. However, in the case of f_{11}, f_{12}, f_{16}, f_{17}, f_{18}, f_{19}, f_{20}, f_{23} and f_{26} benchmarks, the robustness of the most of the CEAs are really higher than the standard EA.

4.2.1.4. Real-time evolution and scalability results Figures 4 and 5 indicate the real-time mean performance of the rival techniques for optimizations of the 200D benchmarks over 1000 iterations, for crossover tests. This figure lets us evaluate the both real-time evolution and accuracy of the algorithms. As it can be seen, for most of the cases, the sinusoidal CEA shows a fast convergence behavior. Besides, except f_3, f_{13}, f_{14}, f_{23}, f_{24} benchmarks, the dominancy/eligibility of the sinusoidal CEA over the other techniques is really obvious. On contrary to some types of metaheuristics which focus on the exploration at the early iterations and then shift to the exploitation, the implemented CEAs try to have a balance between the exploration and exploitation capabilities. Apparently, for most of the benchmark problems, a permanent gradual evolution is observed for the whole optimization period, and also, a smooth evolution towards the global solution can be recognized. Such trait of the designed CEAs is very advantageous as the gradual evolution ensures that the optimizer does not trap into a local pitfall, and thus, an unacceptable premature convergence is prevented.

To evaluate the overall performance of the rival techniques, the bar diagrams of the mean performances for all of the conducted experiments, including the both crossover and mutation tests, are provided in Figs. 6 and 7. As it can be seen, for the crossover tests, the sinusoidal CEA preserves its dominancy for the benchmarks of different dimensionalities (medium

Table 14 Statistical results of the optimizations for 200D version of benchmarks ($f_1 - f_{14}$)

Crossover tests	f_1	f_2	f_3	f_4	f_5	f_6	f_7	f_8	f_9	f_{10}	f_{11}	f_{12}	f_{13}	f_{14}
Chebyshev CEA														
Mean	0.3830	0.4049	− 3.4635	386,255	− 106.68	7.5755	0.2140	0.0023	− 134.48	3.2065	5.8727	− 142.09	1.67E8	− 6.89E−10
Min	0.3128	0.2996	− 3.4705	298,477	− 114.06	6.2478	0.1671	0.0020	− 139.06	0.7099	2.1671	− 143.49	1.35E8	− 2.32E−09
Max	0.4453	0.4531	− 3.4541	514,867	− 101.49	9.0891	0.2851	0.0027	− 132.06	6.7431	9.3464	− 139.90	2.13E8	− 2.11E−12
Std.	0.0493	0.0648	0.0065	90,953	4.9957	1.1165	0.0439	0.0002	2.8426	2.5347	2.9827	1.5099	3.72E7	9.52E−10
Circle CEA														
Mean	0.4021	0.4467	− 3.4687	325,802	− 104.52	6.4904	0.1944	0.0017	− 133.60	2.1879	7.6506	− 140.64	1.64E8	− 1.31E−09
Min	0.3242	0.3259	− 3.4714	271,765	− 110.74	6.0583	0.1500	0.0015	− 137.66	0.1423	2.7380	− 144.45	1.11E8	− 4.37E−09
Max	0.5067	0.6222	− 3.4647	373,383	− 101.67	7.8251	0.2530	0.0024	− 125.05	6.0752	12.806	− 134.94	2.27E8	− 6.96E−11
Std.	0.0824	0.1317	0.0029	36,951	3.6733	0.7533	0.0491	0.0004	4.9523	2.3703	4.3040	3.7887	4.15E7	1.77E−09
Gauss–Mouse CEA														
Mean	0.2580	0.3336	− 3.0324	219,553	− 105.65	**4.4992**	0.1302	0.0013	− 139.60	0.3335	4.9603	− 144.50	1.54E8	− 1.56E−10
Min	0.2372	0.3073	− 3.4819	170,340	− 111.09	3.7652	0.1037	0.0010	− 144.24	0.0745	0.6389	− 150.03	9.98E7	− 4.73E−10
Max	0.2781	0.3690	− 1.2463	260,468	− 96.569	5.9123	0.1714	0.0015	− 135.43	1.2040	13.897	− 141.30	2.15E8	− 5.49E−12
Std.	0.0176	0.0250	0.9984	35,326	5.5700	0.8671	0.0256	0.0001	3.6683	0.4887	5.4145	3.2969	4.19E7	1.86E−10
Liebovitch CEA														
Mean	0.2969	**0.3147**	**− 3.4791**	195,167	− 108.45	4.6561	0.1570	0.0013	− 138.30	4.3475	2.3582	− 144.25	1.97E8	− 3.49E−11
Min	0.2181	0.2760	− 3.4836	160,233	− 112.16	4.3887	0.1008	0.0011	− 142.85	0.0905	0.1394	− 148.65	1.63E8	− 1.32E−10
Max	0.5128	0.4140	− 3.4755	260,472	− 104.19	4.8322	0.2128	0.0017	− 129.85	18.317	3.6654	− 139.89	2.61E8	− 2.11E−12
Std.	0.1228	0.0571	0.0032	41,193	3.4378	0.1740	0.0432	0.0002	5.0469	7.9132	1.5073	3.2562	3.90E7	5.53E−11
Logistic CEA														
Mean	0.2662	0.3570	− 2.0876	206,710	− 108.61	5.2537	0.1547	0.0014	− 139.48	1.1247	1.5546	− 146.46	2.35E8	− 5.08E−12
Min	0.2457	0.2954	− 3.4796	177,994	− 111.87	3.8225	0.1425	0.0010	− 143.10	0.0940	0.0357	− 157.40	1.38E8	− 1.96E−11
Max	0.2777	0.4481	− 0.9945	256,287	− 102.62	6.8176	0.1754	0.0016	− 135.78	4.0959	4.5233	− 136.84	3.12E8	− 1.20E−13
Std.	0.0134	0.0627	1.2731	38,746	3.8514	1.2031	0.0133	0.0002	3.3253	1.6772	1.8311	8.1177	6.88E7	8.28E−12

Table 14 continued

Crossover tests	f_1	f_2	f_3	f_4	f_5	f_6	f_7	f_8	f_9	f_{10}	f_{11}	f_{12}	f_{13}	f_{14}
Piecewise CEA														
Mean	0.3002	0.3295	− 3.0287	246,055	− 105.36	5.8043	0.1449	0.0015	− 133.13	0.1944	3.0936	− 142.63	1.58E8	− 5.43E−10
Min	0.2464	0.2769	− 3.4814	212,978	− 108.93	5.0103	0.0966	0.0012	− 139.90	0.0622	0.5154	− 146.10	9.29E7	− 2.32E−09
Max	0.3364	0.4829	− 1.2399	289,992	− 100.20	6.3308	0.2457	0.0019	− 127.02	0.3452	4.5649	− 138.77	2.04E8	− 1.53E−12
Std.	0.0367	0.0870	0.9999	34,780	3.2010	0.5035	0.0586	0.0002	4.9594	0.1216	1.6827	2.8335	4.53E7	1.00E−09
Sine CEA														
Mean	0.5449	0.6579	− 3.0034	597,302	− 103.84	9.7797	0.2792	0.0027	− 132.77	7.1108	11.583	− 137.34	1.56E8	**− 2.85E−09**
Min	0.4822	0.3945	− 3.4551	499,764	− 106.90	7.2662	0.2524	0.0018	− 136.94	0.7307	3.4518	− 139.95	1.12E8	− 5.98E−09
Max	0.6958	0.8298	− 1.2101	717,159	− 99.690	12.292	0.3150	0.0036	− 126.63	12.351	20.735	− 134.47	2.53E8	− 8.06E−13
Std.	0.0912	0.1822	1.0024	84,134	2.6199	1.9410	0.0226	0.0006	4.1365	5.1712	6.3292	2.0005	5.55E7	3.00E−09
Sinusoidal CEA														
Mean	**0.2447**	0.3336	− 2.0902	**140,436**	**− 125.31**	4.7010	**0.1248**	**0.0013**	**− 144.86**	**0.0465**	**0.3034**	**− 164.31**	2.09E8	− 1.17E−13
Min	0.2002	0.2983	− 3.4844	103,261	− 128.70	4.0360	0.0930	0.0011	− 148.70	0.0398	0.0413	− 167.50	1.58E8	− 4.32E−13
Max	0.3685	0.4124	− 1.0058	168,911	− 122.41	5.1162	0.1600	0.0016	− 140.42	0.0575	0.9562	− 161.13	3.2E8	− 2.64E−15
Std.	0.0699	0.0457	1.2726	30,551	2.2580	0.4299	0.0262	0.0002	2.9419	0.0076	0.3758	2.6825	6.50E7	1.83E−13
Tent CEA														
Mean	0.2745	0.3232	− 3.4739	225,454	− 105.94	4.9440	0.1286	0.0014	− 138.98	1.2784	4.4878	− 142.18	1.52E8	− 1.86E−10
Min	0.1962	0.2632	− 3.4781	180,474	− 108.64	4.5647	0.1075	0.0013	− 144.00	0.1792	0.8885	− 146.25	1.14E8	− 6.50E−10
Max	0.3843	0.4059	− 3.4721	276,333	− 103.37	5.4778	0.1624	0.0016	− 128.71	4.9895	8.2150	− 139.12	1.91E8	− 1.11E−12
Std.	0.0750	0.0748	0.0024	38,164	1.8727	0.3627	0.0205	0.0001	5.9352	2.0773	3.0182	3.2729	3.23E7	2.70E−10
Standard EA														
Mean	0.3051	0.3349	− 2.5787	217,074	− 108.60	4.7489	0.1411	0.0013	− 139.65	0.8069	3.7654	− 143.73	**1.47E8**	− 3.66E−11
Min	0.2614	0.2684	− 3.4762	160,042	− 112.29	4.4284	0.1317	0.0012	− 142.16	0.0914	0.0639	− 149.28	9.47E7	− 1.32E−10
Max	0.3240	0.4430	− 1.2331	257,458	− 104.31	5.0468	0.1591	0.0016	− 136.48	3.1626	10.146	− 139.76	1.82E8	− 2.89E−12
Std.	0.0254	0.0681	1.2265	40,640	3.0578	0.2733	0.0117	0.0001	2.4008	1.3196	4.1529	4.1041	4.07E7	5.38E−11

Table 15 Statistical results of the optimizations for 200D version of benchmarks ($f_{15} - f_{27}$)

Crossover tests	f_{15}	f_{16}	f_{17}	f_{18}	f_{19}	f_{20}	f_{21}	f_{22}	f_{23}	f_{24}	f_{25}	f_{26}	f_{27}
Chebyshev CEA													
Mean	56.532	−5.92E+38	1.3225	2.10E−5	262.20	587.96	3.2798	−55,585	108,308	8.6498	2.1444	724.40	−6.33E+198
Min	53.303	−6.33E+38	1.1691	1.18E−5	233.41	493.24	3.1998	−57,393	96,897	7.8964	1.9846	583.67	−4.80E+198
Max	59.162	−4.97E+38	1.6191	3.74E−5	289.47	688.70	3.3998	−53,616	121,080	9.8103	2.3818	914.64	−2.32E+191
Std.	2.3907	5.41E+37	0.1757	1.14E−5	22.325	82.912	0.0836	1535	10,678	0.8873	0.1583	129.74	Inf
Circle CEA													
Mean	56.000	−3.55E+38	1.2536	1.46E−5	225.56	625.46	2.8798	−51,434	71,176	7.7839	2.1507	769.96	−5.60E+198
Min	53.337	−3.94E+38	1.1172	9.07E−6	215.35	493.60	2.3998	−54,852	57,286	6.6162	1.8720	527.82	−2.80E+199
Max	57.964	−3.26E+38	1.3510	2.02E−5	240.79	885.1	3.3998	−48,076	80,927	8.7468	2.4414	943.48	−6.48E+189
Std.	1.8897	2.44E+37	0.0999	4.02E−6	10.307	152.72	0.4086	2820	10,786	0.7640	0.2117	166.34	3.24E+69
Gauss–Mouse CEA													
Mean	55.744	−7.31E+38	1.1779	5.50E−6	225.07	671.33	2.8198	−55,630	76,148	10.099	1.5473	813.40	−3.31E+200
Min	54.256	−7.80E+38	1.0664	3.30E−6	202.81	526.99	2.6998	−57,714	50,199	8.5064	1.3136	656.99	−1.34E+201
Max	57.145	−6.86E+38	1.3071	7.32E−6	251.45	939.92	2.9998	−52,346	101,939	11.897	1.6542	1005.6	−4.76E+195
Std.	1.3486	4.18E+37	0.0919	1.68E−6	23.866	168.55	0.1303	2141	20,995	1.4012	0.1370	143.79	Inf
Liebovitch CEA													
Mean	56.217	−7.85E+38	1.2080	**5.36E−6**	222.57	815.13	2.9798	−54,850	82,010	8.6407	1.6006	746.16	−3.23E+201
Min	54.302	−8.41E+38	1.0967	3.07E−6	194.26	520.54	2.7998	−56,467	66,845	6.5932	1.4642	533.23	−1.60E+202
Max	58.192	−7.23E+38	1.2699	7.39E−6	242.12	1165.9	3.1998	−52,069	102,890	10.504	1.8569	946.60	−3.66E+196
Std.	1.5557	4.66E+37	0.0655	1.66E−6	21.574	233.70	0.1484	1936	16,159	1.4046	0.1578	169.64	Inf
Logistic CEA													
Mean	53.838	−1.11E+39	1.1937	7.66E−6	202.13	774.83	2.9398	−57,918	96,688	11.342	1.4696	761.10	−2.46E+202
Min	52.061	−1.23E+39	1.0851	4.71E−6	194.28	718.94	2.5998	−59,629	77,607	9.3894	1.2607	593.06	−1.06E+203
Max	56.225	−1.00E+39	1.2787	1.40E−5	210.15	842.07	3.1998	−55,562	126,262	13.093	1.6598	918.97	−7.63E+200
Std.	1.9451	9.09E+37	0.0825	3.67E−6	7.5579	48.913	0.2792	1507	18,752	1.5063	0.1433	116.71	Inf

Table 15 continued

Crossover tests	f_{15}	f_{16}	f_{17}	f_{18}	f_{19}	f_{20}	f_{21}	f_{22}	f_{23}	f_{24}	f_{25}	f_{26}	f_{27}
Piecewise CEA													
Mean	56.452	−6.18E+38	1.2006	9.17E−6	229.37	625.30	2.8598	−53,898	93,988	8.8809	1.5219	**700.12**	−6.88E+202
Min	54.050	−6.33E+38	1.1439	7.01E−6	199.79	446.50	2.5998	−55,080	71,823	7.5594	1.3557	589.44	−3.18E+203
Max	61.158	−5.84E+38	1.2695	1.30E−5	253.14	862.25	3.1998	−52,821	118,909	9.4957	1.6234	798.71	−8.70E+193
Std.	2.7815	1.99E+37	0.0498	2.82E−6	20.521	151.25	0.2701	1060	17,257	0.7775	0.1089	93.733	Inf
Sine CEA													
Mean	57.713	−2.65E+38	1.4266	2.67E−5	258.57	608.94	2.9798	−52,547	**67,204**	**7.5550**	2.8324	779.75	−6.16E+193
Min	55.985	−2.83E+38	1.1964	1.28E−5	213.15	570.16	2.6993	−54,301	49,068	6.7849	2.6060	721.68	−2.59E+194
Max	59.356	−2.42E+38	1.8241	3.52E−5	308.02	659.14	3.1998	−49,669	91,609	8.3740	2.9296	906.94	−1.52E+190
Std.	1.3050	1.79E+37	0.2357	8.88E−6	35.929	38.343	0.2167	1819	16,417	0.6889	0.1390	73.829	Inf
Sinusoidal CEA													
Mean	**45.934**	**−2.14E+39**	**1.0618**	6.06E−6	**182.49**	1082.8	3.2798	−**60,255**	138,330	13.445	**1.4243**	917.22	**−1.79E+217**
Min	41.735	−2.30E+39	1.0463	4.43E−6	155.92	1005.5	2.9998	−61,529	100,678	11.339	1.2464	790.81	−8.92E+217
Max	47.716	−1.96E+39	1.0915	8.94E−6	220.93	1139.4	3.4998	−57,914	158,705	15.430	1.5379	1053.9	−8.61E+211
Std.	2.4726	1.39E+38	0.0177	1.84E−6	30.337	54.584	0.2280	1446	22,309	1.8449	0.1329	120.23	Inf
Tent CEA													
Mean	55.772	−6.44E+38	1.2412	5.90E−6	237.94	**520.15**	2.8798	−55,690	88,085	8.7919	1.6281	759.45	−8.50E+201
Min	54.340	−7.59E+38	1.1493	5.25E−6	224.17	405.45	2.7998	−56,853	73,988	8.2158	1.3905	683.31	−4.24E+202
Max	56.790	−5.99E+38	1.3007	7.99E−6	250.35	610.47	2.9998	−53,133	98,629	9.4948	1.8457	938.07	−3.31E+191
Std.	0.9850	6.66E+37	0.0645	1.17E−6	9.5105	79.031	0.0836	1618	11,397	0.5560	0.2128	102.21	Inf
Standard EA													
Mean	55.857	−6.52E+38	1.2369	9.27E−6	239.59	929.65	**2.8198**	−53,767	82,678	8.3683	1.7081	806.05	−1.11E+200
Min	54.027	−7.07E+38	1.0860	5.26E−6	208.54	616.29	2.5998	−54,612	54,321	7.5019	1.4945	648.59	−4.43E+200
Max	57.660	−5.96E+38	1.3872	1.37E−5	271.26	1779.6	3.0998	−53,126	102,861	9.0702	1.8407	1160.0	−1.74E+196
Std.	1.4337	4.39E+37	0.1388	3.31E−6	29.466	493.92	0.1923	587	19,285	0.7455	0.1428	209.07	Inf

Table 16 Statistical results of the optimizations for 200D version of benchmarks ($f_1 - f_{14}$)

Mutation tests	f_1	f_2	f_3	f_4	f_5	f_6	f_7	f_8	f_9	f_{10}	f_{11}	f_{12}	f_{13}	f_{14}
Chebyshev CEA														
Mean	0.3532	0.3659	− 2.0838	105,186	− **130.345**	5.7754	0.1604	0.0018	− 144.071	0.1215	0.1036	− 164.652	2.16E+8	− 6.26E−13
Min	0.3143	0.3098	− 3.4783	91,167	− 134.681	4.6615	0.1190	0.0016	− 147.154	0.0649	0.0209	− 167.175	1.28E+8	− 1.12E−12
Max	0.4426	0.4487	− 1.0010	135,505	− 125.855	7.0103	0.2029	0.0022	− 139.003	0.2832	0.3549	− 161.933	2.93E+8	− 1.21E−13
Std.	0.0518	0.0525	1.2733	18,295	3.3712	0.9639	0.0369	0.0002	3.4507	0.0913	0.1412	1.9934	6.96E+7	4.91E−13
Circle CEA														
Mean	0.2584	0.3018	− **2.5855**	113,584	− 125.084	3.2850	0.1062	0.0010	− 140.699	0.0456	**0.0504**	− 164.960	1.57E+8	− **6.92E−11**
Min	0.2161	0.2119	− 3.4851	91,500	− 128.901	2.3233	0.0740	0.0009	− 145.038	0.0405	0.0121	− 166.327	1.31E+8	− 2.52E−10
Max	0.3826	0.3574	− 1.2401	140,998	− 116.798	3.7536	0.1299	0.0013	− 135.247	0.0505	0.1673	− 163.892	1.74E+8	− 1.12E−12
Std.	0.0699	0.0580	1.2280	17,761	5.0865	0.5629	0.0252	0.0001	3.5481	0.0046	0.0663	0.9174	1.78E+7	1.06E−10
Gauss–Mouse CEA														
Mean	0.1644	0.2125	− 2.1499	**33,459**	− 123.744	**1.7937**	**0.0698**	**0.0006**	− 144.862	**0.0273**	0.1796	− 162.730	1.54E+8	− 4.59E−12
Min	0.1468	0.1866	− 3.4939	27,978	− 131.873	1.5836	0.0435	0.0006	− 147.743	0.0215	0.0088	− 165.622	1.11E+8	− 1.98E−11
Max	0.1790	0.2366	− 1.2549	38,364	− 119.375	2.1914	0.1550	0.0007	− 143.147	0.0339	0.4282	− 159.717	2.64E+8	− 2.29E−13
Std.	0.0141	0.0232	1.2251	4416	5.1575	0.2323	0.0479	5.15E−5	2.1801	0.0046	0.2235	2.5864	6.29E+7	8.49E−12
Liebovitch CEA														
Mean	**0.1563**	**0.2053**	− 2.1011	37,938	− 124.301	2.4342	0.0777	0.0007	− 145.108	0.0349	0.3848	− 160.640	1.75E+8	− 4.35E−12
Min	0.1393	0.1796	− 3.4928	23,621	− 131.746	2.1643	0.0423	0.0006	− 150.034	0.0272	0.0137	− 164.392	1.19E+8	− 1.97E−11
Max	0.1782	0.2222	− 1.0136	53,912	− 117.178	2.5754	0.1181	0.0007	− 141.452	0.0392	1.0794	− 158.894	2.31E+8	− 1.21E−13
Std.	0.0161	0.0166	1.2729	11,490	5.3481	0.1646	0.0283	2.76E−5	3.5684	0.0046	0.5125	2.2442	4.82E+7	8.61E−12
Logistic CEA														
Mean	0.4320	0.2728	− 1.6416	65,182	− 129.229	5.2618	0.1634	0.0017	− **146.226**	0.2807	0.1927	− **166.393**	2.54E+8	− 7.08E−13
Min	0.1954	0.2153	− 3.4773	36,362	− 133.880	4.1111	0.0985	0.0015	− 149.349	0.0609	0.0157	− 169.545	1.38E+8	− 2.93E−12
Max	0.6772	0.3080	− 1.0004	89,694	− 121.969	7.3065	0.2359	0.0024	− 141.181	1.1143	0.3960	− 164.023	3.84E+8	− 3.64E−15
Std.	0.1957	0.0361	1.0316	22,702	4.4808	1.2273	0.0577	0.0004	3.8469	0.4662	0.1664	2.4792	8.97E+7	1.25E−12

Table 16 continued

Mutation tests	f_1	f_2	f_3	f_4	f_5	f_6	f_7	f_8	f_9	f_{10}	f_{11}	f_{12}	f_{13}	f_{14}
Piecewise CEA														
Mean	0.1970	0.2481	− 1.6998	50,506	− 124.253	2.9710	0.0945	0.0008	− 144.235	0.0373	0.1116	− 163.827	1.62E+8	− 3.98E−12
Min	0.1552	0.2166	− 3.4930	39,859	− 133.138	2.5292	0.0697	0.0007	− 146.688	0.0285	0.0097	− 166.359	1.16E+8	− 1.98E−11
Max	0.2937	0.2697	− 1.2504	68,775	− 119.764	3.5550	0.1467	0.0009	− 142.318	0.0502	0.2858	− 158.963	2.23E+8	− 9.45E−15
Std.	0.0570	0.0232	1.0024	12,078	5.3892	0.4371	0.0319	9.24E−5	1.8003	0.0081	0.1344	2.9589	4.97E+7	8.82E−12
Sine CEA														
Mean	0.3006	0.5650	− 2.5724	135,653	− 124.245	4.7153	0.1466	0.0018	− 138.738	0.0665	0.4705	− 163.058	2.43E+8	− 1.24E−11
Min	0.2648	0.4797	− 3.4702	90,091	− 133.409	3.8251	0.1037	0.0013	− 145.288	0.0555	0.0339	− 164.140	2.14E+8	− 2.70E−11
Max	0.3462	0.7147	− 1.2321	233,213	− 119.061	5.9413	0.1933	0.0025	− 131.603	0.0794	1.4177	− 162.193	3.00E+8	− 4.64E−14
Std.	0.0322	0.0924	1.2234	56,835	5.8520	0.7933	0.0361	0.0005	5.3500	0.0090	0.5568	0.7447	3.52E+7	1.17E−11
Sinusoidal CEA														
Mean	0.5120	0.4083	− 1.0749	54,452	− 140.720	7.8032	0.1748	0.0021	− 145.402	0.1195	0.0187	− 181.522	3.97E+8	− 1.95E−14
Min	0.2910	0.3351	− 1.2375	37,721	− 144.840	6.3901	0.1418	0.0016	− 149.127	0.0522	0.0133	− 182.967	3.27E+8	− 6.43E−14
Max	0.9375	0.5788	− 0.9501	73,552	− 137.842	9.5711	0.2221	0.0027	− 141.982	0.3464	0.0220	− 180.439	4.56E+8	− 3.65E−15
Std.	0.2695	0.1018	0.1474	15,855	2.8950	1.3082	0.0328	0.0004	2.8357	0.1270	0.0037	0.9552	5.59E+7	2.53E−14
Tent CEA														
Mean	0.1961	0.2400	− 2.5939	44,309	− 125.690	3.0463	0.0854	0.0008	− 143.316	0.0339	0.0980	− 164.923	1.59E+8	− 2.13E−11
Min	0.1739	0.1938	− 3.4925	34,576	− 132.028	2.5425	0.0583	0.0007	− 148.889	0.0244	0.0087	− 169.907	1.14E+8	− 7.06E−11
Max	0.2242	0.3021	− 1.2499	60,173	− 120.227	3.2904	0.1105	0.0009	− 136.250	0.0416	0.3407	− 162.675	1.86E+8	− 1.13E−12
Std.	0.0217	0.0410	1.2266	10,316	5.3745	0.3219	0.0225	0.0001	4.7241	0.0067	0.1418	2.9449	2.82E+7	2.95E−11
Standard EA														
Mean	0.3051	0.3349	− 2.5787	217,074	− 108.6	4.7489	0.1411	0.0013	− 139.65	0.8069	3.7654	− 143.73	**1.47E+8**	− 3.66E−11
Min	0.2614	0.2684	− 3.4762	160,042	− 112.29	4.4284	0.1317	0.0012	− 142.16	0.0914	0.0639	− 149.28	9.47E+7	− 1.32E−10
Max	0.324	0.443	− 1.2331	257,458	− 104.31	5.0468	0.1591	0.0016	− 136.48	3.1626	10.146	− 139.76	1.82E+8	− 2.89E−12
Std.	0.0254	0.0681	1.2265	40,640	3.0578	0.2733	0.0117	0.0001	2.4008	1.3196	4.1529	4.1041	4.07E+7	5.38E−11

Table 17 Statistical results of the optimizations for 200D version of benchmarks ($f_{15} - f_{27}$)

Mutation tests	f_{15}	f_{16}	f_{17}	f_{18}	f_{19}	f_{20}	f_{21}	f_{22}	f_{23}	f_{24}	f_{25}	f_{26}	f_{27}
Chebyshev CEA													
Mean	47.0318	**− 3.77E+39**	1.0784	9.93E−6	167.395	991.49	3.6799	− 65,229	107,853	9.1970	1.8422	883.85	**− 3.67E+224**
Min	45.6480	− 3.86E+39	1.0543	7.54E−6	155.296	871.51	3.2999	− 67,433	74,339	8.2671	1.6451	658.89	− 1.83E+225
Max	48.5657	− 3.68E+39	1.0975	1.56E−5	193.094	1198.77	3.7999	− 63,600	124,821	11.6220	2.0507	1061.76	− 1.84E+220
Std.	1.2517	7.36E+37	0.0161	3.28E−6	15.4547	145.12	0.2168	1806	21,676	1.3815	0.1874	147.22	Inf
Circle CEA													
Mean	45.0867	− 1.75E+39	1.0676	2.23E−6	158.221	826.87	2.9799	− 58,070	96,412	**3.8021**	1.5044	**744.10**	− 8.57E+219
Min	41.8548	− 1.80E+39	1.0466	1.90E−6	154.425	670.65	2.7999	− 59,022	61,608	3.1774	1.3791	597.41	− 3.95E+220
Max	47.6586	− 1.63E+39	1.0816	2.65E−6	165.790	1044.87	3.0999	− 56,555	122,572	5.1479	1.5930	1040.88	− 1.07E+217
Std.	2.5144	6.68E+37	0.0158	3.32E−7	4.6882	150.00	0.1304	1029	24,881	0.8047	0.0964	185.16	Inf
Gauss–Mouse CEA													
Mean	45.1691	− 1.82E+39	**1.0165**	2.00E−6	154.609	1165.41	3.7399	− 59,578	108,083	8.3532	0.8186	764.31	− 1.86E+224
Min	41.5084	− 1.99E+39	1.0120	1.23E−6	136.082	1000.48	3.3999	− 60,162	76,420	6.7484	0.7573	608.62	− 5.85E+224
Max	47.6283	− 1.73E+39	1.0241	3.02E−6	170.970	1340.90	3.9999	− 58,405	133,175	10.0641	0.9170	1029.15	− 9.19E+219
Std.	2.3351	9.79E+37	0.0049	6.74E−7	15.0576	134.60	0.2608	708	20,663	1.3293	0.0642	160.62	Inf
Liebovitch CEA													
Mean	46.9638	− 2.30E+39	1.0214	**1.64E−6**	160.056	1102.14	3.8199	− 61,704	95,029	9.8069	**0.8408**	845.02	− 3.29E+222
Min	43.9840	− 2.37E+39	1.0164	8.52E−7	146.063	1023.15	3.1999	− 63,022	84,851	8.4351	0.8022	667.10	− 1.25E+223
Max	48.7390	− 2.18E+39	1.0258	2.26E−6	169.048	1248.74	4.0999	− 61,069	111,960	10.9716	0.9579	1186.19	− 2.64E+220
Std.	1.8961	7.26E+37	0.0041	5.08E−7	9.3332	97.08	0.3564	795	10,449	1.0238	0.0661	212.29	Inf
Logistic CEA													
Mean	**43.9405**	− 3.65E+39	1.0300	1.08E−5	**135.728**	1221.36	4.5999	**− 66,419**	131,629	13.6115	1.2810	1012.56	− 1.35E+224
Min	41.4520	− 3.80E+39	1.0228	5.30E−6	116.961	1064.76	4.1999	− 68,862	103,899	11.9584	1.0841	805.35	− 5.51E+224
Max	45.7864	− 3.40E+39	1.0372	2.28E−5	158.518	1462.05	4.8999	− 64,696	153,996	15.1497	1.4583	1200.01	− 3.59E+220
Std.	1.9240	1.62E+38	0.0062	7.16E−6	20.5536	157.10	0.3240	1532	22,477	1.1496	0.1358	159.78	Inf

Table 17 continued

Mutation tests	f_{15}	f_{16}	f_{17}	f_{18}	f_{19}	f_{20}	f_{21}	f_{22}	f_{23}	f_{24}	f_{25}	f_{26}	f_{27}
Piecewise CEA													
Mean	45.4781	−2.12E+39	1.0351	3.02E−6	160.316	1013.21	3.4199	−60,165	96,151	6.5490	1.0776	844.74	−4.33E+221
Min	44.3144	−2.23E+39	1.0223	1.32E−6	134.251	821.03	2.9999	−61,226	68,441	5.5776	0.9463	675.23	−1.16E+222
Max	48.0556	−1.95E+39	1.0677	4.43E−6	168.485	1175.87	3.7999	−58,240	124,126	7.0905	1.1614	973.89	−1.54E+220
Std.	1.6717	1.14E+38	0.0190	1.13E−6	14.6638	127.42	0.3033	1278	23,544	0.6009	0.0828	118.74	Inf
Sine CEA													
Mean	46.6048	−2.05E+39	1.0990	4.17E−6	185.148	**660.83**	3.0599	−59,336	**89,790**	4.3577	2.0174	844.57	−2.33E+217
Min	44.5921	−2.19E+39	1.0782	2.82E−6	156.979	483.05	2.7999	−60,464	66,611	3.4634	1.8680	701.07	−1.14E+218
Max	50.0655	−1.92E+39	1.1290	5.47E−6	209.859	958.63	3.2999	−58,587	107,999	5.6310	2.2024	1097.11	−2.28E+214
Std.	2.1072	1.13E+38	0.0197	1.17E−6	21.7248	178.18	0.1949	904	15,481	0.8570	0.1473	153.44	Inf
Sinusoidal CEA													
Mean	36.6800	−4.28E+39	1.0522	8.15E−6	71.4813	1379.16	7.6599	−67,719	173,279	27.8893	2.2756	1547.00	−4.44E+227
Min	35.0564	−4.75E+39	1.0468	4.57E−6	58.7745	1189.86	7.1999	−69,360	135,874	24.0397	1.9489	1268.02	−1.60E+228
Max	40.2311	−4.11E+39	1.0627	1.17E−5	88.4667	1627.77	7.9999	−66,402	213,079	35.4935	2.6359	1765.21	−3.86E+226
Std.	2.1907	2.64E+38	0.0064	2.74E−6	11.0656	162.70	0.3130	1092	29,450	4.6572	0.2705	218.10	Inf
Tent CEA													
Mean	45.5315	−2.11E+39	1.0369	2.77E−6	153.025	1315.97	3.6399	−60,027	111,639	7.1572	1.0588	779.34	−1.68E+225
Min	39.2572	−2.29E+39	1.0269	1.52E−6	123.448	1047.80	3.2999	−61,796	98,010	5.9049	0.9899	621.47	−8.41E+225
Max	49.6800	−1.83E+39	1.0655	5.35E−6	168.346	2171.27	3.8999	−58,635	128,667	7.9224	1.1512	908.00	−5.01E+219
Std.	4.0871	1.80E+38	0.0163	1.53E−6	17.4550	480.89	0.2408	1291	14,568	0.8866	0.0620	118.37	Inf
Standard EA													
Mean	55.857	−6.52E+38	1.2369	9.27E−6	239.59	929.65	**2.8198**	−53,767	82,678	8.3683	1.7081	806.05	−1.11E+200
Min	54.027	−7.07E+38	1.086	5.26E−6	208.54	616.29	2.5998	−54,612	54,321	7.5019	1.4945	648.59	−4.43E+200
Max	57.66	−5.96E+38	1.3872	1.37E−5	271.26	1779.6	3.0998	−53,126	102,861	9.0702	1.8407	1160	−1.74E+196
Std.	1.4337	4.39E+37	0.1388	3.31E−6	29.466	493.92	0.1923	587	19,285	0.7455	0.1428	209.07	Inf

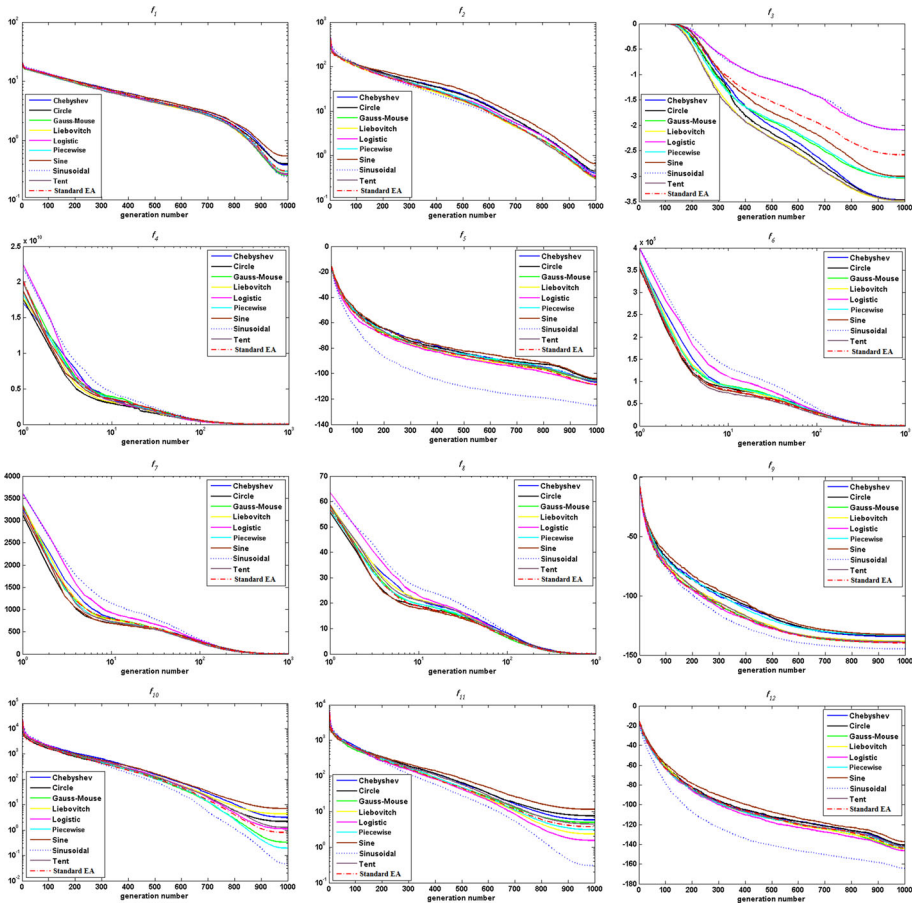

Fig. 4 Real-time mean performances of the rival techniques for optimization of 200D benchmark problems over 1000 iterations ($f_1 - f_{12}$)

scale, semi large scale and large scale). This, in turn, endorses the scalability of this type of chaotic map. For the mutation tests, the results are a little bit different. It can be seen that the logistic CEA yields the superior performance for the medium scale version of benchmarks while the Gauss/mouse CEA surpasses the other rival methods for the semi large scale and large scale benchmarks. Furthermore, the results show that, for the large scale benchmarks, it is impossible to discriminate one of the approaches as the superior method. To be more to the point, it seems that the circle, logistic, and Gauss/mouse maps closely follow each other. For the mutation experiments, it can be interpreted that the performance of the methods are very sensible to the dimensionality (scale) of the benchmarks.

4.2.1.5. Time complexity analysis At this point, it can be concluded that the CEAs with sinusoidal crossover and Gauss–Mouse mutation can show very promising outcomes with respect to the accuracy, robustness and scalability. However, these features are not enough to substantiate the applicability of the mentioned CEAs for practical applications. Maybe, the computational power of those algorithms is guaranteed at the cost of a higher computational complexity. To be more to the point, without performing a time complexity analysis, we cannot claim that the CEAs with sinusoidal crossover and Gauss–Mouse mutation are the

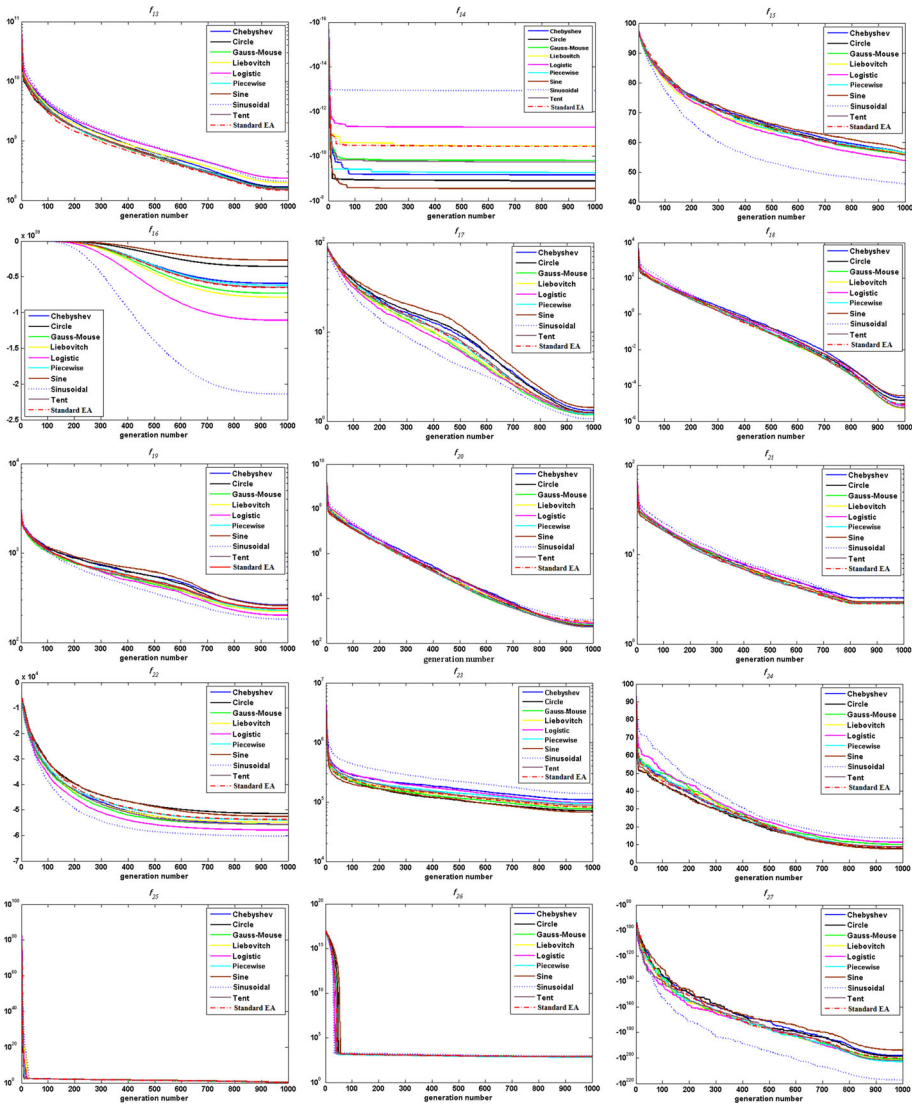

Fig. 5 Real-time mean performances of the rival techniques for optimization of 200D benchmark problems over 1000 iterations ($f_{13} - f_{27}$)

best choices among the existing rival methods. Thus, here, a time complexity analysis is performed to check whether the CEAs with sinusoidal crossover and Gauss–Mouse mutation are computationally efficient as well.

Table 18 lists the results of a time complexity analysis for f_4 benchmark problem in 3 different dimensions using both chaotic mutation and crossover operators. As it can be observed, the algorithmic complexities of the CEAs with sinusoidal map and the embedded crossover and the Gauss–Mouse mutation operators are quite acceptable. In most of the cases, the CEAs with sinusoidal crossover and Gauss–Mouse mutation operators are among the algorithms with the lowest computational complexities. The results of the complexity

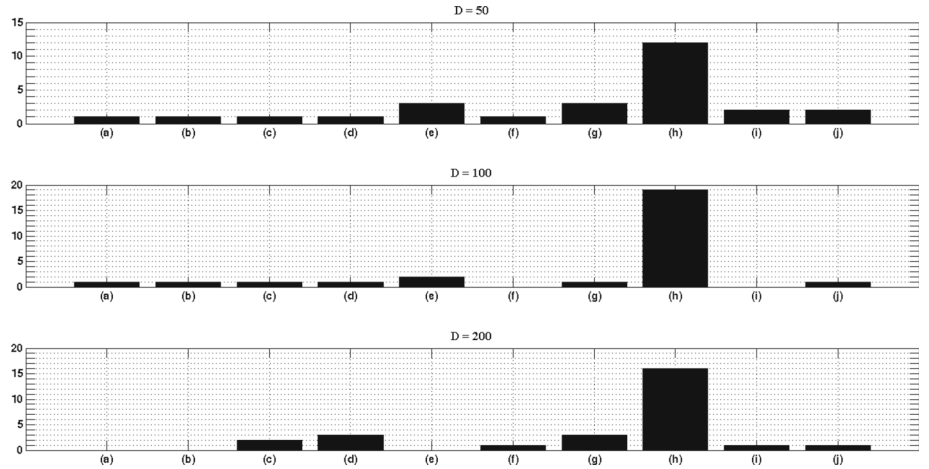

Fig. 6 Number of success of the standard EAs for crossover tests, **a** Chebyshev CEA, **b** circle CEA, **c** Gauss/mouse CEA, **d** Liebovitch CEA, **e** logistic CEA, **f** piecewise CEA, **g** sine CEA, **h** sinusoidal CEA, **i** tent CEA, **j** standard EA

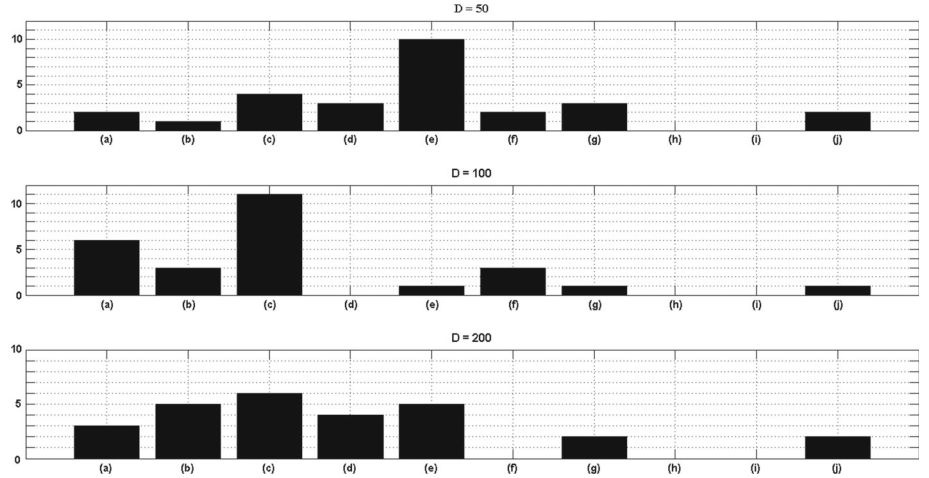

Fig. 7 Number of success of the standard EAs for mutation tests, **a** Chebyshev CEA, **b** circle CEA, **c** Gauss/mouse CEA, **d** Liebovitch CEA, **e** logistic CEA, **f** piecewise CEA, **g** sine CEA, **h** sinusoidal CEA, **i** tent CEA, **j** standard EA

experiments confirm the high potential of the CEAs with sinusoidal crossover and Gauss–Mouse mutation operators for the optimization tasks.

4.2.1.6. Convergence analysis At the final stage of the numerical experiments, the authors are to investigate the convergence behavior of the sinusoidal CEA. This helps the readers to discern whether embedding the sinusoidal chaos into the EA does not undermine its ability in balancing the exploration/exploitation over the optimization process. Previously, through a tentative experiment, it was indicated that the basic EA has the power of balancing the exploration/exploitation of the chromosomes. Here, the same experiment is conducted for sinusoidal CEA.

Table 18 Time complexity analysis of the rival algorithms for f_4 benchmark function

Algorithms	HX crossover operator				AGS mutation operator			
	T_0	T_1	T_2	Complexity	T_0	T_1	T_2	Complexity
D = 50								
Chebyshev CEA	0.917616	1.000128	3.959233	3.2247	0.917616	1.000128	4.126456	3.4070
Circle CEA	0.917616	1.000128	3.882333	3.1409	0.917616	1.000128	4.012745	3.2831
Gauss–Mouse CEA	0.917616	1.000128	3.828227	3.0820	0.917616	1.000128	3.909475	3.1705
Logistic CEA	0.917616	1.000128	4.040570	3.3134	0.917616	1.000128	4.124656	3.4050
Liebovitch CEA	0.917616	1.000128	3.821975	3.0751	0.917616	1.000128	3.865736	3.1229
Piecewise CEA	0.917616	1.000128	4.103777	3.3823	0.917616	1.000128	4.109385	3.3884
Sine CEA	0.917616	1.000128	3.860645	3.1173	0.917616	1.000128	3.878495	3.1368
Sinusoidal CEA	0.917616	1.000128	3.881615	3.1401	0.917616	1.000128	3.898475	3.1586
Tent CEA	0.917616	1.000128	4.042638	3.3156	0.917616	1.000128	4.085734	3.3626
Standard EA	0.917616	1.000128	3.912586	3.1739	0.917616	1.000128	3.912586	3.1739
D = 100								
Chebyshev CEA	0.917616	1.747036	5.585297	4.1828	0.917616	1.747036	5.717355	4.3268
Circle CEA	0.917616	1.747036	5.395774	3.9763	0.917616	1.747036	5.424676	4.0078
Gauss–Mouse CEA	0.917616	1.747036	5.327894	3.9023	0.917616	1.747036	5.523861	4.1159
Logistic CEA	0.917616	1.747036	5.643388	4.2461	0.917616	1.747036	5.774867	4.3895
Liebovitch CEA	0.917616	1.747036	5.233707	3.7997	0.917616	1.747036	5.334576	3.9096

Table 18 continued

Algorithms	HX crossover operator				AGS mutation operator			
	T_0	T_1	T_2	Complexity	T_0	T_1	T_2	Complexity
Piecewise CEA	0.917616	1.747036	6.018872	4.6553	0.917616	1.747036	5.960386	4.5916
Sine CEA	0.917616	1.747036	5.316153	3.8845	0.917616	1.747036	5.442052	4.0268
Sinusoidal CEA	0.917616	1.747036	5.333344	3.9082	0.917616	1.747036	5.384756	3.9643
Tent CEA	0.917616	1.747036	5.495722	4.0852	0.917616	1.747036	5.478571	4.0666
Standard EA	0.917616	1.747036	5.306763	3.8791	0.917616	1.747036	5.306763	3.8793
D = 200								
Chebyshev CEA	0.917616	3.735394	10.43521	7.3013	0.917616	3.735394	10.45526	7.3232
Circle CEA	0.917616	3.735394	10.13627	6.9755	0.917616	3.735394	10.01274	6.8409
Gauss–Mouse CEA	0.917616	3.735394	9.922562	6.7426	0.917616	3.735394	9.989375	6.8155
Logistic CEA	0.917616	3.735394	10.62156	7.5044	0.917616	3.735394	10.85989	7.7641
Liebovitch CEA	0.917616	3.735394	9.790479	6.5987	0.917616	3.735394	9.901924	6.7202
Piecewise CEA	0.917616	3.735394	11.14322	8.0729	0.917616	3.735394	11.27452	8.2160
Sine CEA	0.917616	3.735394	10.11779	6.9554	0.917616	3.735394	10.15242	6.9931
Sinusoidal CEA	0.917616	3.735394	10.00222	6.8294	0.917616	3.735394	10.02846	6.8581
Tent CEA	0.917616	3.735394	10.36193	7.2214	0.917616	3.735394	9.919285	6.7391
Standard EA	0.917616	3.735394	9.865378	6.6803	0.917616	3.735394	9.865378	6.6803

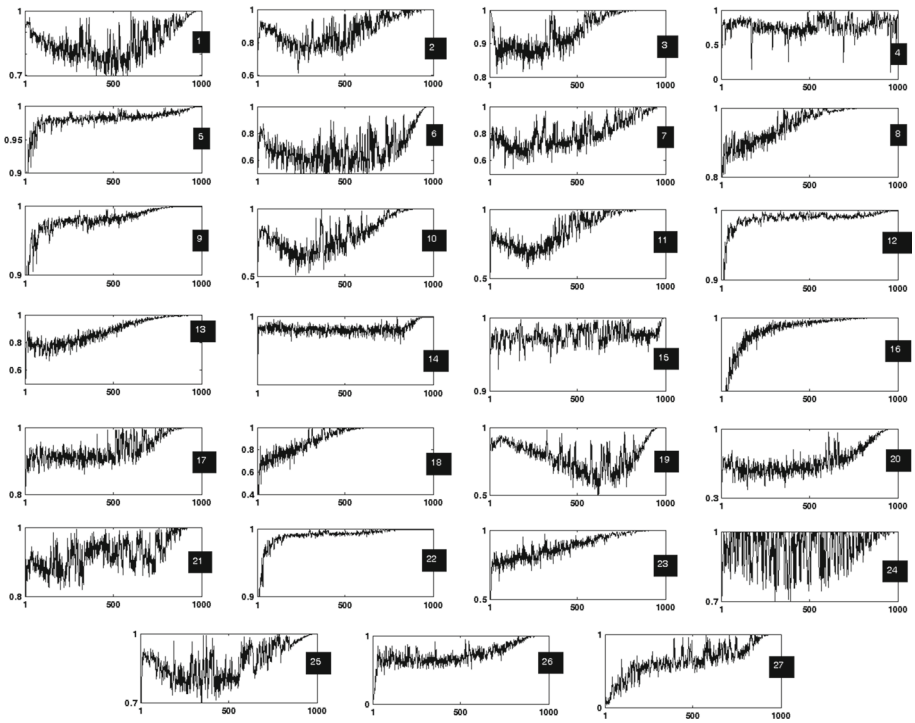

Fig. 8 Convergence behavior of the sinusoidal CEA for the benchmark problems

The convergence test is done for the 50D version of the benchmark problems with chaotic crossover operators to avoid any miss-judgment. Figure 8 reveals the convergence behavior of sinusoidal CEA for the considered problems. As it is obvious, the convergence behaviors of CEAs are very acceptable. It seems that the chaotic agents of the CEA are really capable of balancing their exploration/exploitation characteristics which results in a correct convergence at the end of the optimization procedure.

4.2.2 Optimizing the operating parameters of Damavand power plant

At the second stage, the experiments are continued by applying the rival algorithms to a demanding real-life problem. In general, optimizing the operating parameters of a power plant can be really demanding. This is because of the steps required for implementing a proper objective function. The optimization of power plants is not possible unless several constraints and decision variables are taken into account. Besides, the objective function should be formulated by coupling several non-linear mathematical equations. This in turn produces a non-convex, highly multimodal and nonlinear objective function. Therefore, exposing the rival algorithms to such a problem can provide us with reliable feed-back regarding their potentials in handling demanding practical problems. In a recent study by the authors' research group, a very large-scale power plant known as Damavand power plant has been analyzed based on different laws of thermodynamics (Mozaffari et al. 2012b). Damavand power plant is the biggest power plant in the middle-east sited in Iran consisting of 12 symmetric phases which work in parallel, and each phase hosts one steam turbine (ST) and two gas turbine (GT) power systems. This power plant plays an important role by supplying

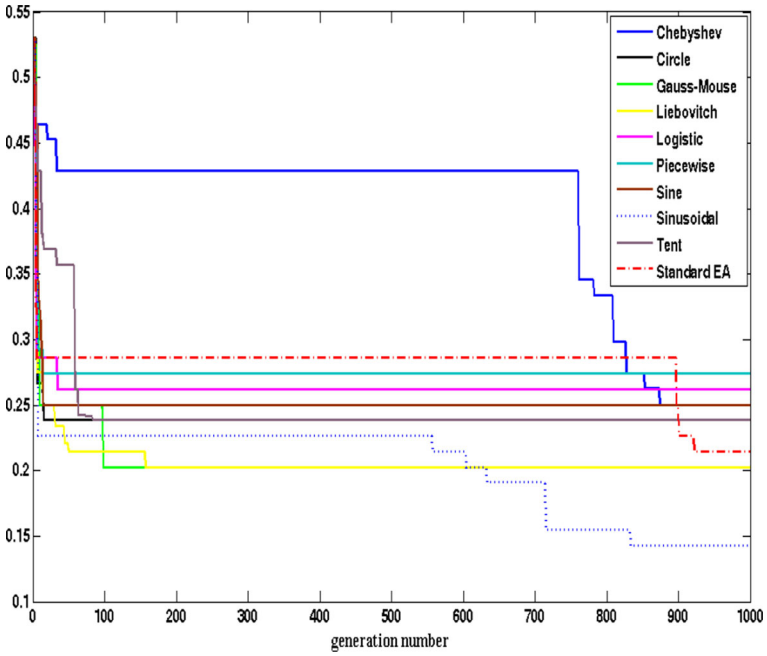

Fig. 9 Performances of the rival techniques for optimizing the operating parameters of Damavand power plant

over 2300 MW electricity for industrial, agricultural, civil and domestic regions for various provinces of Iran. The stepwise and detailed procedures required for implementing the constraints and objective functions of the power plant are presented in (Mozaffari et al. 2012b). Therefore, here, for the sake of brevity, the detailed formulations required for simulating the power plant are not provided. To optimize the Damavand power plant, 9 decision variables, i.e. compressor pressure ratio (r_p), isentropic efficiency of compressor (η_C), isentropic efficiency of gas turbine (η_T), temperature of combustion products (T_5, T_{14}), temperatures of air preheater products entering the combustion engines (T_3, T_{12}), temperatures of compression products (T_2, T_{11}) air temperature (T_1, T_{10}), air mass flow rate (m_a) and fuel mass flow rate (m_f), should be considered. Besides, to obtain practical results, a set of nonlinear constraints should be devised [for more information please see (Mozaffari et al. 2012b)]. The optimal design of operating parameters is not possible unless two conflicting objective functions, i.e. maximizing the power output (energetic efficiency) and minimizing the total cost, are taken into account. The mathematical formulation required for implementing these two objective functions are given in the online supplementary file. Here, the concept of self-adaptive penalty function (SAPF) is used to equalize the impact of constraints in the objective function (Tessema 2006). Therefore, all of the rival techniques should optimize a single objective function which always yields the normalized objective values within the range of unity. Considering the SAPF strategy, the objective function can be formulated as:

$$F_{SAPF}(X) = -f_1(X) + 10^{-6} f_2(X) + \frac{1}{23} \sum_{j=1}^{23} \frac{c_j(X)}{c \ \max_j} \tag{15}$$

The mathematical procedures which yield the above function are given in the online supplementary file. Figure 9 indicates the performance of the rival techniques for optimizing

Table 19 Obtained results of the power plant optimization problem

Decision variables	r_p	η_T	η_c	T_5, T_{14}	T_3, T_{12}	T_2, T_{11}	T_1, T_{10}	$m_{a,1}, m_{a,2}$	$m_{f,1}, m_{f,2}$	f_1	f_2
Chebyshev CEA	9.93	87	81	1342.6	783.5	605.3	299.1	475.9	8.8	45.5	5.32E+2
Circle CEA	10.31	86	83	1424.8	776.1	603.3	299.1	482.4	9.9	45.8	4.89E+2
Gauss–Mouse CEA	10.15	89	82	1356.8	783.3	604.6	299.1	483.2	9.5	46.7	5.45E+2
Logistic CEA	10.23	88	84	1393.3	784.9	603.7	300.2	490.5	9.7	48.6	5.32E+2
Liebovitch CEA	10.15	89	82	1356.8	783.3	604.6	299.1	483.2	9.5	46.7	5.45E+2
Piecewise CEA	10.24	88	84	1381.8	777.2	603.6	299.1	494.2	9.4	47.8	5.32E+2
Sine CEA	9.93	87	81	1342.6	783.5	605.3	299.1	475.9	8.8	45.5	5.32E+2
Sinusoidal CEA	9.95	90	85	1445.8	771.5	604.4	300.2	498.8	10.1	**49.2**	**5.41E+2**
Tent CEA	10.31	86	83	1424.8	776.1	603.3	299.5	482.4	9.9	45.8	4.89E+2
Standard EA	10.65	89	84	1376.9	791.5	604.4	300.2	498.8	10.3	47.4	5.53E+2

the operating parameters of Damavand power plant. To avoid any miss-judgment, all of the rival metaheuristics start the optimization with the same initial population. As it can be seen, sinusoidal CEA converges to a more qualified solution. It is worth noting that the sinusoidal CEA is the only algorithm which can neatly balance its exploration/exploitation capabilities. Apparently, after the iteration of 560, this algorithm fosters its exploitation capability and therefore, escapes from the local pitfalls and finally converges to the most optimum solution. The numerical results including the values of the decision variables and the corresponding objective values are listed in Table 19. Obviously, the sinusoidal CEA suggests a vector of parameters which can consequently suggest an acceptable rate of energetic efficiency at a logical amount of cost.

5 Conclusions

In this research, the authors proposed a rigor test bed to effectively study the impact of chaotic maps into the algorithmic functioning of evolutionary algorithms (EAs). The experiments were composed of two different phases. At the first stage, several benchmark problems in medium, semi-large and large scale dimensions were utilized to investigate the convergence, scalability, accuracy and robustness of different versions of chaotic EAs (CEAs). Besides, the exploration/exploitation characteristics of the most successful CEA were evaluated empirically. At the next stage, a constraint real-life engineering problem was used to find out whether the derived conclusions are valid for practical problems. Based on the experiments, the following remarks were concluded:

(1) It was observed that the proposed boundary constraint handling technique (BCHT) can be reliably used within the structure of CEAs to direct the infeasible solutions towards feasible regions in the solution domain.
(2) By exposing the rival techniques to the various types of benchmarks with different scales, it was inferred that the CEAs with sinusoidal crossover and with Gauss–Mouse mutation can show very acceptable results in terms of the robustness, convergence and accuracy. Besides, it was observed that this approach could retain its acceptable quality during the optimization, and also, its performance did not degrade by increasing the dimensionality of the problems.
(3) Another important observation is that CEAs are not only capable of improving the accuracy of standard EA (because of their chaotic exploitation instinct) but also can retain an acceptable amount of robustness over the process. This fact was demonstrated in the both stages of the experiments.
(4) Through the conducted complexity analysis, it was revealed that embedding the chaos into the algorithmic functioning of EAs does not increase their computational complexity. Also, it was observed that the CEAs with sinusoidal crossover and with the Gauss–Mouse mutation (the most successful CEA) can show a similar convergence behavior as compared to the standard EA.

In the future, the authors will design an ensemble optimization frame based on the integration of different chaotic CEAs to find out whether it can improve the performance of single chaotic based metaheuristics.

Appendix A: Benchmark problems

See Table 20.

Table 20 Characteristics of the benchmark problems

Test problem	Objective function	Solution domain	Optimum value
f_1: Ackley	$-20\exp\left(-0.2\sqrt{\frac{1}{D}\sum_{i=1}^{D}x_i^2}\right)-\exp\left(-0.2\sqrt{\frac{1}{D}\sum_{i=1}^{D}\cos 2\pi x_i}\right)+20+e$	$[-32,32]^D$	$F([0,0,\ldots,0])=0$
f_2 : Alpine	$\sum_{i=1}^{D}\lvert x_i\sin(x_i)+0.1x_i\rvert$	$[-10,10]^D$	$F([0,0,\ldots,0])=0$
f_3: Sinusoidal	$-\left[2.5\prod_{i=1}^{D}\sin\left(\frac{(x_i-30)\pi}{180}\right)+\prod_{i=1}^{D}\sin\left(\frac{5(x_i-30)\pi}{180}\right)\right]$	$[0,180]^D$	$F([120,120,\ldots,120])=-3.5$
f_4: High Conditioned Elliptic	$\sum_{i=1}^{D}10^{\frac{6(i-1)}{D-1}}x_i^2$	$[-100,100]^D$	$F([-100,-100,\ldots,-100])=0$
f_5: Epistatic Michalewicz	$-\sum_{i=1}^{D}\sin\left(y_i^2\right)\sin^{20}\left(\frac{iy_i^2}{\pi}\right),\quad y_i=\begin{cases}x_i\cos(\pi/6)-x_{i+1}\sin(\pi/6) & i=1,3,5,\ldots<D\\ x_i\sin(\pi/6)+x_{i+1}\cos(\pi/6) & i=2,4,6,\ldots<D\\ x_i & i=D\end{cases}$	$[0,\pi]^D$	Dimension specific
f_6: Sphere	$\sum_{i=1}^{D}x_i^2$	$[-100,100]^D$	$F([0,0,\ldots,0])=0$
f_7: Griewank	$\frac{1}{4000}\sum_{i=1}^{D}x_i^2-\prod_{i=1}^{D}\cos(\frac{x_i}{\sqrt{i}})+1$	$[-600,600]^D$	$F([0,0,\ldots,0])=0$
f_8: Inverted Cosine Mixture	$0.1D-\left(0.1\sum_{i=1}^{D}\cos(5\pi x_i)-\sum_{i=1}^{D}x_i^2\right)$	$[-1,1]^D$	$F([0,0,\ldots,0])=0$
f_9: Inverted Cosine Wave	$-\sum_{i=1}^{D-1}(\exp(\frac{-(x_i^2+x_{i+1}^2+0.5x_ix_{i+1})}{8})\times(\cos(4\sqrt{x_i^2+x_{i+1}^2+0.5x_ix_{i+1}})))$	$[-5,5]^D$	$F([0,0,\ldots,0])=-D+1$

Table 20 continued

Test problem	Objective function	Solution domain	Optimum value
f_{10}: Levy	$\sin^2(\pi x_i) + \sum_{i=1}^{D-1}\left((x_i-1)^2(1+10\sin^2(\pi x_{i+1}))\right) + \left((x_D-1)^2(1+10\sin^2(\pi x_D)\right)$	$[-10, 10]^D$	$F([1, 1, \ldots, 1]) = 0$
f_{11}: Levy Montalvo 2	$0.1(\sin^2(3\pi x_1) + \sum_{i=1}^{D-1}\left((x_i-1)^2(1+10\sin^2(3\pi x_{i+1}))\right) + \left((x_D-1)^2(1+10\sin^2(2\pi x_D))\right)$	$[-5, 5]^D$	$F([1, 1, \ldots, 1]) = 0$
f_{12}: Michalewicz	$-\sum_{i=1}^{D}(\sin(x_i)\sin^{20}(\frac{ix_i^2}{\pi}))$	$[0, \pi]^D$	Dimension specific
f_{13}: Neumaier 3	$\sum_{i=1}^{D}(x_i-1)^2 - \sum_{i=2}^{D} x_i x_{i-1}$	$[-D^2, D^2]^D$	$F([D, \ldots, i(D+1-i)]) = -\frac{D(D+4)(D-1)}{6}$
f_{14}: Odd Square	$-\left(1+\frac{0.2\sqrt{\sum_{i=1}^{D}(x-b_i)^2}}{\sqrt{D}\max_{i\in[1,D]}\lvert x_i-b_i\rvert+0.1}\right)\cos(\pi\sqrt{D}\max_{i\in[1,D]}\lvert x_i-b_i\rvert)e^{-\frac{\sqrt{D}\max_{i\in[1,D]}\lvert x_i-b_i\rvert}{2\pi}}$	$[-15, 15]^D$	Dimension specific
f_{15}: Pathological	$\sum_{i=1}^{D-1}(0.5+\frac{\sin^2\sqrt{100x_i^2+x_{i+1}^2}-0.5}{1+0.001(x_i^2-2x_ix_{i+1}+x_{i+1}^2)^2})$	$[-100, 100]^D$	$F([0, 0, \ldots, 0]) = 0$
f_{16}: Paviani	$\sum_{i=1}^{D}[(\ln(x_i-2))^2+(\ln(10-x_i))^2] - \left(\prod_{i=1}^{D}x_i\right)^{0.2}$	$[2, 10]^D$	dimension specific

Table 20 continued

Test problem	Objective function	Solution domain	Optimum value
f_{17}: Periodic	$1+\sum_{i=1}^{D}(\sin x_i)^2-0.1\prod_{i=1}^{D}\exp(-x_i^2)$	$[-10,10]^D$	$F([0,0,\ldots,0])=0$
f_{18}: Quartic	$\sum_{i=1}^{D} ix^4+rand[0,1]$	$[-1.28,1.28]^D$	$F([0,0,\ldots,0])=0$
f_{19}: Rastrigin	$\sum_{i=1}^{D}\left[x_i^2-10\cos(2\pi x_i)+10\right]$	$[-5.12,5.12]^D$	$F([0,0,\ldots,0])=0$
f_{20}: Rosenbrock	$\sum_{i=1}^{D-1}\left[100(x_i^2-x_{i+1})^2+(1-x_i)^2\right]$	$[-2,2]^D$	$F([1,1,\ldots,1])=0$
f_{21}: Salomon	$1-\cos(2\pi\sqrt{\sum_{i=1}^{D}x_i^2})+0.1\sqrt{\sum_{i=1}^{D}x_i^2}$	$[-100,100]^D$	$F([0,0,\ldots,0])=0$
f_{22}: Schwefel 2.26	$-\sum_{i=1}^{D}x_i\sin\sqrt{\lvert x_i\rvert}$	$[-500,500]^D$	$F([420.96,\ldots,420.96])=-418.98D$
f_{23}: Schwefel 1.2	$\sum_{i=1}^{D}\left(\sum_{j=1}^{i}x_j\right)^2$	$[-100,100]^D$	$F([0,0,\ldots,0])=0$
f_{24}: Schwefel 2.21	$\max_{i\in[1,D]}\lvert x_i\rvert$	$[-100,100]^D$	$F([0,0,\ldots,0])=0$
f_{25}: Schwefel 2.22	$\sum_{i=1}^{D}\lvert x_i\rvert+\prod_{i=1}^{D}\lvert x_i\rvert$	$[-10,10]^D$	$F([0,0,\ldots,0])=0$
f_{26}: Zakharov	$\sum_{i=1}^{D}x_i^2+\left(\sum_{i=1}^{D}0.5ix_i\right)^2+\left(\sum_{i=1}^{D}0.5ix_i\right)^4$	$[-5,10]^D$	$F([0,0,\ldots,0])=0$
f_{27}: Schubert	$\prod_{i=1}^{D}\left(\sum_{j=1}^{5}j\cos((j+1)x_j+j)\right)$	$[-10,10]^D$	$F(x)\approx-186.73$

References

Abdechiri M, Meybodi MR, Bahrami H (2013) Gases Brownian motion optimization: an algorithm for optimization (GBMO). Appl Soft Comput 5:2932–2946

Abdechiri M, Faez K, Amindavar H, Bilotta E (2017a) Chaotic target representation for robust object tracking. Signal Process Image Commun 54:23–35

Abdechiri M, Faez K, Amindavar H (2017b) Visual object tracking with online weighted chaotic multiple instance learning. Neurocomputing 247:16–30

Abdechiri M, Faez K, Amindavar H, Bilotta E (2017c) The chaotic dynamics of high-dimensional systems. Nonlinear Dyn 87:2597–2610

Alatas B (2010a) Chaotic harmony search algorithms. Appl Math Comput 216:2687–2699

Alatas B (2010b) Chaotic bee colony algorithms for global numerical optimization. Expert Syst Appl 37:5682–5687

Alatas B (2011) Uniform big bang–chaotic big crunch optimization. Commun Nonlinear Sci Numer Optim 16:3696–3703

Alatas B, Akin E (2009) Chaotically encoded particle swarm optimization algorithm and its applications. Chaos Solitones Fractals 41:939–950

Alatas B, Akin E, Bedri Ozer A (2009) Chaos embedded particle swarm optimization algorithms. Chaos Solitons Fractals 40:1715–1734

Alikhani KJ, Hosseini SMM (2015) A new hybrid algorithm based on chaotic maps for solving systems of nonlinear equations. Chaos Solitons Fractals 81:233–245

Alikhani KJ, Hosseini SMM, Ghaini FMM (2016) A new optimization algorithm based on chaotic maps and golden section search method. Eng Appl Artif Intell 50:201–214

Arena P, Caponetto R, Fortuna L, Rizzo A, La Rosa M (2000) Self organization in non-recurrent complex systems. Int J Bifurc Chaos 10(5):1115–1125

Askarzadeh A, Coelho LDS (2014) A backtracking search algorithm combined with Burger's chaotic map for parameter estimation of PEMFC electrochemical model. Int J Hydrog Energy 39(21):11165–11174

Beyer HG, Schwefel HP (2002) Evolution strategies: a comprehensive introduction. Nat Comput 1(1):3–52

Bingol H, Alatas B (2016) Chaotic league championship algorithms. Arab J Sci Eng 41(12):5123–5147

Brameier M, Banzhaf W (2007) Linear genetic programming. Springer, New York

Caponetto R, Fortuna L, Fazzino S, Xibilia MG (2003) Chaotic sequences to improve the performance of evolutionary algorithms. IEEE Trans Evol Comput 7(3):289–304

Chelliah TR, Thangaraj R, Allamsetty S, Pant M (2014) Coordination of directional overcurrent relays using opposition based chaotic differential evolution algorithm. Int J Electr Power Energy Syst 55:341–350

Chen LN, Aihara K (1995) Chaotic simulated annealing by a neural network model with transient chaos. Neural Netw 8:915–930

Chen F, Tang B, Song T, Li L (2014) Multi-fault diagnosis study on roller bearing based on multi-kernel support vector machine with chaotic particle swarm optimization. Measurement 47:576–590

Cheng MY, Tran DH, Wu YW (2014) Using a fuzzy clustering chaotic-based differential evolution with serial method to solve resource-constrained project scheduling problems. Autom Constr 37:88–97

Civicioglu P, Besdok E (2013) A conceptual comparison of the Cuckoo-search, particle swarm optimization, differential evolution and artificial bee colony algorithms. Artif Intell Rev 39(4):315–346

Coelho LDS, Mariani VC, Guerra FA, da Luz MVF, Leite JV (2014) Multiobjective optimization of transformer design using a chaotic evolutionary approach. IEEE Trans Magn 50(2), Article ID: 7016504

Davendra D, Senkerik R, Zelinka I, Pluhacek M, Bialik-Davendra M (2014) Utilising the chaos-induced discrete self organising migrating algorithm to solve the lot-streaming flowshop scheduling problem with setup time. Soft Comput 18(4):669–681

Deb K, Agrawal RB (1995) Simulated binary crossover for continuous search space. Complex Syst 9:115–148

Deep K, Thakur M (2007) A new crossover operator for real coded genetic algorithms. Appl Math Comput 188(1):895–911

Devaney RL (1987) An introduction to chaotic dynamical systems. Addison-Wesley, Boston

El-Shorbagi MA, Mousa AA, Nasr SM (2016) A chaos-based evolutionary algorithm for general nonlinear programming problems. Chaos Solitons Fractals 85:8–21

Emami M, Mozaffari A, Azad NL, Rezaie B (2016) An empirical investigation into the effects of chaos on different types of evolutionary crossover operators for efficient global search in complicated landscapes. Int J Comput Math 93:3–26

Fathi A, Mozaffari A (2013) Modeling a shape memory alloy actuator using an evolvable recursive black-box and hybrid heuristic algorithms inspired based on the annual migration of salmons in nature. Appl Soft Comput 14:224–251

Fathi A, Mozaffari A (2014) Vector optimization of laser solid freeform fabrication system using a hierarchical mutable smart bee-fuzzy inference system and hybrid NSGA-II/self-organizing map. J Intell Manuf 25(4):775–795
Fogel LJ, Owens AJ, Walsh MJ (1966) Artificial intelligence through simulated evolution. Wiley, New York
Fourcade B, Tramblay AMS (1990) Universal multifractal properties of circle maps from the point of view of critical phenomena. J Stat Phys 61:639–665
Gandomi AH, Yang XS (2012) Evolutionary boundary constraint handling scheme. Neural Comput Appl 21:1449–1462
Gandomi AH, Yang XS (2013) Chaotic bat algorithm. J Comput Sci 5(2):224–232
Gandomi AH, Yang XS, Talatahari S, Alavi AH (2013a) Firefly algorithm with chaos. Commun Nonlinear Sci Numer Simul 18:89–98
Gandomi AH, Yun GJ, Yang XS, Talatahari S (2013b) Chaos-enhanced accelerated particle swarm optimization. Commun Nonlinear Sci Numer Simul 18:327–340
Gao H, Zhang Y, Liang S, Li DA (2006) New chaotic algorithm for image encryption. Chaos Solitons Fractals 29:393–399
Gao J, Xiao M, Zhang W (2010) A rapid chaos genetic algorithm. Lect Notes Comput Sci 6145:425–431
Goldberg DE (1989) Genetic algorithms in search optimization and machine learning. Addison-Wesley, Boston
Gong W, Wang S (2009) Chaos ant colony optimization and applications. In: 4th international conference on internet computing for science and engineering, pp 301–303
He Y, Xu Q, Yang S, Han A, Yang L (2014) A novel chaotic differential evolution algorithm for short-term cascaded hydroelectric system scheduling. Int J Electr Power Energy Syst 61:455–462
Heidari AA, Abbaspour RA, Jordehi AR (2017) An efficient chaotic water cycle algorithm for optimization tasks. Neural Comput Appl 28(1):57–85
Holland JH (1975) Adaption in natural and artificial systems. University of Michigan Press, Ann Arbor
Huaguang Z, Yongbing Q (2001) Modeling, identification and control of a class of nonlinear systems. IEEE Trans Fuzzy Syst 9:349–354
Huang X (2012) Image encryption algorithm using Chebyshev generator. Nonlinear Dyn 67:2411–2417
Jiang C, Bompard E (2005) A hybrid method of chaotic particle swarm optimization and linear interior for reactive power optimization. Math Comput Simul 68:57–65
Karaboga D, Akay B (2009) A survey: algorithms simulating bee swarm intelligence. Artif Intell Rev 31:61–85
Karaboga D, Basturk B (2007) A powerful and efficient algorithm for numerical function optimization: artificial bee colony algorithm. J Glob Optim 39(3):459–471
Kaveh A, Sheikholeslami R, Talatahari S, Keshvari-Ikhihci M (2014) Chaotic swarming of particles: a new method for size optimization of truss structures. Adv Eng Softw 67:136–147
Kuang F, Zhang S, Jin Z, Xu W (2015) A novel SVM by combining kernel principal component analysis and improved chaotic particle swarm optimization for intrusion detection. Soft Comput 19:1187–1199
Kuru L, Ozturk A, Kuru E, Kandara O et al (2015) Determination of voltage stability boundary values in electrical power systems by using the chaotic particle swarm optimization algorithm. Int J Electr Power Energy Syst 64:873–879
Li MW, Hong WC, Geng J, Wang J (2017) Berth and quay crane coordinated scheduling using multi-objective chaos cloud particle swarm optimization algorithm. Neural Comput Appl 28(11):3163–3182
Liu B, Wang L, Jin Y, Tang F, Huang D (2005) Improved particle swarm optimization combined with chaos. Chaos Solitons Fractals 25:1261–1271
Lu P, Zhou J, Zhang H, Zhang R, Wang C (2014) Chaotic differential bee colony optimization algorithm for dynamic economic dispatch problem with valve-point effects. Int J Electr Power Energy Syst 62:130–143
Manganaro G, Pine dade Gyvez J (1997) DNA computing based on chaos. In: IEEE international conference on evolutionary computation, Piscataway, pp 255–260
Michalewicz Z (1995) Genetic algorithms numerical optimization and constraints. In: Eshelmen LJ (ed) Proceedings of the 6th international conference on genetic algorithms, Morgan Kaufmann, San Mateo, CA, pp 151–158
Mingjun J, Huanwen T (2004) Application of chaos in simulated annealing. Chaos Solitons Fractals 21:933–941
Mirjalili S, Gandomi AH (2017) Chaotic gravitational constants for the gravitational search algorithm. Appl Soft Comput 53:407–419
Mozaffari A, Gorji-Bandpy M, Gorji TB (2012a) Optimal design of constraint engineering systems: application of mutable smart bee algorithm. Int J Bio Inspir Comput 4:167–180
Mozaffari A, Gorji-Bandpy M, Samadian P, Mohammadrezaei Noudeh S (2012b) Analyzing, controlling and optimizing Damavand power plant operating parameters using a synchronous parallel shuffling self-organized Pareto strategy and neural network: a survey. Proc IMECHE A J Power Energy 226:848–866

Mozaffari A, Fathi A, Behzadipour S (2012c) The great salmon run: a novel bio-inspired algorithm for artificial system design and optimization. Int J Bio Inspir Comput 4(5):286–301
Mozaffari A, Azimi M, Gorji-Bandpy M (2013a) Ensemble mutable smart bee algorithm and a robust neural identifier for optimal design of a large scale power system. J Comput Sci 5(2):206–223
Mozaffari A, Ramiar A, Fathi A (2013b) Optimal design of classical Atkinson engine with dynamic specific heat using adaptive neuro-fuzzy inference system and mutable smart bee algorithm. Swarm Evolut Comput 12:74–91
Mozaffari A, Emami M, Azad NL, Fathi A (2015) On the efficacy of chaos-enhanced heuristic walks with nature-based controllers for robust and accurate intelligent search, part A: an experimental analysis. J Exp Theor Artif Intell 27:389–422
Ott E, Grebogi C, Yorke JA (1990) Controlling chaos. Phys Rev Lett 64:1196–1199
Pecora L, Carroll T (1990) Synchronization in chaotic systems. Phys Rev Lett 64:821–824
Schuster HG (1988) Deterministic chaos: an introduction, 2 revised edn. Federal Republic of Germany: Physick-Verlag GmnH, Weinheim
Senkerik R, Pluhacek M, Zelinka I, Davendra D, Oplatkova ZK (2014) Comparison of chaos driven PSO and differential evolution on the selected PID tuning problem. Lect Notes Comput Sci 8838:67–76
Singh H, Srivastava L (2014) Modified differential evolution algorithm for multi-objective VAR management. Int J Electr Power Energy Syst 55:731–740
Storn R, Price K (1997) Differential evolution: a simple and efficient heuristic for global optimization over continuous space. J Glob Optim 11(4):341–341
Talatahari S, Azar BF, Sheikholeslami R, Gandomi AH (2012) Imperialist competitive algorithm combined with chaos for global optimization. Commun Nonlinear Sci Numer Simul 17:1312–1319
Tavazoei MS, Haeri M (2007) Comparison of different one-dimensional maps as chaotic search pattern in chaos optimization algorithms. Appl Math Comput 187:1076–1085
Tessema B (2006) A self-adaptive genetic algorithm for constrained optimization. M.Sc. Thesis, Oklahoma State University
Thakur M (2013) A new genetic algorithm for global optimization of multimodal continuous functions. J Comput Sci 5(2):298–311
Tian H, Yuan X, Ji B, Chen Z (2014) Multi-objective optimization of short-term hydrothermal scheduling using non-dominated sorting gravitational search algorithm with chaotic mutation. Energy Convers Manag 81:504–519
Wang GG, Guo L, Gandomi AH, Hao GS, Wang H (2014) Chaotic krill herd algorithm. Inf Sci 274:17–34
Wolpert DH, Macready WG (1997) No free lunch theorems for optimization. IEEE Trans Evolut Comput 1:67–82
Wong K, Man KP, Li S, Liao X (2005) More secure chaotic cryptographic scheme based on dynamic look-up table circuits. Circuit Syst Signal Process 24(5):571–584
Wright AH (1991) Genetic algorithms for real parameter optimization. In: Rawlins GJE (ed) Foundations of genetic algorithms I. Morgan Kaufmann, San Mateo, pp 205–218
Xiang T, Liao X, Wong K (2007) An improved particle swarm optimization algorithm combined with piecewise linear chaotic map. Appl Math Comput 190:1637–1645
Yang XS (2008) Nature-inspired metaheuristic algorithms. Luniver Press, Beckington
Yang L, Chen T (2002) Application of chaos in genetic algorithms. Commun Theor Phys 38:168–172
Yuan XH, Yuan YB, Zhang YC (2002) A hybrid chaotic genetic algorithm for short-term hydro system scheduling. Math Comput Model 59:319–327
Yuan X, Dai X, Wu L (2015) A mutative-scale pseudo-parallel chaos optimization algorithm. Soft Comput 19:1215–1227
Zelinka I, Jasek R (2010) Evolutionary decryption of chaotically encrypted information. Studi Comput Intell Evolut Algorithms Chaotic Syst 267:329–343
Zelinka I, Celikovsky S, Richter H, Chen G (2010) Evolutionary algorithms and chaotic systems. Studies in computational intelligence, vol 267. Springer, Berlin
Zhang H, Ma T, Huang GB, Wang Z (2010) Robust global exponential synchronization of uncertain chaotic delayed neural networks via dual-stage impulsive control. IEEE Trans Syst Man Cybern B (Cybern) 40:831–844
Zhang H, Wang Z, Liu D (2014) A comprehensive review of stability analysis of continuous-time recurrent neural networks. IEEE Trans Neural Netw Learn Syst 25:1229–1262
Zhang H, Yan Q, Zhang G, Jiang Z (2016) A chaotic differential evolution algorithm for flexible job shop scheduling. In: Asian simulation conference: theory, methodology, tools and applications for modeling and simulation of complex systems, pp 79–88
Zhou A, Qu BY, Li H, Zhao SZ, Suganthan PN, Zhang Q (2011) Multiobjective evolutionary algorithms: a survey of the state of the art. Swarm Evolut Comput 1(1):32–49

Zhu W, Duan H (2014) Chaotic predator–prey biogeography-based optimization approach for UCAV path planning. Aerosp Sci Technol 32(1):153–161

Zuo XQ, Fan YSA (2006) Chaos search immune algorithm with its application to neuro-fuzzy controller design. Chaos, Solitons Fractals 30:94–109